

JAERI-M

8 7 6 6

STUDIES ON ENTRAPPING OF ENZYMES AND DRUGS  
IN MATRICES BY RADIATION-INDUCED  
POLYMERIZATION AT LOW TEMPERATURES  
AND THEIR CAPABILITIES

March 1980

Masaru YOSHIDA

日 本 原 子 力 研 究 所  
Japan Atomic Energy Research Institute

この報告書は、日本原子力研究所が JAERI-M レポートとして、不定期に刊行している研究報告書です。入手、複製などのお問い合わせは、日本原子力研究所技術情報部（茨城県那珂郡東海村）あて、お申しこしてください。

JAERI-M reports, issued irregularly, describe the results of research works carried out in JAERI. Inquiries about the availability of reports and their reproduction should be addressed to Division of Technical Information, Japan Atomic Energy Research Institute, Tokai-mura, Naka-gun, Ibaraki-ken, Japan.

Studies on Entrapping of Enzymes and Drugs in Matrices by Radiation-Induced Polymerization at Low Temperatures and Their Capabilities

Masaru Yoshida

Pilot Scale Research Station, Takasaki Radiation Chemistry Research Establishment, JAERI

(Received February 5, 1980)

The author has studied a immobilization method for enzymes and drugs by means of radiation-induced polymerization at low temperatures in a supercooled state using glass-forming monomers. The proposed technique using glass-forming monomer has features as follows. (1) Inactivation of the bio-component by heat and radiation is almost eliminated due to the low temperature treatment. (2) Moulding or shaping of the mixture of monomer and bio-component in difference forms and sizes of polymerized composite is easy due to high viscosity of the supercooled monomer. (3) The carrier matrix may be selected from a wide range of hydrophilic and hydrophobic vinyl monomers and polymers. (4) No impurities such as a polymerization catalyst are introduced in the system. (5) A bio-component can be easily distributed in high stability, either concentrated on surface of the monomer or homogeneously within the monomer, due to large viscosity of the monomer. Furthermore, the author attempted practical usage of the technique in such as enzyme fixation for long continuous or repeated application (PART I) and controlled slow release of medicine in efficient and durable without secondary reaction (PART II).

Keywords; Immobilization, Radiation-Induced Polymerization, Enzyme, Controlled-Release, Drug, Glass-Forming Monomer, Polymer Matrix, Low Temperature.

低温放射線重合による生物活性物質の包括とその応用に関する研究

日本原子力研究所高崎研究所開発試験場

吉田 勝

(1980年2月5日受理)

低温では結晶化せず安定な過冷却状態になり、低温重合反応性が大きい特徴をもつガラス化性モノマーを利用して、これと生物活性物質の混合物に低温で照射して放射線重合させる方法により、広く親水性および疎水性の合成高分子担体に酵素、生理活性物質を固定する研究を行った。この方法の特徴は、低温反応のため放射線、熱による生物活性物質の失活がないこと、複合体内部に不純物が混在しないこと、固定化の担体として材質および加工性の変化に富むビニルポリマーの適応性が広いこと、マイルドな条件下で固定できること、生物活性物質を担体表面もしくは内部に均一に分散させることができること、などである。第1編は比較的分子量、分子サイズの大きい酵素を固定して長期連続酵素反応を行い、第2編は制癌剤に徐放性と特効性を付与させ副作用なしに効率よく作用せしめることを目的とした基礎的研究を行った。

## CONTENTS

INTRODUCTION -----	1
PART I IMMOBILIZATION OF ENZYMES BY RADIATION-INDUCED POLYMERIZATION OF GLASS-FORMING MONOMERS AT LOW TEMPERATURES -----	2
CHAPTER 1 Immobilization of enzymes by poly(2-hydroxyethyl methacrylate) -- Effect of monomer-solvent composition on porosity of matrix and activity of immobilized enzymes -----	3
CHAPTER 2 Immobilization of enzymes by copolymerization of 2-hydroxyethyl methacrylate and other hydrophilic or hydrophobic comonomer -----	24
CHAPTER 3 Immobilization of enzymes by hydrophobic glass-forming monomers at low temperatures	
3-1 Immobilization of some enzymes in particle form -----	35
3-2 Immobilization of cellulase in the swollen polymer microsphere -----	41
CHAPTER 4 Continuous enzyme reaction by immobilized enzymes -----	48
PART II ENTRAPPING AND CONTROLLED RELEASE OF DRUGS BY RADIATION- INDUCED POLYMERIZATION OF GLASS-FORMING MONOMERS AT LOW TEMPERATURES -----	53
CHAPTER 5 Entrapping and controlled release of potassium chloride from various matrices -----	54
CHAPTER 6 Controlled release of drugs from matrix having pH dependency of solubility -----	66
CHAPTER 7 Controlled release of drugs from variously shaped matrices	
7-1 Release of drugs from polymerized beads -----	73
7-2 Release of chemotherapeutic drugs from variously shaped matrices -----	78
CHAPTER 8 Controlled release of 5-fluorouracil from polymer matrices containing adsorbents -----	90
CHAPTER 9 Controlled release of multi-component cytotoxic agents from radiation polymerized composites -----	97
REFERENCES -----	104
ACKNOWLEDGEMENT -----	110

## INTRODUCTION

The author has studied the new immobilization technique for enzymes and drugs by means of radiation-induced polymerization at low temperatures in a supercooled state using glass-forming monomers<sup>1,2</sup>. These monomers were suitable as the carrier materials for entrapping because of large viscosity in supercooling state and also of their high polymerizability even at low temperatures<sup>3</sup>. This immobilization was carried out by mixing the glass-forming monomer and biologically active substance in the presence or absence of solvent (usually water), cooling it to low temperatures and then irradiating. It was found that according to this method, the biologically active substances can be entrapped efficiently on surface or inside matrix of vinyl polymer with various forms and structures. The characteristic merits of the method can be summarized as follows;

- (1) Inactivation of biologically active substances by heat and irradiation can be almost completely retarded due to low temperature
- (2) No impurities such as catalyst exist in the matrix
- (3) Mixing and dispersion of biologically active substances to the monomer matrix is easy in monomeric state due to viscous liquid at low temperatures
- (4) Preparation and control of specific matrix such as porous structure is easily done
- (5) Molding and shaping of the mixture to various forms are easy in supercooled state of monomers
- (6) Selection of carrier matrix is free among widely ranged chemical, physical and biological properties of vinyl polymers
- (7) General application to various kinds of biologically active substances is possible

Recently, immobilization of biologically active substances such as enzyme has been the problem of increased interest and a number of methods has been proposed<sup>4-19</sup>. Among them, entrapping method is one of the most advantageous for its general applicability to any kind of biologically active substance and for the multiple uses not only to fixation of biological components but also to controlled slow release of them<sup>20-27</sup>. However, hitherto entrapping methods are not satisfactory in functionalities such as activity yield, stability, moldability to desired shape and size, and freedom of widely selection of carrier polymer.

In this study, the author investigated on the fundamental conditions

of this new immobilization technique as well as its some variations and also on the characteristic properties of the method and materials. Furthermore, the author tried to apply this method for practical applications such as an enzyme fixation for continuous or repeated long use (PART I) and a controlled slow release of medicine for efficient and durable cure without secondary reaction (PART II).

## PART I

### IMMOBILIZATION OF ENZYMES BY RADIATION-INDUCED POLYMERIZATION OF GLASS-FORMING MONOMERS AT LOW TEMPERATURES

In this PART, the biologically active substances such as enzymes were immobilized in porous polymer matrices by radiation-induced polymerization of glass-forming monomers at low temperatures.  $\alpha$ -Amylase and glucoamylase were mainly used as water soluble enzymes to know the fundamental properties of this method, because these enzymes are industrially useful. Furthermore, in the stage of advanced research the immobilization of glucose isomerase (microbial cells) and cellulase (water soluble enzyme) were investigated to clarify the characteristic of the immobilized materials for the cell reaction and also for the enzyme reaction with water insoluble substrate. In CHAPTER 1, the enzymes were immobilized in porous poly(2-hydroxyethyl methacrylate) (PHEMA) and the relation between the activity and the porosity was clarified. The effect of hydrophilicity in matrix on the porosity and the activity was investigated in CHAPTER 2 by means of radiation-induced copolymerization of HEMA with other monomers. The maximum activity of immobilized glucoamylase was observed in a certain composition of HEMA with hydrophobic monomer. On the other hand, the immobilization of cellulase in completely hydrophobic monomer system was carried out in CHAPTER 3. The sufficient reactivity between immobilized enzyme and water insoluble substrate was proved. On the basis of the fundamental study in CHAPTER 1-3, the continuous enzyme reaction was tested for 30 days by column method, in CHAPTER 4. The durabilities of immobilized enzymes in this process were excellent results.

of this new immobilization technique as well as its some variations and also on the characteristic properties of the method and materials. Furthermore, the author tried to apply this method for practical applications such as an enzyme fixation for continuous or repeated long use (PART I) and a controlled slow release of medicine for efficient and durable cure without secondary reaction (PART II).

## PART I

### IMMOBILIZATION OF ENZYMES BY RADIATION-INDUCED POLYMERIZATION OF GLASS-FORMING MONOMERS AT LOW TEMPERATURES

In this PART, the biologically active substances such as enzymes were immobilized in porous polymer matrices by radiation-induced polymerization of glass-forming monomers at low temperatures.  $\alpha$ -Amylase and glucoamylase were mainly used as water soluble enzymes to know the fundamental properties of this method, because these enzymes are industrially useful. Furthermore, in the stage of advanced research the immobilization of glucose isomerase (microbial cells) and cellulase (water soluble enzyme) were investigated to clarify the characteristic of the immobilized materials for the cell reaction and also for the enzyme reaction with water insoluble substrate. In CHAPTER 1, the enzymes were immobilized in porous poly(2-hydroxyethyl methacrylate) (PHEMA) and the relation between the activity and the porosity was clarified. The effect of hydrophilicity in matrix on the porosity and the activity was investigated in CHAPTER 2 by means of radiation-induced copolymerization of HEMA with other monomers. The maximum activity of immobilized glucoamylase was observed in a certain composition of HEMA with hydrophobic monomer. On the other hand, the immobilization of cellulase in completely hydrophobic monomer system was carried out in CHAPTER 3. The sufficient reactivity between immobilized enzyme and water insoluble substrate was proved. On the basis of the fundamental study in CHAPTER 1-3, the continuous enzyme reaction was tested for 30 days by column method, in CHAPTER 4. The durabilities of immobilized enzymes in this process were excellent results.



## CHAPTER I

## IMMOBILIZATION OF ENZYMES BY POLY(2-HYDROXYETHYL METHACRYLATE) — EFFECT OF MONOMER-SOLVENT COMPOSITION ON POROSITY OF MATRIX AND ACTIVITY OF IMMOBILIZED ENZYMES —

## 1.1. Introduction

The author has studied radiation-induced polymerization at low temperatures using glass-forming monomers<sup>3,28</sup>, and has found in relation to its application that glass-forming monomers were very suitable as the entrapping matrix owing to their property of forming highly viscous liquids or amorphous solids on supercooling at low temperatures and also to their high polymerizability even at low temperatures. This method can be applied to the entrapping of any kind of biologically active substance for the purpose not only of immobilization, but also of controlled release<sup>29</sup>.

Recently, many studies have been reported on the immobilization of enzymes<sup>30-37</sup>. A number of methods has been proposed for immobilization. Among these the entrapping method is considered to be one of the most promising, because it can be most generally applied to the entrapping of any kind of enzymes, microbial cells and organelles with different sizes and properties, with little destruction of biological activity as compared with the covalent bonding method. Moreover, by using various techniques in polymer synthesis to control the polymer structure, enzymically stable and mechanically very firm entrapment conjugates might be possible. Such conjugates would compare very favourably with conjugates prepared by the adsorption method. Entrapment has been performed by using radiation techniques, such as cross-linking of poly(vinyl alcohol)<sup>20,38</sup> and polymerization of acrylamide<sup>22</sup> by irradiation. However, in these methods enzyme entrapped inside the cross-linked polymer and the substrate has to diffuse inside the matrix for enzyme reaction. There is also a difference between the tighter enzyme immobilization by increased cross-linking and the faster enzyme reaction by increased substrate diffusion. Moreover, water insoluble or high molecular weight substrates cannot be utilized for enzyme reaction using immobilized enzymes that are entrapped inside the carrier matrix.

In this CHAPTER, the author has tried to clarify the effect and characteristics of the new entrapping immobilization method using radiation

induced polymerization of a typical and moderately hydrophilic glass-forming monomer, 2-hydroxyethyl methacrylate, in the presence of enzymes which are relatively stable for radiation<sup>39,40</sup>.

## 1.2. Experimental

### 1.2.1. Materials

Bacillus subtilis liquefying  $\alpha$ -amylase (Nagase Sangyo Co.): crystalline bacterial  $\alpha$ -amylase, 1500000 DUN/g, one DUN is defined as that amount of enzyme activity causing a decreasing of absorbance at 660 nm of 1% per minute at 40°C in blue value of 1% soluble starch; Aspergillus niger glucoamylase (NOVO Industry A.S., Denmark): 150 NOVO AG-units/ml; Rhizopus niveus glucoamylase (Seikagaku Kogyo Co.): fine grade, 16.8 units/mg; Trichoderma viride cellulase (Kinki Yakult Co.): [ONOZUKA] R-10, 10000 units/g, assay is based on that of Kitamikado<sup>41</sup>; Aspergillus niger glucose oxidase (Sigma Chemical Co.): purity grade, type II, 20300 units/g, one unit will oxidize 1.0  $\mu$ mole of glucose to gluconic acid per minute at pH 5.1 at 35°C; Yeast  $\alpha$ -glucosidase (Tokyo Kasei Kogyo Co.): purity grade, type I, one mg liberates approx. 6.9  $\mu$ moles of glucose per minute from p-nitrophenyl-D-glucoside at pH 6.8 at 30°C, were used as enzymes.

Soluble starch (Katayama Chemical Co.) for  $\alpha$ -amylase, maltose ( $[\alpha]_D^{20}$  +129.0 - +130.5) (Tokyo Kasei Kogyo Co.) for glucoamylase and  $\alpha$ -glucosidase, carboxymethyl cellulose sodium, n=500 (CMC) (Kanto Chemical Co.) for cellulase, and glucose ( $[\alpha]_D^{20}$  +52.5 - +53.0) (Kishida Chemical Co.) for glucose oxidase were used as substrates.

2-Hydroxyethyl methacrylate (HEMA) obtained from Mitsubishi Chemical Co. was used as a carrier and purified by passing through ion exchange resin to remove polymerization inhibitor.

Drierite obtained from W.A. Hamond Drierite Co. was used as an adsorbent.

### 1.2.2. Immobilization

The immobilization enzymes were prepared as follows. The enzyme was dissolved in 0.02M phosphate buffer solution (pH 6.9) in the case of  $\alpha$ -amylase or  $\alpha$ -glucosidase, in 0.1M acetate buffer solution (pH 4.5) in the case of glucoamylase or cellulase, and in 0.1M citrate buffer solution

(pH 5.4) with the above solution to a total volume of 1 ml. The monomer concentration ([M]) is given as;

$$[M] (\%) = \frac{\text{Monomer (ml)}}{\text{Monomer (ml) + Buffer (ml)}} \times 100 \quad (1)$$

The enzyme-HEMA mixture was then charged into an 8 mm diameter glass ampoule and sealed off under a vacuum of  $10^{-3}$  mmHg.  $\gamma$ -ray from a  $^{60}\text{Co}$  source was carried out at various temperatures using various cryostats: liquid nitrogen ( $-196^\circ\text{C}$ ), dry ice-ethanol ( $-78^\circ\text{C}$ ), carbon tetrachloride ( $-24^\circ\text{C}$ ) and ice ( $0^\circ\text{C}$ ), respectively. In general, the irradiation dose rate was carried out at  $5 \times 10^5$  R/hr.

After irradiation, the immobilized enzymes were cut into 10 samples 8 mm diameter x 2 mm long and used to study leakage and activity yield. The polymer composites obtained using concentrations of HEMA in the ranges 10-40, 50-80 and 90-100% were in the form of a sponge-like white gel, a hard sponge-like white gel and a rigid transparent glass-like gel, respectively.

In the case of  $\alpha$ -amylase immobilized in the presence of drierite as an adsorbent, enzyme was dissolved in 0.02M phosphate buffer solution (pH 6.9) containing HEMA, and then this solution was poured into a glass ampoule containing an adsorbent. The ampoule was sealed and kept overnight at  $25^\circ\text{C}$ . The immobilization was carried out with  $1 \times 10^6$  R ( $5 \times 10^5$  R/hr) at  $-24^\circ\text{C}$ . The resultant immobilized enzyme composite was in a pellet form of 16 mm diameter and 5 mm long.

### 1.2.3. Enzyme Reaction and Activity Yield

Native or immobilized enzymes were mixed with a 1% corresponding buffer solution of each substrate. A 2% soluble starch solution (phosphate buffer, pH 6.9) was used for  $\alpha$ -amylase. A 1% maltose solution (acetate buffer, pH 4.5) was used for glucoamylase or  $\alpha$ -glucosidase. A 0.5% CMC solution (acetate buffer, pH 4.5) was used for cellulase. A 1% glucose solution (citrate buffer, pH 5.4) was used for enzyme reaction by glucose oxidase.

Then, the reaction was carried out at determined conditions chosen by preliminary reaction tests. Reaction conditions were as follows;

$\alpha$ -amylase (40°C for 1 hr), glucoamylase from *Aspergillus niger* (45°C for 30 min), glucoamylase from *Rhizopus niveus* (40°C for 30 min), cellulase (40°C for 1 hr),  $\alpha$ -glucosidase (35°C for 1 hr) and glucose oxidase (30°C for 30 min), respectively.

Then the reacted solution was separated from immobilized enzymes by filtration and the product was assayed as follows. For  $\alpha$ -amylase assay total reducing sugars were measured by the absorption at 492 nm using Shimazu Model QV-50 spectrophotometer according to the 3,5-dinitrosalicylic acid method<sup>42</sup>. The relation between the amount of  $\alpha$ -amylase (native) and the increase in reducing power is shown in Figure 1. In this case, reducing power was expressed as corresponding maltose yield, which was

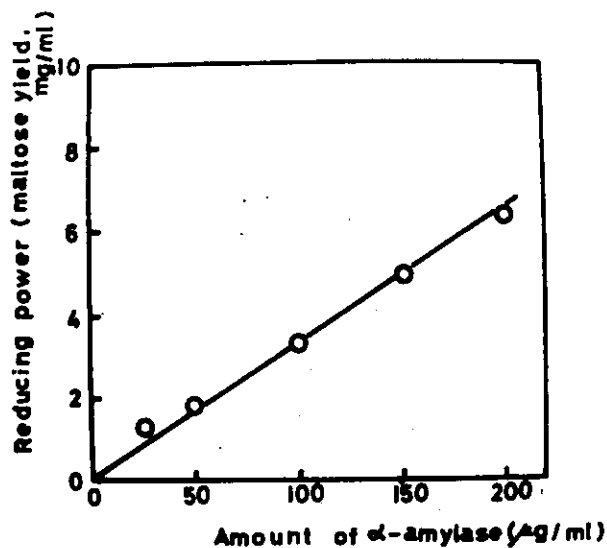
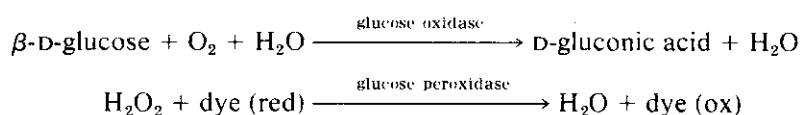


Figure 1 Relationship between the amount of  $\alpha$ -amylase (native) and the increase in reducing power expressed as the maltose yield.  
Incubation: 40°C, 1 hr

obtained from the conversion relationship between the absorbance and maltose quantity.

The glucose oxidase assay was carried out colourimetrically measuring the absorption at 465 nm after addition of sodium p-diphenylamine sulfonate as a colouring reagent<sup>43</sup>.

For  $\alpha$ -glucosidase assay glucose formation was determined colourimetrically from absorption at 505 nm. In cellulase assay, glucose was detected by absorption at 505 nm, adding GOD-PODLK (from Nagase Sangyo Co.), which consists of glucose oxidase, glucose peroxidase and chromogen (colouring reagent) and catalyzes the following reaction<sup>20</sup>.



For the glucoamylase assay native or immobilized glucoamylase was mixed with 5 ml 1% maltose solution of acetate buffer (pH 4.5) in 20 mm diameter glass ampoule. The reaction was carried out by standing the mixture at 40°C for 30 min. After reaction, the amount of glucose produced was determined by measuring the absorption intensity at 505 nm. The activity yield of the immobilized enzymes may be represented as follows;

$$\text{Activity yield (\%)} = \frac{I_a}{N_a} \times 100 \quad (2)$$

where  $I_a$  is the quantity of hydrolysis product formed by immobilized enzymes during each batch reaction and  $N_a$  is the quantity of hydrolysis product formed by native enzymes.

The pH of the reaction mixture was measured with a Toa Denpa Kogyo Co., Model HA-5A pH meter. Buffer solutions of varying pHs for the pH stability test were prepared (hydrochloric acid-acetic acid buffer for pH 1.0, tartrate buffer for pH 2.0-4.0, acetic acid buffer for pH 4.5-5.0, phosphate buffer for pH 6.0 and ammonium buffer for pH 9.0-10.0).

#### 1.2.4. Differential Thermal Analysis (DTA)

The glass transition temperature ( $T_g$ ) and melting point ( $T_m$ ) were measured using the DTA equipment described previously<sup>3</sup>. The phase diagram was also determined by DTA.

#### 1.2.5. Determination of Pore Structure and Water Content of the Composite

The polymerized composite was cut into slices 15-25  $\mu\text{m}$  thick using a freezing-type microtome (Yamato Koki Co.). The micrograph of its membrane (polymerized composite with a porous structure) was then taken using an Olympus Model FHF microscope with Olympus PM-10-M equipment.

The average area of a pore was read directly from the micrograph. The average diameter of a pore in the porous structure was determined from Equation (3);

$$\text{Average diameter of pore, } \mu\text{m} = 2 \times \left( \frac{\text{Average area of a pore}}{\pi} \right)^{1/2} \quad (3)$$

The porosity was defined as;

$$\begin{aligned} \text{Porosity (\%)} &= \frac{\text{Total area of pores}}{\text{Total area of visual field in microscopy (pores and polymer matrix)}} \times 100 \\ &= \frac{(\text{Average pore diameter}) \times (\text{number of pores/cm}^2)}{\text{Total area of visual field in microscopy/cm}^2} \times 100 \end{aligned} \quad (4)$$

The water content (W) in the polymerized composite was defined as;

$$\text{Water content (\%)} = \frac{(A+B)}{(A+B)+C} \times 100 \quad (5)$$

where A is the weight of water in the saturated porous structure of the polymerized composite before (in the case of wet composite), or after (in the case of dried composite) the drying treatment; B is the weight of water absorbed in the saturated polymer matrix itself before or after the drying treatment; and C is the weight of the polymer composite after the drying treatment. In the case, B takes a constant value and a water content (W) of 25-35 wt% of the pure polymer is found.

### 1.3. Results and Discussion

#### 1.3.1. Effect of Irradiation on Native Enzyme Activity

Effect of irradiation on native enzyme activity was investigated to find the suitable irradiation condition for immobilization. The results are shown in Figures 2 and 3.

Enzyme radiation damage can be prevented by limiting the irradiation dose within  $1 \times 10^6$  R under vacuum as shown in Figure 2 for glucoamylase from *Rhizopus niveus*. The same tendency has been observed for glucoamylase from *Aspergillus niger*<sup>23</sup>. Furthermore, according to Figure 3, it is obvious that radiation damage can be retarded remarkably and scarcely has a significant effect on activity by carrying out the irradiation at low temperatures not only for glucoamylase but also any type of enzyme. But excess irradiation doses or extremely low irradiation temperatures are not

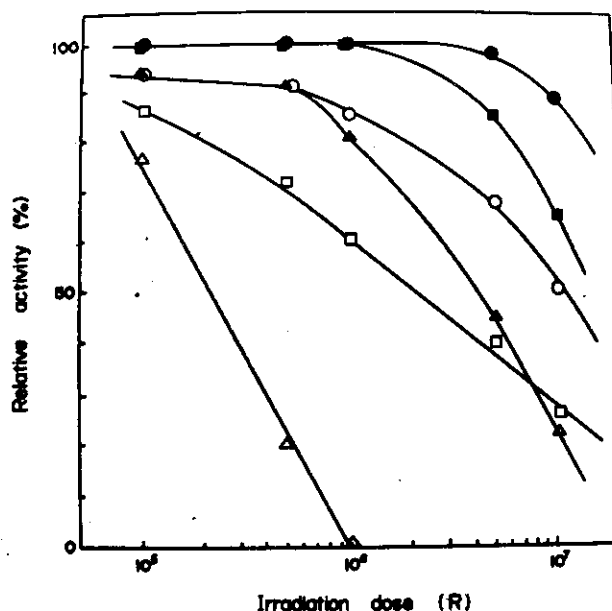


Figure 2 Effect of irradiation dose on relative activity of native glucoamylase from *Rhizopus niveus* at various temperatures. Temperature and atmosphere: (●) -196°C, in vacuo, (■) -78°C, in vacuo, (▲) 25°C, in vacuo, (○) -196°C, in air, (□) -78°C, in air, (Δ) 25°C, in air. Enzyme concentration: 600  $\mu$ g in 1 ml buffer solution. Dose rate: 0.5 MR/hr

suitable because of lower polymer yields. The preferred condition is between -24°C and -78°C and  $5 \times 10^5$  -  $1 \times 10^6$  R.

### 1.3.2. Effect of Polymerization Temperature on Immobilized Enzyme Activity Yield

Activity yields of glucoamylase and some other enzymes immobilized by HEMA (as typical hydrophilic glass-forming monomer) are shown as a function of polymerization temperature in Figure 4.

It is obvious that activity yield increases with lower polymerization temperatures not only in immobilized glucoamylase but also in all other immobilized enzymes. One of the important reasons can be due to less enzyme radiation damage at low temperatures as shown in Figure 2. But, a rather sudden increase in activity than expected from the temperature dependency of radiation damage was observed in Figure 3 at certain temperatures (near -20°C - +24°C in all immobilized enzymes). This boundary temperature approximately agreed to that of phase in the monomeric system from a homogeneous aqueous solution to a ice-in-supercooled monomer

suspension.

The phase diagram of this monomer-water system was then investigated as shown in Figure 5, to identify the immobilization mechanism. This phase diagram was characterized by the fact that the melting peak of the eutectic

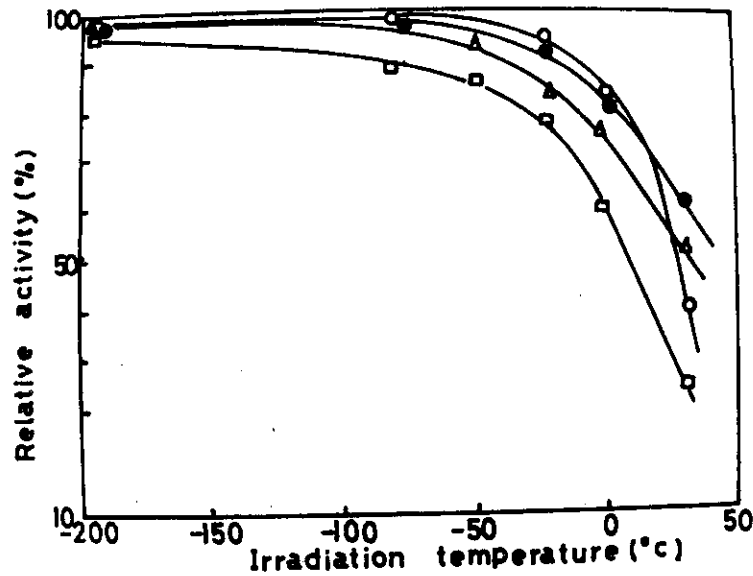


Figure 3 Effect of irradiation temperature on relative activity of native enzymes. Enzyme and its concentration (in 1 ml of total mixture): (●) 600  $\mu$ g glucoamylase from *Rhizopus niveus*, (○) 100  $\mu$ g glucose oxidase, (△) 20 mg  $\alpha$ -glucosidase, (□) 500  $\mu$ g cellulase. Irradiation: 1 MR, in vacuo

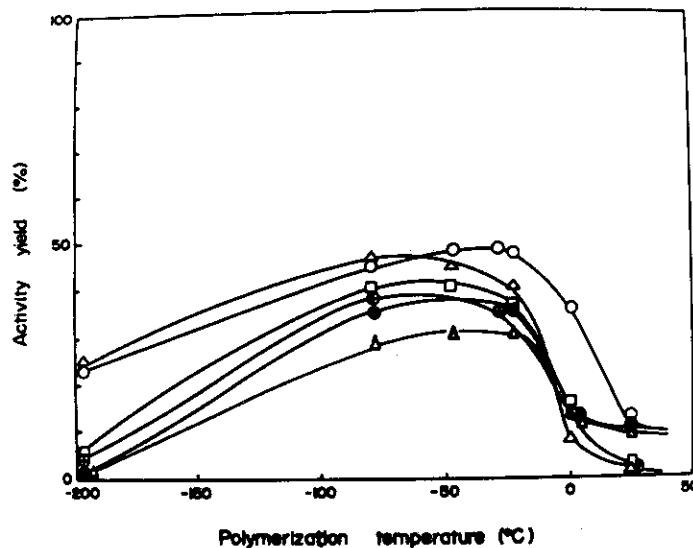


Figure 4 Effect of polymerization temperature on activity yield of enzymes polymerized by HEMA. Enzyme and monomer concentration in monomer-buffer solution: (○)  $\alpha$ -amylase, 50% HEMA, (▲) glucoamylase, 50% HEMA, (●) glucoamylase, 30% HEMA, (⊙) glucose oxidase, 50% HEMA, (△)  $\alpha$ -glucosidase, 50% HEMA, (□) cellulase, 50% HEMA. Irradiation: 1 MR, in vacuo. Enzyme concentration: same as in Figure 3.



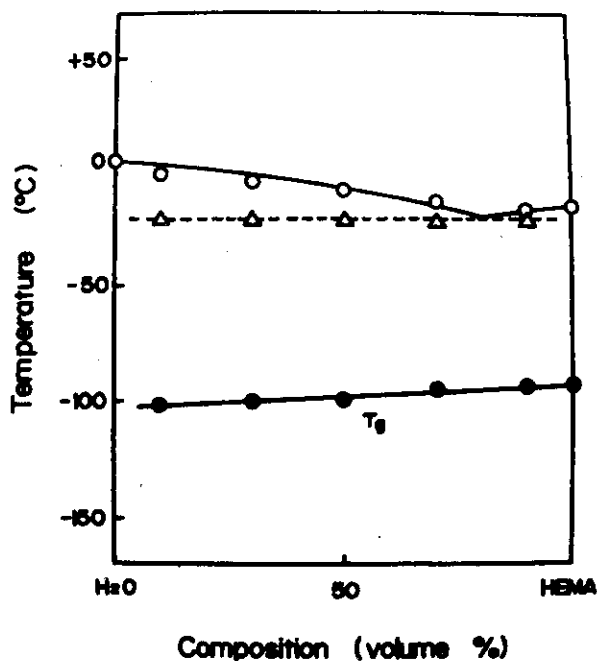


Figure 5 Phase diagram of HEMA-water system.

composition at the eutectic point (above  $-24^{\circ}\text{C}$ ) could hardly, or only slightly, be distinguished and that the change of apparent specific heat corresponding to glass transition temperature could clearly be observed. This fact proved that in the temperature region below  $-24^{\circ}\text{C}$ , most of the water has crystallized to ice, while all eutectic compositions consisting mainly of monomer with a small amount of water have undergone supercooling. That is, the monomeric system is a suspension of ice in supercooled monomer, acting as the dispersion medium at low temperatures. Consequently, the polymerization phase, the mechanism and the structure of the polymerized composite were completely different at temperatures above and below  $-24^{\circ}\text{C}$ . In aqueous solution above  $-24^{\circ}\text{C}$ , heterogeneous precipitation polymerization occurred forming a polymer which was isolated from the monomeric phase due to the lower solubility of poly(2-hydroxyethyl methacrylate) (PHEMA) in water; a continuous pore structure in the polymer composite was formed. On the other hand, at lower temperatures, homogeneous, almost bulk polymerization took place in the supercooled phase due to good compatibility of PHEMA with monomer, forming an almost independent pore structure due to the dispersed ice. It is natural to expect that the great differences in the polymerization phase and polymer structure have an important effect on immobilization. In polymerization by precipitation, the enzyme is concentrated and remains in the water phase (monomer phase)

without effectively being trapped by the polymer. On the other hand, in a cooled system, the enzyme is apt to become isolated from crystallized water, to shift and be dispersed on the surface of the supercooled viscous monomer phase and then effectively to be trapped by homogeneous polymerization. Moreover, excess continuous pore structure in solution polymerization is disadvantageous in preventing enzyme leakage, though it is advantageous for the release of low molecular weight substances<sup>23</sup>. These are probably the other important reasons for the sharp change in activity between the temperatures above and below  $-24^{\circ}\text{C}$  seen in Figure 4. On the other hand, the relationship between the irradiation dose and the activity yield of immobilized enzyme shown in Figure 6 shows that the activity yield was optimal in a certain dose range; the activity yield decreased due to radiation damage in a dose range in excess of this and also decreased by enzyme loss due to lower polymer conversion in the much smaller dose range. The polymer conversion in a suitable dose range was shown to be almost 100%.

### 1.3.3. Dependence of Activity Yield on Monomer Concentration and the Change in Activity Yield with Repeated Use

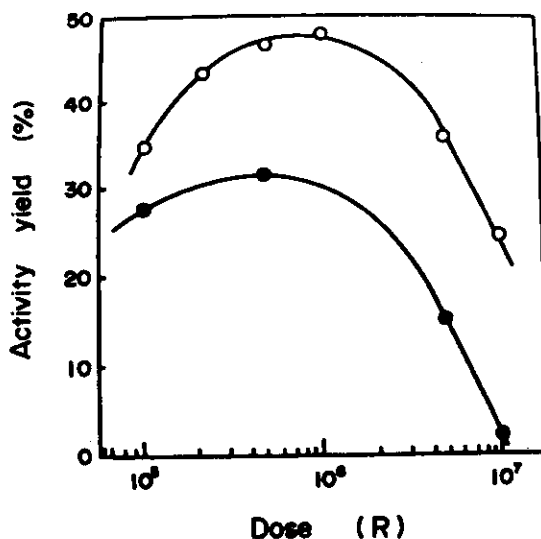


Figure 6 Relationship between the irradiation dose and the activity yield of immobilized enzymes. Immobilized  $\alpha$ -amylase: 200  $\mu\text{g}$  enzyme, 1 ml 50% HEMA in buffer (pH 6.9), and 0.5 MR/hr at  $-24^{\circ}\text{C}$ , in vacuo; immobilized glucoamylase (from *Aspergillus niger*): 0.8  $\mu\text{g}$  enzyme, 1 ml 50% HEMA in buffer (pH 4.5), and 0.5 MR/hr at  $-78^{\circ}\text{C}$ , in vacuo. Substrate: 6 ml 2% starch solution ( $\alpha$ -amylase), 5 ml 1% maltose solution (glucoamylase). Batch enzyme reaction was carried out repeatedly up to 20 times. Enzyme: (○)  $\alpha$ -amylase, (●) glucoamylase

The formation of a pore structure due to ice is one of the most characteristic features of polymers obtained by the present method, and the key factor in determining activity. The monomer concentration should have a direct effect on porosity and activity. Figure 7 shows the dependence of activity yield on monomer concentration. The Figure shows that the activity yield decreases steadily with increasing monomer

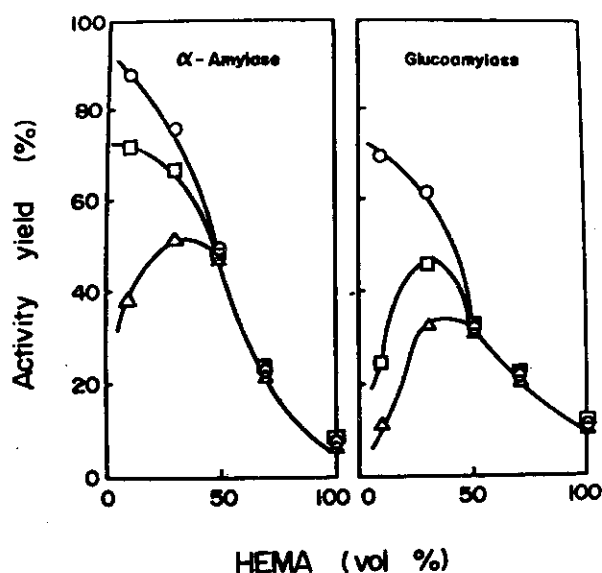


Figure 7 Relationship between the HEMA concentration and the activity yield of immobilized enzymes. (a) Immobilized  $\alpha$ -amylase: 200  $\mu$ g enzyme, 1 ml HEMA in buffer (pH 6.9), and 1 MR at  $-24^{\circ}\text{C}$ , in vacuo. (b) Immobilized glucoamylase (from *Aspergillus niger*): 0.8  $\mu$ g enzyme, 1 ml HEMA in buffer (pH 4.5), and 0.5 MR at  $-78^{\circ}\text{C}$ , in vacuo. Substrate: 6 ml 2% starch solution ( $\alpha$ -amylase), 5 ml 1% maltose solution (glucoamylase). Batch enzyme reaction (times): (O) 1, ( $\square$ ) 5, ( $\Delta$ ) 20

concentration after a small number of batch reactions. However, when a steady state is reached after repeated use in the enzyme assay, the activity yield curve shows an optimum at a certain monomer concentration. From an analysis of the reacted solution, it was shown that the initial decrease in activity in the low monomer concentration system could be attributed mainly to leakage of enzyme due to an excess of large pores. On the other hand, in the high monomer concentration system there was very little enzyme leakage from the polymer; but activity decreased because the dense polymer matrix caused an increase in diffusion resistance to the substrate. Moreover, the proportion of deeply embedded enzyme, not contributing to the enzyme reaction, increased with increasing monomer concentrations. This probably explains the peak in Figure 7.

The limiting condition for enzyme leakage can be determined as a function of both the monomer and enzyme concentrations as shown in Figure 8. The leakage takes place at high enzyme concentration and smaller monomer concentration (above the limiting curve) and no enzyme leakage occurs in the region below the curve.

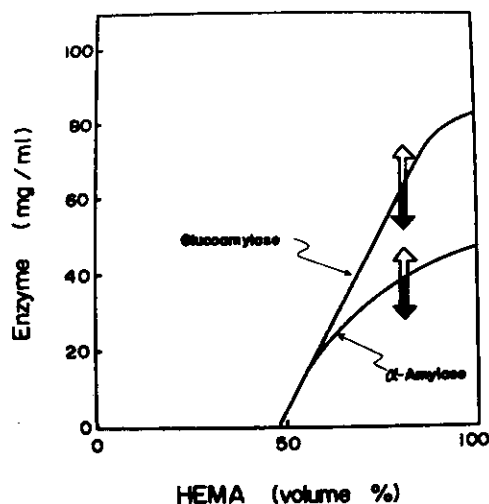


Figure 8 Entrapping limitation curves of immobilized enzymes. Immobilized  $\alpha$ -amylase: 1 ml the HEMA-enzyme-buffer (pH 6.9) mixture was irradiated for 1 hr at a dose rate of 1 MR/hr at  $-24^{\circ}\text{C}$ , in vacuo. Immobilized glucoamylase (from *Aspergillus niger*): 1 ml the HEMA-enzyme-buffer (pH 4.5) mixture was irradiated for 1 hr at a dose rate of 0.5 MR/hr at  $-78^{\circ}\text{C}$ , in vacuo. Substrate: 20 ml 10% starch ( $\alpha$ -amylase), 20 ml 20% maltose (glucoamylase). Batch enzyme reaction was carried out repeatedly up to 20 times, ( $\uparrow$ ) decrease of activity occurred with repeating the batch reaction, ( $\downarrow$ ) no decrease of activity occurred with repeating the batch reaction

#### 1.3.4. Double Entrapping Immobilization of Enzymes by Polymerization of HEMA in the Presence of Inorganic Adsorbent

The immobilization was carried out by polymerizing the mixture which was prepared by mixing the enzyme-additive adsorption mixture with monomer. Optimum concentrations of additive, monomer and enzyme were determined. These preparations showed stable activity and no losses due to enzyme leakage. The quantity 0.3-0.5 g/ml of additive, 30% monomer and the range 0.2-10 mg/ml enzyme were found to be the optimum. Furthermore, limiting concentrations of these components which permitted enzyme leakage on repeated batch reactions were observed and could be set as shown in Figures 9 and 10. In these two Figures, enzymatic activity decreases with the

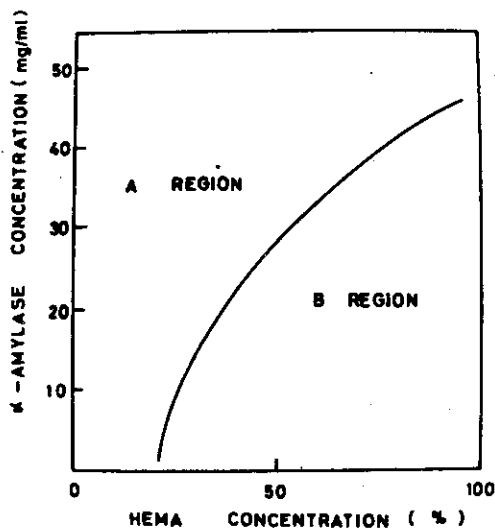


Figure 9 Entrapping limitation curve of immobilized  $\alpha$ -amylase as the function of the enzyme and HEMA concentration. Additive concentration: 0.3 g/ml. A region: decrease of enzymatic activity occurred with increase of the reaction number. B region: decrease of the enzymatic activity did not occur with increase of the reaction number

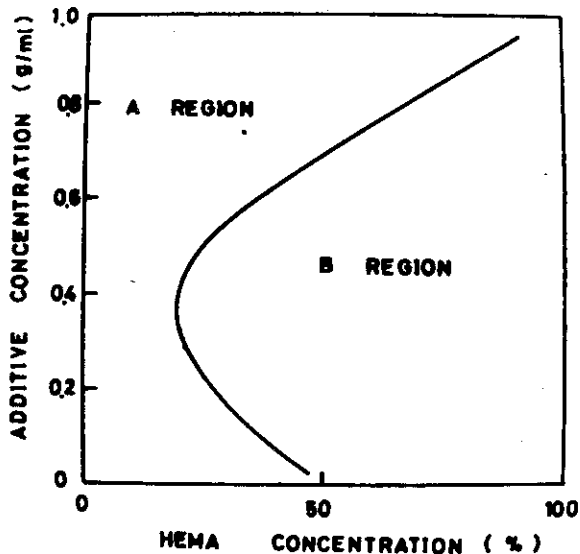


Figure 10 Entrapping limitation curve of immobilized  $\alpha$ -amylase as the function of additive and HEMA concentration.  $\alpha$ -Amylase concentration: 0.2 mg/ml

repeated batch enzyme reaction due to enzyme leakage under the conditions of region A and no enzyme leakage is observed under the conditions of region B. Enzymatic activity decreases because of enzyme leakage from higher enzyme concentration and because lower monomer concentration regions in single trapping systems have an absence of additives as shown in Figure 9. The addition of additives moved the limiting condition curve to the left, thereby enlarging region B. According to Figure 10, the additive concentration range was enlarged as was the no leakage condition region for the monomer concentration as well as for the enzyme concentration. Excess addition of the additives, however, again narrowed the no leakage region. Consequently, it could be concluded that double entrapping by adsorbent and by polymer was effective in increasing the efficiency and firmness of the enzyme trapping. It also heightened enzymatic activity and prevented enzyme leakage on repeated use even at lower monomer concentrations and higher enzyme concentrations as compared to the single trapping enzymes which do not include additives.

#### 1.3.5. Estimation of Porosity by Microscopy and Water Content and Its Effect on Activity

Microscopic observation was adopted for the estimation of the porous structure. The micrographs obtained at various monomer concentrations are shown in Figure 11. It can clearly be seen that the porous structure becomes richer with a decrease in monomer concentration. The average pore diameter and number of pores per unit surface area of the sample in the microscopic visual field were read and estimated. The porosity can be compared with water content, because the water content (subtracting the water absorption of matrix itself at 100% HEMA monomer concentration) is equal to the amount of water occupying the pores, and thus increases in a manner proportional to the porosity.

These pore factors are plotted against irradiation temperature and monomer concentration in Figures 12 and 13. The distribution of pore diameter at various monomer concentrations is shown in Figure 14. Pore diameter decreased steadily but the number of pores reached a maximum with an increase of monomer concentration as shown in Figure 13. The decrease in the number of pores at low monomer concentrations can be attributed to the mutual joining of very large pores. The porosity also decreased steadily with the increase in monomer concentration. The trend in porosity

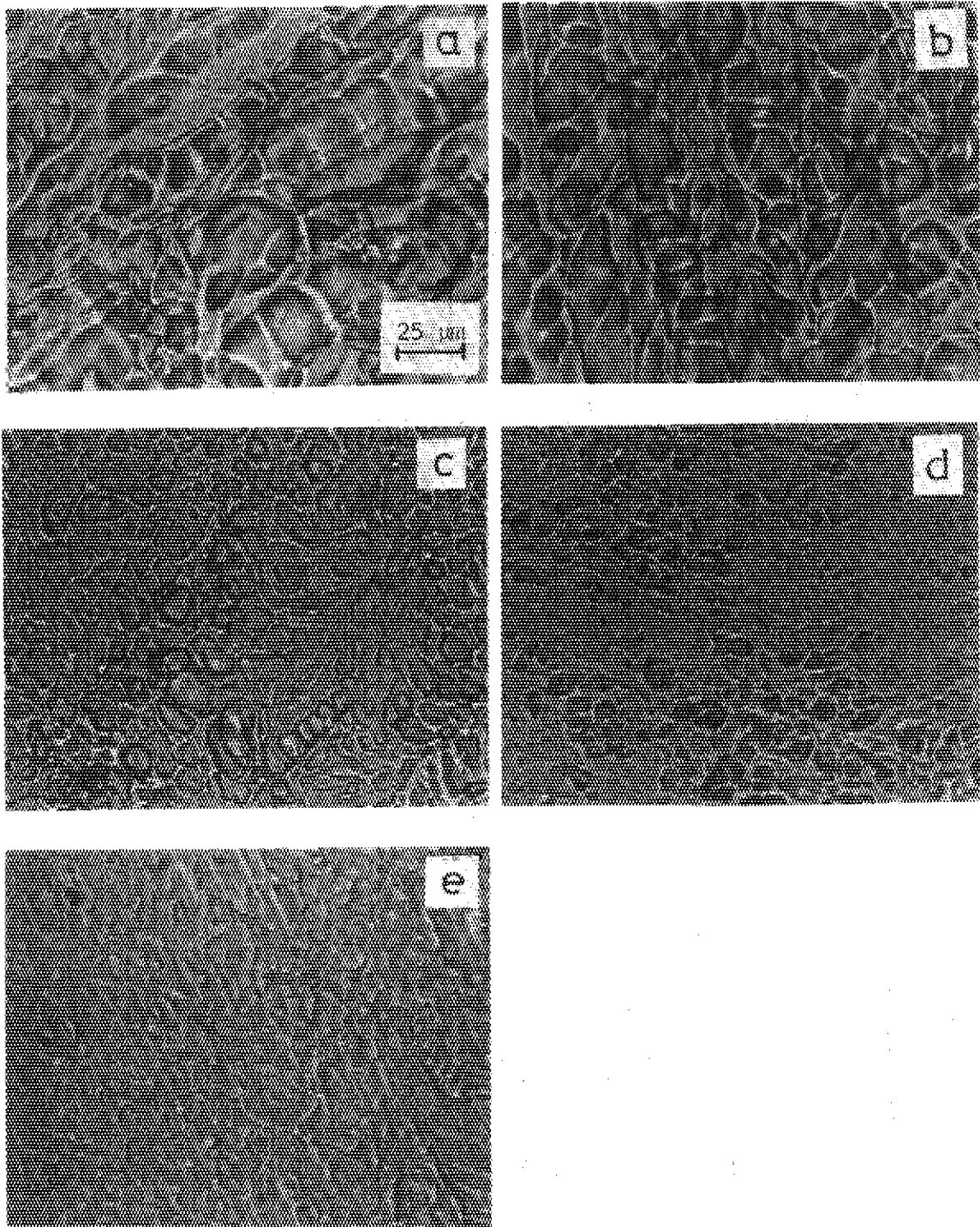


Figure 11 Optical microphotographs of pore structure in polymerized composite obtained in various HEMA concentrations. Experimental conditions were the same as those in Figure 7. HEMA concentration: (a) 10%, (b) 30%, (c) 50%, (d) 70%, (e) 100%

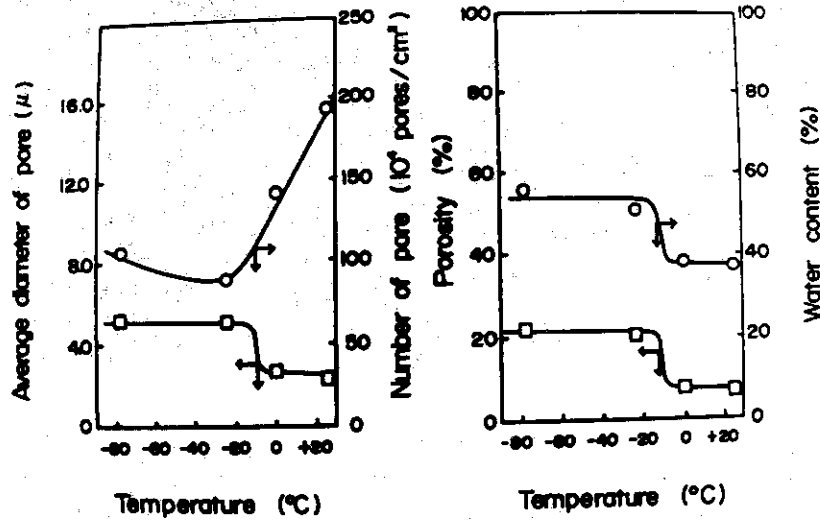


Figure 12 Relationship between the irradiation temperature and the physical properties of pore structure such as average pore diameter, pore number, porosity and water content of polymer composite. Experimental conditions were the same as those in Figure 3 except for irradiation temperature. The activity yield is shown in Figure 14 as a function of pore factors, in the case of immobilized glucoamylase

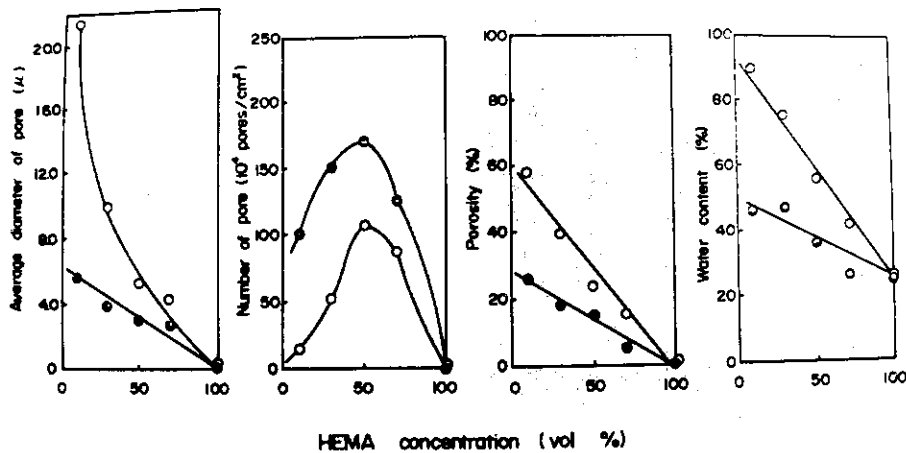


Figure 13 Relationship between the HEMA concentration and the physical properties of pore structure such as average pore diameter, pore number, porosity and water content of polymer composite. Experimental conditions were the same as those in Figure 7. Polymer composite: (O) as-polymerized, (●) after drying treatment



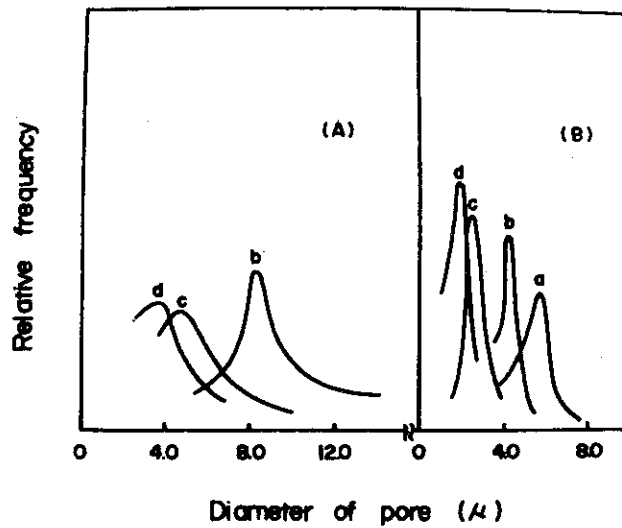


Figure 14 Relationship between the diameter of pore and the relative frequency. Polymer composite: (A) as-polymerized, (B) after drying treatment. HEMA concentration: (a) 10%, (b) 30%, (c) 50%, (d) 70%

obtained by microscopic estimation agreed with that observed by water content measurements.

The pore factors exhibited a discontinuous change over the temperature region between 0°C and -24°C, as shown in Figure 12. This fact can be related to the change in polymerization phase and mechanism as already started. The activity yield was studied in relation to the pore factors as shown in Figure 15. It increased with an increase in porosity at an

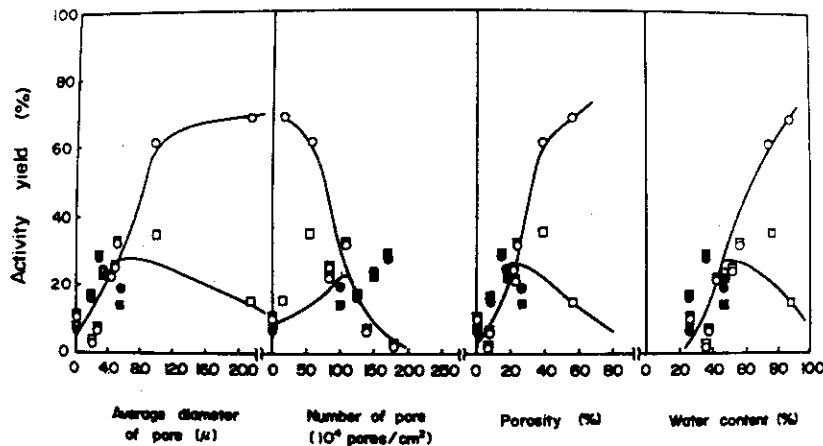


Figure 15 Relationship between the pore factors and the activity yield plotted from the data given in Figures 7 and 11. Batch reaction number (times): (○) 1, (□) 20, in the case of as-polymerized composite; (●) 1, (■) 20, in the case of polymer composite after drying treatment

early stage of repeated use, but it showed a maximum value at a certain porosity at a later stage of repeated use for the same reason described in the interpretation of Figure 7. The effect on the porous structure of drying the as-polymerized polymer was also investigated and plotted in Figure 13. Generally, the pore structure was reduced in size and porosity decreased by drying treatment. However, the degree of shrinkage was rather limited and the pore structure was still present after drying, because of the less hydrophilic properties of the PHEMA matrix. That is, permanent pores could be obtained in spite of the drying treatment. The activity yield in the dry polymer also showed the same dependence on the porosity as in the wet system in Figure 15.

#### 1.3.6. Effect of Cooling Rate on Porosity and Enzymatic Activity

The pore structure depends on the space occupied by the crystallized component. The cooling rate might be one of the important factors affecting the porosity, because the crystal size of ice varies with the crystallization rate. The effect of cooling rate on pore factors such as average pore diameter, number of pores, porosity and water content are shown in Figure 16. According to this result, the average pore diameter increases but the number of pores decreases with a decrease in cooling rate. Apparent porosity increases with a decrease in cooling rate. This means that porosity can be controlled to some degree by the cooling rate; slow cooling increases the size of the crystal and gives the same effect on pore structure as a decrease in monomer concentration. It is reasonable that the activity yield is larger in the early stages of repeated use of the immobilized enzyme but becomes smaller in the later stages of repeated use, owing to enzyme leakage. This trend is more marked for immobilized enzyme as the cooling rate used in the pre-treatment step decreases.

#### 1.3.7. Heat and pH Stabilities of Immobilized Enzymes

Heat and pH stabilities of glucoamylase and  $\alpha$ -amylase immobilized by HEMA are shown in Figure 17. According to these results, heat stability increased considerably at higher temperatures region and pH dependency on activity was expanded by immobilization in comparison with those of the native enzyme. Similar results were also observed in other immobilized enzymes obtained by the same method.

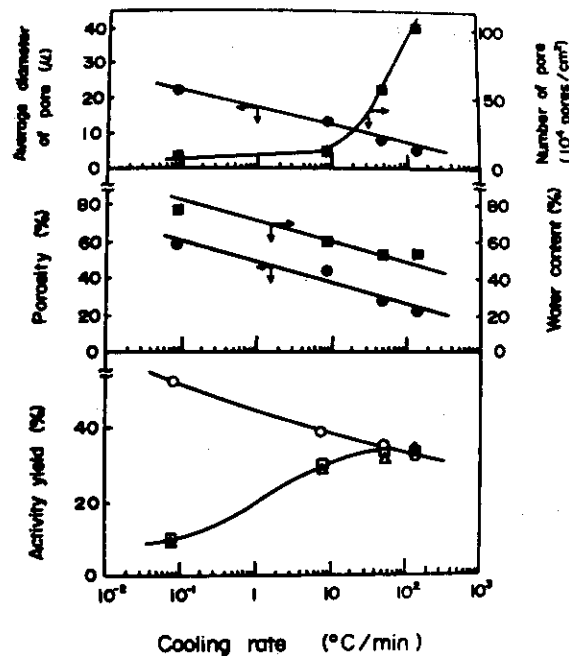


Figure 16 Effects of cooling rate on the physical properties of the pore structure in polymerized composite and on the activity yield of immobilized glucoamylase from *Aspergillus niger*. HEMA solution containing enzyme was cooled at various rates from 25 to  $-78^{\circ}\text{C}$ , and the immobilization was carried out under 0.5 MR at  $-78^{\circ}\text{C}$ , in vacuo. Number of batch reaction (times): (O) 1, ( $\square$ ) 5, ( $\Delta$ ) 20

### 1.3.8. Leakage Property of Glucoamylase in Porous PHEMA Matrix

A bio-material such as *Aspergillus niger* glucoamylase (enzyme), maltose (substrate) and glucose (hydrolyzed product) was entrapped in porous PHEMA matrix. The leakage test was carried out according to the experimental conditions as described in CHAPTER 5, with acetate buffer solution (pH 4.5) at  $45^{\circ}\text{C}$ . The amount of glucoamylase leaked from porous PHEMA matrix was assayed spectrophotometrically by measuring optical density at 268 nm. In the case of maltose, the maltose leaked from the matrix was completely hydrolyzed with excess glucoamylase and its amount estimated from the hydrolyzed product as glucose. The glucose was assayed from optical density at 505 nm.

On the basis of the Higuchi's equation<sup>44</sup> (CHAPTER 5 in PART II), the relation between the  $Q/t^{1/2}$  (a measure of leakage rate) and the HEMA monomer concentration (or average diameter of pore) is shown in Figure 18. The  $Q/t^{1/2}$  values showed a decrease tendency with increasing HEMA concentration

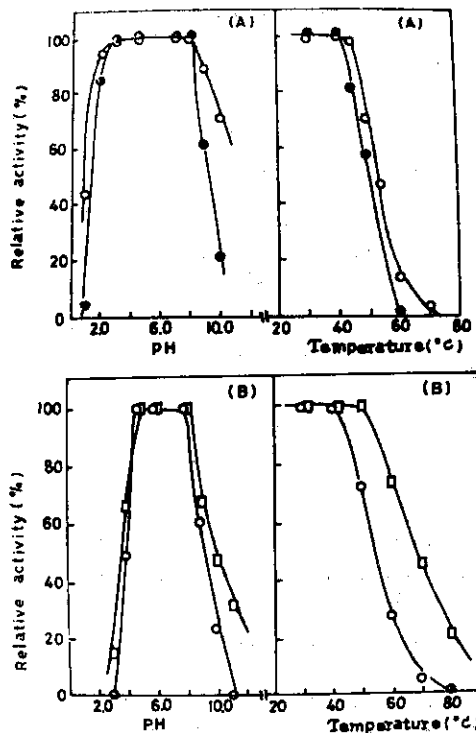


Figure 17 Heat and pH stabilities of immobilized enzymes. (a) Glucoamylase from *Rhizopus niveus* (●) 600  $\mu$ g/ml native enzyme, (○) immobilized enzyme obtained by polymerization of 50% HEMA containing 600  $\mu$ g enzyme at  $-78^{\circ}\text{C}$  with 1 MR, in vacuo; incubation: 1 hr in acetate buffer solution at pH 4.5 for heating test and at  $40^{\circ}\text{C}$  for pH test. (b)  $\alpha$ -Amylase (○) 200  $\mu$ g/ml native enzyme, (□) immobilized enzyme obtained by polymerization of 50% HEMA containing 200  $\mu$ g enzyme at  $-24^{\circ}\text{C}$  with 1 MR, in vacuo; incubation: 1 hr in phosphate buffer solution at pH 6.9 for heating test and at  $40^{\circ}\text{C}$  for pH test

as shown in Figure 18. In the case of immobilized glucoamylase, this inflection point corresponded to a maximal of activity yield represented as a function of batch enzyme reaction in Figure 7(b). Furthermore, the  $Q/t^{1/2}$  values of each bio-material differed by kind of bio-material. The leakage order was glucose > maltose > glucoamylase. It may be concluded in comparison of Figure 7(b) and Figure 18 that the activity yield of immobilized glucoamylase keeps a balance owing to the difference of diffusion rate of the leakage in the matrix of glucose and maltose (low molecular weight material) and glucoamylase (high molecular weight material).

#### 1.4. Summary

The immobilization of some enzymes has been studied by radiation-

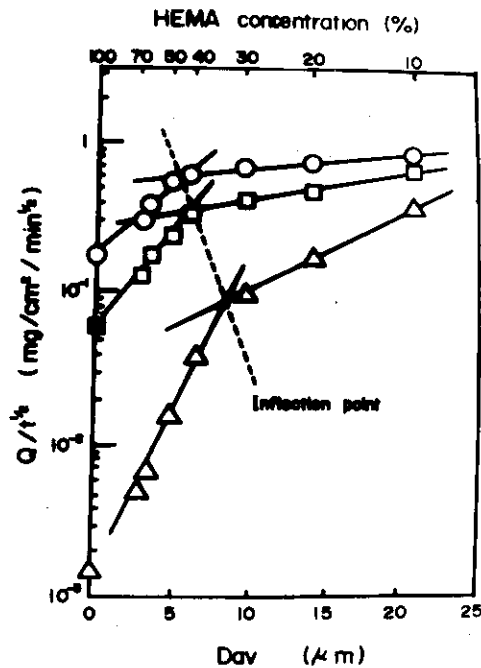


Figure 18 Relationship between the magnitude of bio-material leakage profile and the average diameter of pore. 1 ml of the HEMA-buffer (pH 4.5) mixture in the presence of a bio-material such as glucose, maltose and glucoamylase was charged into an 8 mm diameter glass ampoule. The ampoule was sealed in vacuo and then irradiated for 1 hr at a dose rate of 0.5 MR/hr at  $-78^{\circ}\text{C}$ . Bio-material concentration: 40 mg, (O) glucose, (□) maltose, (Δ) glucoamylase. The leakage test was carried out under the same conditions as described in chapter 5

induced polymerization using HEMA as a glass-forming monomer. Radiation damage of enzymes was slight after irradiation at low temperatures. Moreover, the activity yield of immobilized enzymes increased markedly at polymerization temperatures below  $-24^{\circ}\text{C}$ . The polymer formed was characterized by its porous structure which was studied in detail in relation to the activity and its activity retention with repeated use. It was deduced that enzymes were partly trapped at the pore surface within the polymer matrix and partly within the pores from which they were able to leak out with repeated use. Hence, the use of low temperature and supercooled monomer was necessary for effective enzyme immobilization. On the other hand, it was found that the heat stability increased considerably at higher temperatures region and pH dependency on activity was expanded by immobilization in comparison with those of native enzyme.

## CHAPTER 2

### IMMOBILIZATION OF ENZYMES BY COPOLYMERIZATION OF 2-HYDROXYETHYL METHACRYLATE AND OTHER HYDROPHILIC OR HYDROPHOBIC COMONOMERS

#### 2.1. Introduction

In CHAPTER 1, the author studied a new method of enzyme immobilization by means of radiation-induced polymerization of hydrophilic glass-forming monomer, such as HEMA, at low temperatures<sup>1,45,46</sup>. The characteristic of enzyme composite made by this method had a porous structure and the enzyme was considerably trapped on the pore surface area, dependent on the monomer concentration. In general, the entrapping method is one of the promising, because it may be applicable to biologically active substances under relative mild conditions<sup>47-60</sup>.

In this method, the author choose a suitable carrier from widely hydrophilic or hydrophobic vinyl monomers. Furthermore, a suitable combination of those monomers is also utilizable. The hydrophilic property of the matrix by copolymerization is effective on the control of porous structure. In this CHAPTER, the hydrophilic and hydrophobic property in the matrix was investigated in relation between the porous structure and the enzymatic activity in copolymerization of HEMA.

#### 2.2. Experimental

##### 2.2.1. Materials

Aspergillus niger glucoamylase, 2-hydroxyethyl methacrylate (HEMA) and maltose were the same as described in CHAPTER 1.

Hydrophilic monomers such as hydroxyethyl acrylate (HEA), acrylamide (AAM) and N-vinyl-2-pyrrolidone (NVP) were obtained from Tokyo Kasei Kogyo Co. and purified by distillation or recrystallization. On the other hand, hydrophobic monomers such as hexanediol monomethacrylate (HDMM), diethylene glycol dimethacrylate (DGDA) and methyl methacrylate (MMA) were obtained from Shin-Nakamura Chemical Co. and purified by distillation.

##### 2.2.2. Immobilization

The enzyme (0.8  $\mu\text{g}$ ) was dissolved in 0.5 ml of 0.1M acetate buffer solution (pH 4.5). Various comonomer compositions (0.5 ml) of HEMA-HEA, HEMA-AAm, HEMA-NVP, HEMA-HDMM, HEMA-DGDA and HEMA-MMA were added to the above enzyme solution. The monomer concentration was prepared to be 50% of the total mixture (1 ml in volume). The enzyme-comonomer solution was charged into an 8 mm diameter glass ampoule. The ampoule was sealed off under a vacuum of  $10^{-3}$  mm Hg and shaken enough to form a suspension (hydrophobic system) or a homogeneous solution (hydrophilic system). Then, the sealed ampoule was immersed in a Dewar vessel kept at  $-78^\circ\text{C}$  by dry ice-methanol and irradiated by  $\gamma$ -ray at  $-78^\circ\text{C}$  for 1 hr at a dose rate of  $5 \times 10^5$  R/hr, with a  $^{60}\text{Co}$  source.

After irradiation, the immobilized enzyme composite obtained was cut to be an 8 mm diameter and 2 mm thickness slices in the case of hydrophilic composition. The granular composite obtained from hydrophobic composition was used without cutting. In all cases, the composites were used for the enzyme reaction as in the polymerized state without drying treatment.

The other experiments were carried out under same conditions as described in CHAPTER 1.

## 2.3. Results and Discussion

### 2.3.1. Hydrophilicities of Polymer Used as Components

Hydrophilicities of polymer of comonomer component used in this work are shown in Table I. The hydrophilicity of the copolymer increases in copolymerization of HEMA with HEA, AAm and NVP, while it decreases by copolymerization with HDMM, DGDA and MMA. Among them, HEA, HDMM, DGDA and HEMA are glass-forming monomers. The other comonomers have no glass-forming property but they can be used with HEMA in certain composition range without destroying the glass-forming properties.

### 2.3.2. Microscopic Observation of Pore Structure in the Copolymer

The microphotographs of various polymer matrices are shown in Figure 19. The matrices of (a), (b), (c) and (d) in Figure show sponge-like pore structure, because the monomeric systems are still hydrophilic and hardly form suspension of monomer-in-water in those HEMA rich monomer compositions. The photographs (e) and (f) are the matrices in HEMA poor monomer

compositions. The HEMA-AAm system contains few pores, while the HEMA-DGDA system has many pore structures. This may very well be the reason for the difference in hydrophilicity of the copolymer, that is, swelling by water.

Table I Apparent water contents of each pure polymer

Sample	Monomer	water content (%)
1	HEMA; $\text{CH}_2=\text{C}(\text{CH}_3)\text{COO}(\text{CH}_2)_2\text{OH}$	26.0
2	NVP; $\text{CH}_2=\text{CH}-\text{N}(\text{C}_4\text{H}_6\text{O})$	93.7
3	AAm; $\text{CH}_2=\text{CHCONH}_2$	84.8
4	HEA; $\text{CH}_2=\text{CHCOO}(\text{CH}_2)_2\text{OH}$	45.9
5	HDMM; $\text{CH}_2=\text{C}(\text{CH}_3)\text{COO}(\text{CH}_2)_6\text{OH}$	13.5
6	DGDA; $\text{CH}_2=\text{C}(\text{CH}_3)\text{COO}(\text{CH}_2\text{CH}_2\text{O})_2\text{OC}(\text{CH}_3)=\text{CH}_2$	2.5
7	MMA; $\text{CH}_2=\text{C}(\text{CH}_3)\text{COOCH}_3$	2.1

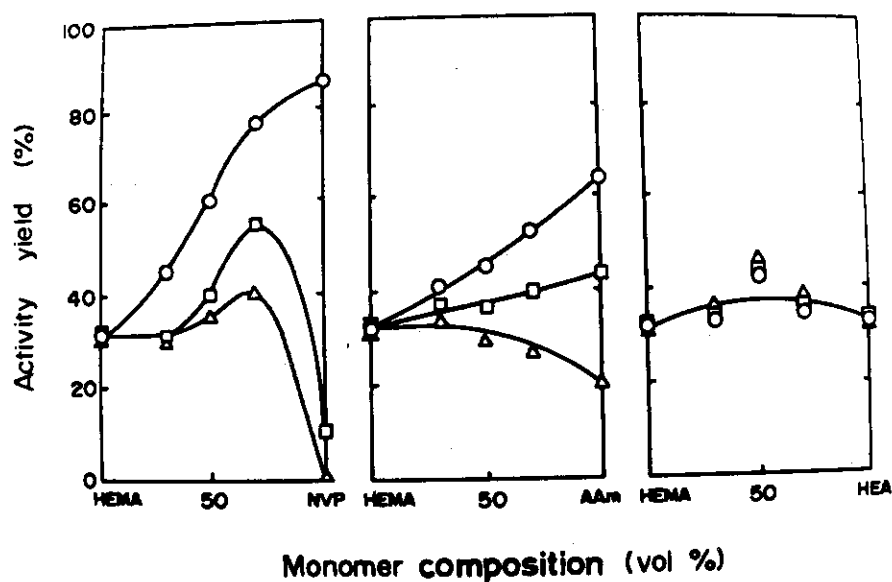


Figure 20 Effect of monomer composition on activity yield of immobilized glucoamylase in various HEMA-hydrophilic comonomer systems. Number of batch reaction (times): (O) 1, (□) 5, (Δ) 15



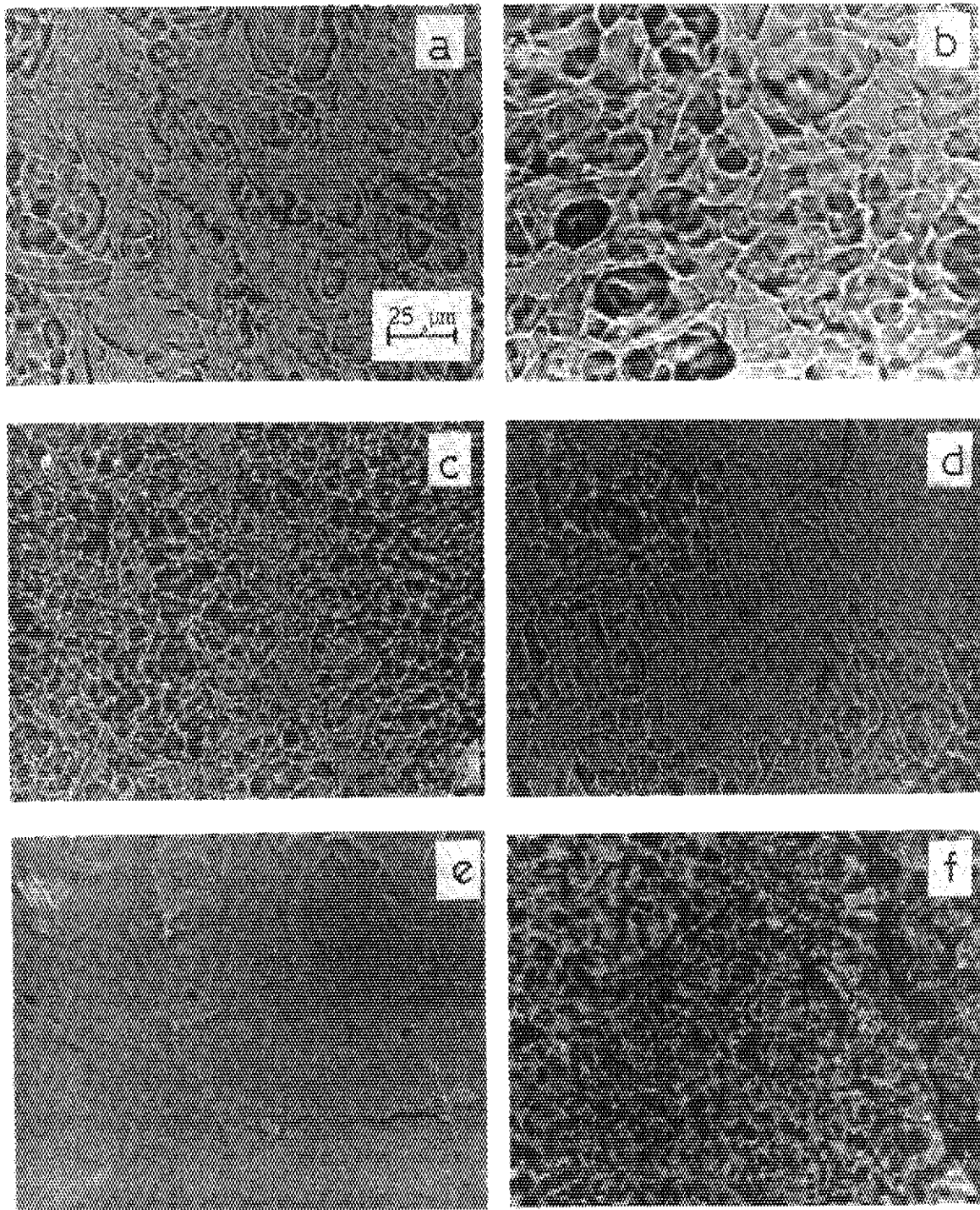


Figure 19 Optical microphotographs of pore structure in as-polymerized composite obtained by copolymerization of HEMA with other comonomers. Monomer concentration: 50% monomer-50% acetate buffer (pH 4.5). Monomer composition: (a) 70% HEMA-30% NVP, (b) 70% HEMA-30% AAm, (c) 70% HEMA-30% DGDA, (d) 70% HEMA-30% HDMM, (e) 30% HEMA-70% AAm, (f) 30% HEMA-70% DGDA

### 2.3.3. Effect of Copolymerization of HEMA with More Hydrophilic Comonomers on Porosity and Enzymatic Activity

The various factors relating to the properties of the porous structure were read and estimated by microscopic observation. In the HEMA-hydrophilic comonomer systems, the porosity generally showed the tendency to decrease with increasing content of strongly hydrophilic comonomer, that is, with increasing hydrophilic property and water content in copolymer. This result is perhaps attributed to expansion of the polymer matrix by water swelling so as to narrow the pore diameter and to join the individual pores. The pore factors (average pore diameter and pore number) and porosity scarcely decreased in the copolymer with HEA. This may be due to the relatively similar hydrophilic properties of HEMA and HEA.

The changes of the enzymatic activity with repeated use for the enzyme reaction are shown as a function of monomer composition in Figure 20. According to the result, the activity decrease with repeated use become remarkable with increasing the composition of hydrophilic comonomer. That is, the initial activity yield decreased quickly with repeated use in those strongly hydrophilic systems. On the other hand, in the relatively less hydrophilic system such as HEMA-HEA system, no decrease of the initial activity was observed at all in the composition range as long as the monomer concentration to water was at a relatively high range such as 50% in the studied systems. The difference in activity between the first reaction and the later reactions indicates the decrease of activity with repeated use. This difference remarkably increased in strongly hydrophilic composition. It was ascertained by analysis of the enzyme content in the solution after the reaction that the decrease of the initial activity with repeated use could be attributed to leakage of the enzyme being isolated freely in the pore structure. In the case of strongly hydrophilic matrices, it is probable that enzyme leakage is promoted by strong swelling of the polymer not only from the pore space but also from near the surface of the matrix. This is probably the reason for the results described above.

The relations between the enzymatic activity and the pore factors in HEMA-hydrophilic comonomer systems were shown in Figure 21. The enzyme leakage can be evaluated by the difference in activity between the first and 15th times of repeated use. This difference increased with decreasing pore diameter, pore number and porosity in the strongly hydrophilic systems. On the other hand, in relatively less hydrophilic systems such as the pure

HEMA system and HEMA-HEA system, enzyme leakage decreased with decreasing the values of those factors. These facts suggest that in strongly hydrophilic systems, enzyme leakage occurs not only from the pore but also from inside the matrix (perhaps from near the surface area of the porous matrix) by swelling of the polymer. In contrast, the leakage of the enzyme takes place mainly by diffusion out the freely isolated enzyme in pore space in less hydrophilic matrix systems. That is probably the reason for the different results in dependency of activity retention with repeated use on the pore factors or porosity.

#### 2.3.4. Effect of Copolymerization of HEMA with More Hydrophobic Comonomers on Porosity and Enzymatic Activity

The relation between the pore factors and the monomer composition in HEMA-hydrophobic comonomer systems is shown in Figures 22 and 23. The complicated monomer composition dependency of pore number in Figure 22

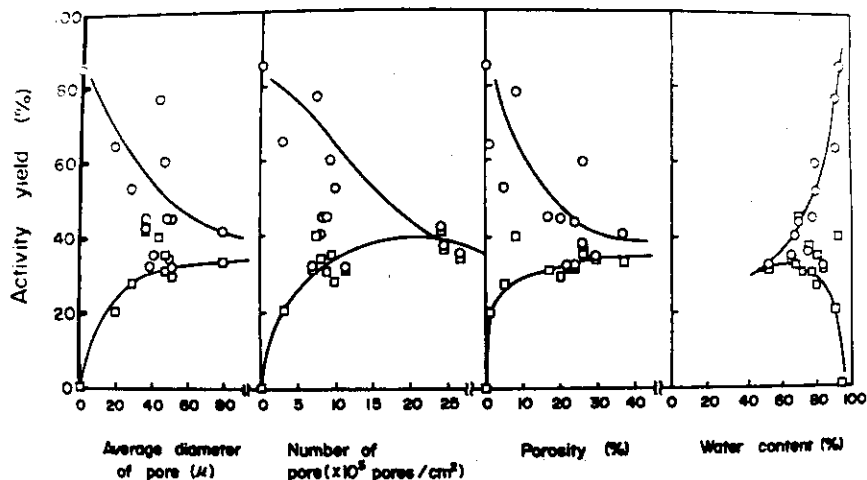


Figure 21 Effect of pore factors on activity yield of immobilized glucoamylase plotted by using the data given in Figures 19 and 20 in various HEMA-hydrophilic comonomer systems. Number of batch reaction (times): (O) 1, (□) 15

can be reduced to phase changes of the monomeric and polymeric systems by monomer composition. That is, the monomeric phase of these systems gradually changes to suspension of monomer-in-water or water-in-monomer from the homogeneous solution with increasing hydrophobic monomer

compositions. Therefore, the formed polymer changes from a porous sponge-like polymer to a microsphere particle in corresponding to the change of monomeric phase at hydrophobic compositions. However, the formed hydrophobic as-polymerized matrix has some apparent water content as

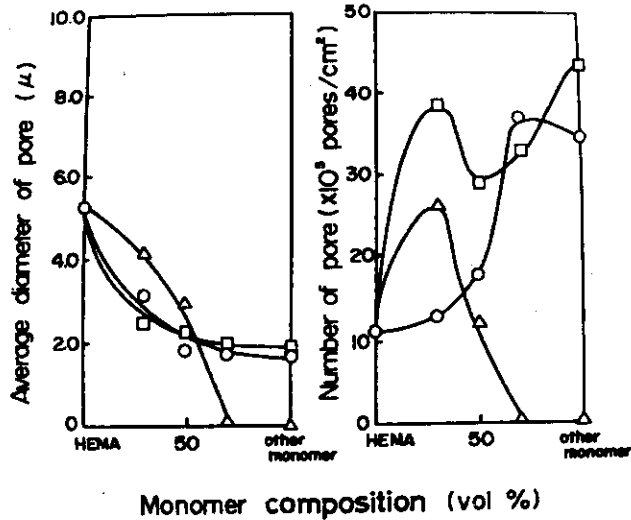


Figure 22 Effect of monomer composition on pore factors such as average pore diameter and pore number in various HEMA-hydrophobic comonomer systems. Monomer concentration: 50% monomer-50% acetate buffer solution, pH 4.5. Monomer system: (○) HEMA-HMM, (□) HEMA-DGDA, (△) HEMA-MMA

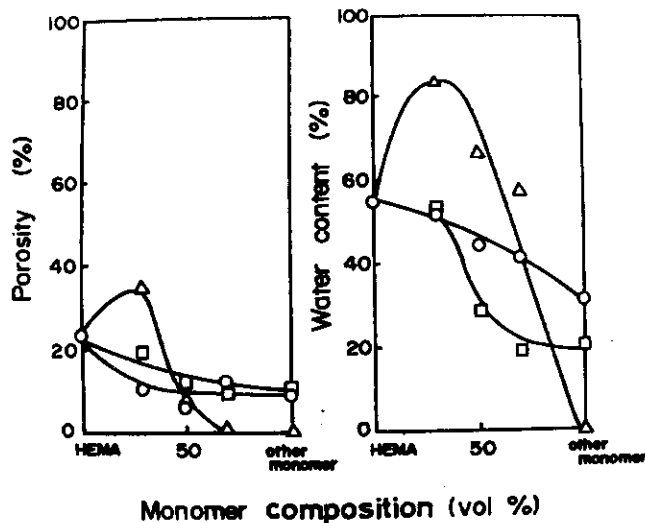


Figure 23 Effect of monomer composition on porosity and water content in various HEMA-hydrophobic comonomer systems. Experimental conditions were the same as those in Figure 22

shown in Figure 23. Because, in this monomer concentration of 50% water, the monomeric system does not form a complete monomer-in-water suspension, but contain some water-in-monomer system. Then, the formed polymer is not a completely independent microsphere, but has some continuously jointed matrix structure including water, though the microsphere particle is easily obtained by drying this polymer. The perfect microsphere polymer in its polymerized state is obtained at a lower monomer concentration, at which the monomeric systems form perfect monomer-in-water suspensions. Generally, the copolymer system with hydrophobic comonomers showed the tendency to decrease for the pore diameter and porosity as the content of the hydrophobic comonomer was increased. The reason might be attributed to the change of the monomeric phase from solution to suspension and also polymeric phase from sponge-like gel to sphere particle.

In HEMA-MMA system, the polymerizability decreased with increasing the MMA content and was lost at a certain MMA composition owing to the crystallization of the MMA. The change of enzymatic activity with repeated use at various monomer composition is shown in Figure 24. The

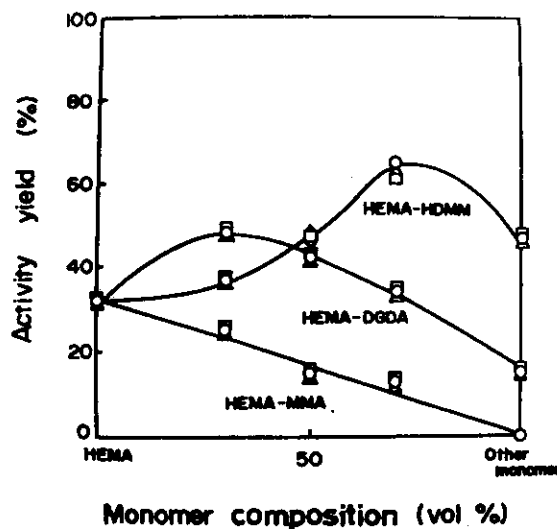


Figure 24 Effect of monomer composition on activity yield of immobilized glucoamylase in various HEMA-hydrophobic comonomer systems. Number of batch reaction (times): (O) 1, (□) 5, (Δ) 15

activity decrease due to enzyme leakage with repeated use was hardly observed in each system at all monomer compositions, because freely isolated enzymes in the pore scarcely exist in this monomer concentration (50%) even in the pure HEMA system, and much more in hydrophobic copolymer system

having less property than pure HEMA system.

The activity yield of the hydrophobic copolymer systems was larger than that of the hydrophilic systems in general and showed a maximum at a certain hydrophobic monomer composition in HEMA-HDMM and HEMA-DGDA systems as shown in Figure 24. These results might be due to some hydrophobic affinity between the hydrophobic bond in enzymes and that in monomer or polymer, because the contribution of hydrophobic bonding to the activity of the enzyme is known, though the mechanism is not clear. The considerable activity of hydrophobic systems supports the conclusion that the enzyme is trapped on the surface area of the matrix pore or of the microsphere and the reaction is carried out on these surface parts without much inner diffusion of substrate into the matrix as in hydrogel type cross-linked polymers in the hitherto conventional entrapping method.

### 2.3.5. Model Scheme for Immobilization Mechanism

The proposed model schemes for immobilization mechanism are shown in Figures 25 and 26. The Figure 25 is the model scheme for low temperature immobilization by hydrophilic glass-forming monomer and Figure 26 is the model scheme for low temperature immobilization by hydrophobic glass-forming monomer. In the former, some part of the enzyme remains in freely isolated state in pores or pore-matrix interface to leak out easily in repeated use, while considerable part of the enzyme firmly trapped on the surface of matrix and some part of enzyme is buried inside matrix without contributing the activity. In the later, some part of the enzyme is freely isolated to be lost easily out of polymer spheres or continuous matrix, and other considerable part of the enzyme is trapped on the surface of microspheres of matrix. The free enzyme outside the polymer is lost with water in polymer isolation step, while the remaining enzyme bound on the polymer surface does not leak.

On the other hand, fluorescein isothiocyanate (FITC) as a phosphor was conjugated to trapped enzyme in porous sponge-like or rigid spherical matrix, made by low temperature polymerization method. After the removal of free FITC, the conjugated enzyme was observed with a fluorescence microscope (Nippon Kogaku Co., Model FT)<sup>61</sup>. According to this result, the fluorescence was observed only on the surface of the particle in the case of particle matrix (rigid spherical matrix), while in the case of porous sponge-like matrix the fluorescence was observed mainly on the interface

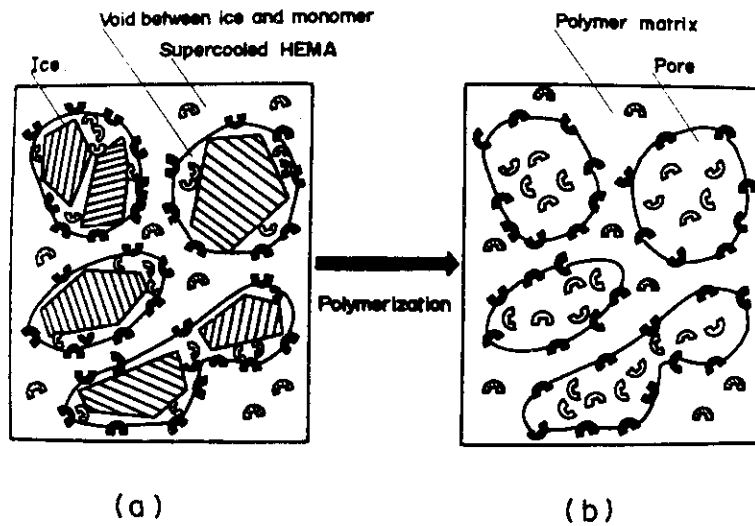


Figure 25 Model scheme for immobilization by hydrophilic glass-forming monomer system at low temperatures. Model scheme: (a) for cooled monomer system, (b) for polymerized system, (U) entrapped enzyme, (⊖) entrapped enzyme inside the matrix, (⊕) freely isolated enzyme

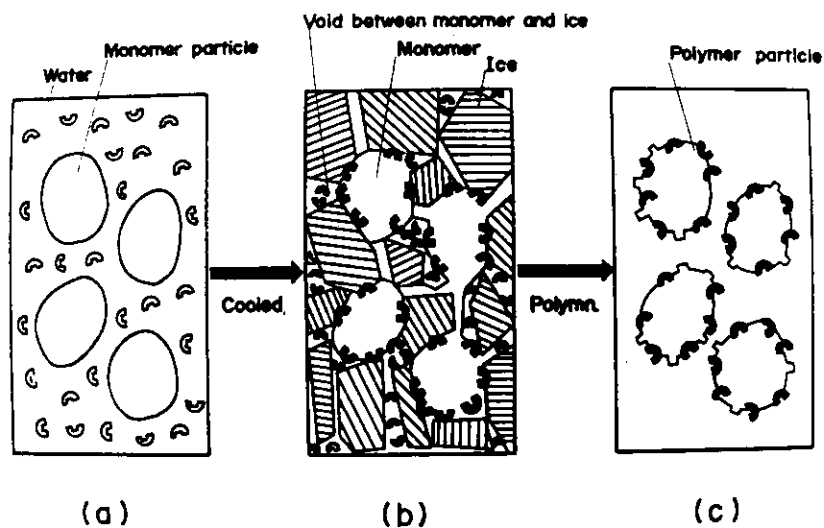


Figure 26 Model scheme for immobilization by hydrophobic glass-forming monomer system at low temperatures. Model scheme: (a) for non cooled monomer system, (b) for cooled monomer system, (c) for polymerized system

between polymer membrane and porous structure and partly on the polymer membrane. Accordingly, it was suggested that the model scheme in Figures 25 and 26 was reasonable from a fluorescent point of view.

Consequently, it is characteristic and advantage of the present method that considerable part of the enzyme is trapped on surface of the polymer matrix having porous sponge-like or microsphere structure formed by suspension structure of the monomeric phase, which consists of ice and supercooled monomer at low temperatures. Glass-forming property of the monomer is necessary not only to obtain high polymerizability but also to give effective pore or sphere structure at low temperatures.

#### 2.4. Summary

Immobilization of enzymes by radiation-induced polymerization was studied at low temperatures using various comonomer systems consisting of hydrophilic and hydrophobic comonomers. The porosity of the matrices obtained by copolymerization with more hydrophilic and more hydrophobic comonomers was lower in comparison with the matrix from hydrophilic monomers. The initial activity of immobilized enzyme in the more hydrophilic and more hydrophobic matrices decreased rapidly with repeated use owing to the enzyme leakage from the matrix. On the other hand, the enzyme leakage was completely retarded and no activity changed with repeated use in the more hydrophobic matrices. Moreover, the activity yield showed a maximum at a certain monomer composition in copolymerization with hydrophobic and hydrophilic comonomers. Finally, it was found that the maximum activity yield of the hydrophobic copolymer matrix was larger than that of the hydrophilic copolymer matrix.



## CHAPTER 3

## IMMOBILIZATION OF ENZYMES BY HYDROPHOBIC GLASS-FORMING MONOMERS AT LOW TEMPERATURES

## 3-1. IMMOBILIZATION OF SOME ENZYMES IN PARTICLE FORM

## 3.1.1. Introduction

The activity yield of enzymes immobilized by this entrapping method were markedly affected by the two factors such as porous structure and hydrophilicity of the polymerized composite as described in CHAPTERS 1 and 2. It was found that the enzyme was considerably trapped on the surface area of porous structure<sup>2,62</sup>.

This characteristic structure was caused by suspension structure of monomeric system of ice in supercooled monomer at low temperatures. On the other hand, a monomeric suspension of hydrophobic monomer and enzyme buffer solution would make a water (ice) suspension structure at low temperatures to form a polymer particle. In this CHAPTER, immobilization by hydrophobic monomer (polymer) as a carrier investigated, expecting more predominant trapping of enzyme on the carrier surface.

## 3.1.2. Experimental

## 3.1.2.1. Materials

Microbial cells having glucose isomerase activity (Streptomyces phaeochromogenes cells, 2000 units/g, assay is based on that of Takasaki<sup>66</sup>) were obtained from Nagase Sangyo Co. and 0.05M phosphate buffer solution (pH 7.2) was used for immobilization. Urokinase (UK) (1200 I.U./vial, assay is based on that of Nishizaki<sup>63</sup>) from urin was obtained as a product of Midori Juji Co. and 0.1M phosphate buffer solution (pH 7.4) was used.

Other enzymes such as glucoamylase from Rhizopus niveus and glucose oxidase from Aspergillus niger were the same as used in CHAPTER 1.

All hydrophobic glass-forming monomers such as diethylene glycol diacrylate (ADGDA), neopentyl glycol dimethacrylate (NPG), tetramethylene glycol diacrylate (ATGDA), hexanediol monomethacrylate (HDMM), trimethylolpropane triacrylate (ATMPT) and hexanediol monoacrylate (HDMA)

used in this CHAPTER were obtained from Shin-Nakamura Chemical Co. and purified through ion exchange resin to remove impurities.

### 3.1.2.2. Immobilization and Activity Assay

All irradiation and immobilization experiments were carried out in the same methods as in CHAPTER 1, using a mixture of hydrophobic monomer and enzyme buffer solution. The only difference from the previous study was that the starting mixture to be cooled was a suspension of monomer and buffer instead of a homogeneous solution. Enzyme reaction and activity assay of immobilized enzymes were carried out using the same methods as in CHAPTER 1, except for glucose isomerase and UK. For the glucose isomerase assay, a 1% buffer solution of glucose was added to the immobilized glucose isomerase cell. After reaction at 65°C for 1 hr, the reacted solution was analyzed by the cystein-carbazol method<sup>64</sup> detecting the absorption at 500 nm. For UK assay, a 0.638% buffer solution of acetylglycyl-L-lysine methyl ester acetate as a substrate was added to immobilized UK, reacted at 37°C, and assayed according to Johnson's method<sup>65</sup>.

### 3.1.2.3. Other Experiments

The average particle diameter of the polymerized composite was estimated by microscopic observation using an Olympus, Model FHF microscope with Olympus, Model PM-10-M equipment. The other experiments were carried out under the same conditions as described in CHAPTER 1.

## 3.1.3. Results and Discussion

### 3.1.3.1. Effect of Repeated Use for Enzyme Reaction on Activity of Enzymes Immobilized by Hydrophobic Polymers

A change in the enzymatic activity of immobilized glucose isomerase (microbial cell) and some other enzymes obtained by polymerization of various hydrophobic glass-forming monomers was plotted in Figure 71 as a function of repeated use for the enzyme reaction.

It is noticed that no activity decrease was observed with repeated use even at low monomer concentrations, i.e., 10% in enzyme immobilized by stark hydrophobic monomers such as ADGDA and GMA. A slight decrease in

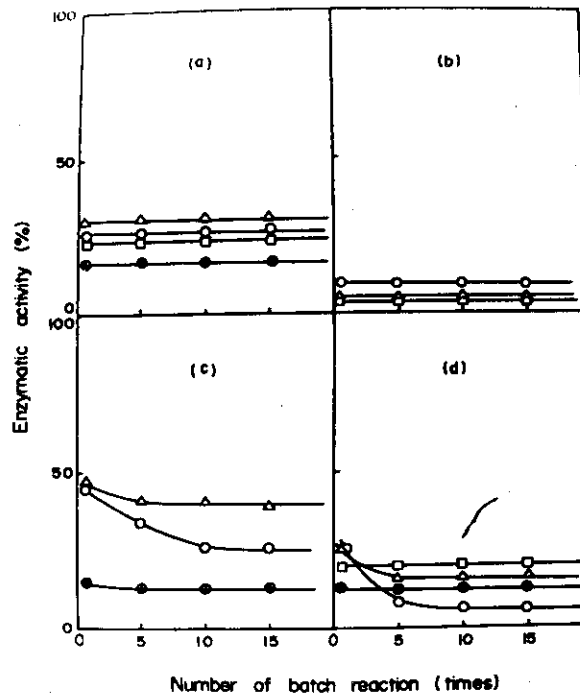


Figure 27 Effect of repeated use of enzyme reaction on enzymatic activity of enzymes immobilized by hydrophobic monomers. Enzyme-monomer system: (a) glucoamylase-ADGDA, (b) glucose isomerase-GMA, (c) glucose oxidase-ATGDA, (d) glucoamylase-HDMA. Monomer concentration in monomer-buffer solution: (O) 10%, ( $\Delta$ ) 30%, ( $\square$ ) 50%, ( $\oplus$ ) 70%. Enzyme content (added quantity for immobilization to 1 ml monomer-buffer solution): 600  $\mu$ g glucoamylase, 50 mg glucose isomerase, 100  $\mu$ g glucose oxidase. Irradiation:  $-78^{\circ}\text{C}$ , 0.5 MR

activity was observed with repeated use at a low monomer concentrations, immobilized by relatively hydrophobic monomers such as ATGDA and HDMA. In general, the activity decrease, which was probably due to enzyme leakage from polymer, was much less in enzymes immobilized by hydrophobic monomers than those by hydrophilic monomers. However, activity yield itself in the hydrophobic carrier system was not as high as in hydrophilic systems. The reason for these discrepancies was discussed in the former section (CHAPTER 2) in relation to the model immobilization scheme.

### 3.1.3.2. Effect of Monomer Concentration on Activity Yield of Enzyme Immobilized by Hydrophobic Monomers

Activity yield of various immobilized glucose isomerase (microbial cell) and some other enzymes by polymerization of various hydrophobic monomers is shown in Figure 28 as a function of monomer concentration.

According to these results, the activity yield had a maximum at a certain monomer concentration in every system. This follows the same relationship as was observed in hydrophilic carrier systems. However, the reason for the maximum activity yield might be quite different between the hydrophobic and hydrophilic carrier systems. As described in CHAPTER 1, an optimum in monomer concentration dependency on activity yield occurred as a result of the optimum balance between the least leakage of isolated enzyme in pore and the least inactive occlusion of enzyme inside polymer

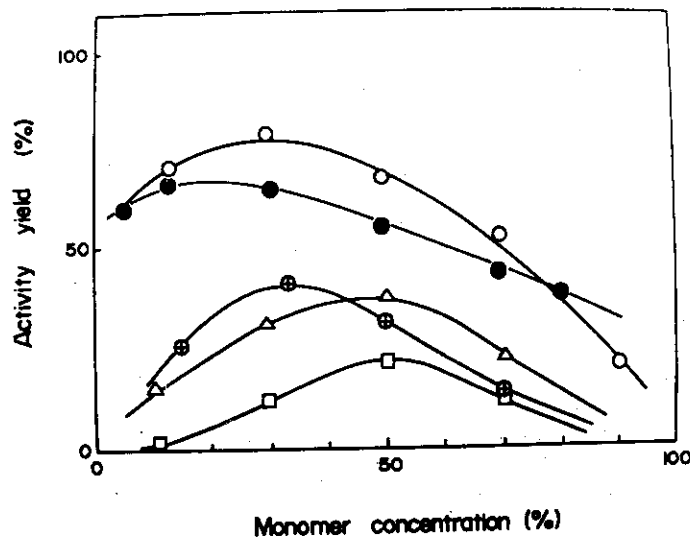


Figure 28 Effect of monomer concentration on activity yield of enzymes immobilized by hydrophobic monomers. (○) urokinase-ATGDA, (△) glucoamylase-HDM, (+) glucose oxidase-ATGDA, (□) glucoamylase-HDMA, (●) glucose isomerase-ATGDA. Irradiation:  $-78^{\circ}\text{C}$ , 0.5 MR. Repeated enzyme reaction: 15 times. Enzyme content (see, Figure 27): 100 IU urokinase, 600  $\mu\text{g}$  glucoamylase, 100  $\mu\text{g}$  glucose oxidase, 50 mg glucose isomerase

matrix in the hydrophilic carrier system. On the other hand, the hydrophobic polymerized composite had little porous structure, having neither isolated enzyme in the pore nor occluded enzyme in the matrix. Usually the hydrophobic polymerized composite was microspheric or fine particulate in the monomer concentration range lower than about 60%, as shown in Figure 29.

That is, in this monomer concentration region, the monomeric systems is a monomer-in-water type suspension. With crystallization of ice on cooling, part of the enzyme transfers to the surface of the supercooled monomer particle from the water phase, but other part of the enzyme remains in the ice phase, which is removed with the ice when isolating the

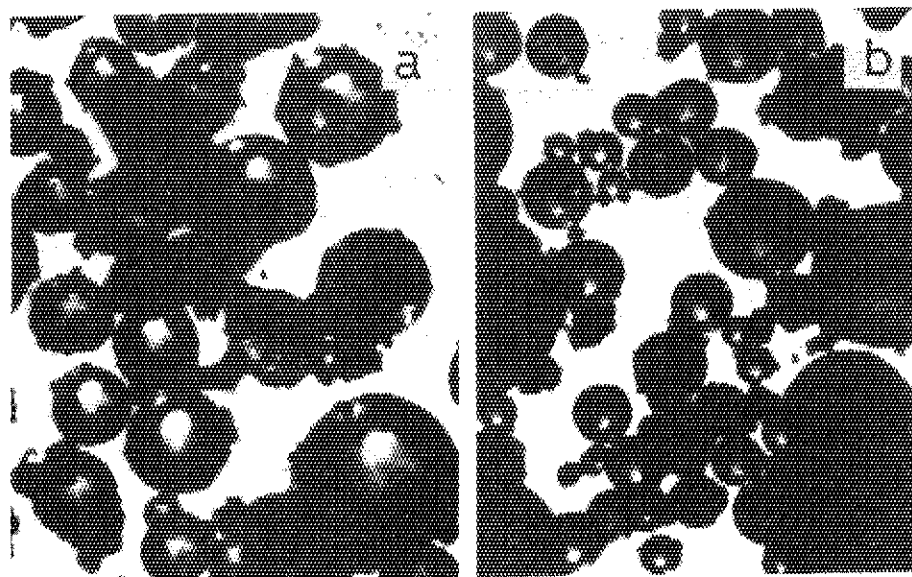


Figure 29 Microphotographs of polymerized composite by hydrophobic monomers. (a) glucose isomerase-30% ATMPT, (b) glucose isomerase-50% NPG. Polymerization:  $-78^{\circ}\text{C}$ , 0.5 MR. Multiplication: 80 times

polymerized composite by filtration. This is probably the reason why activity yield decreased with a decreasing monomer concentration (with increasing water concentration). On the contrary, with an increasing monomer concentration, the monomeric phase changes to a water-in-monomer type suspension and the polymerized composite becomes a hard sponge-like composite having independent cells separated by the water molecules. In this case, enzyme might be trapped on the surface of these inner cells, independent (discontinuousness) of an increase in the monomer concentration, making substrate diffusion difficult. This is probably the reason why activity yield again decreases at a monomer concentration. Consequently, it is reasonable that an optimum monomer concentration also exists in hydrophobic carrier systems.

### 3.1.3.3. Relationship Between Polymerization Monomer Concentration, Polymerized Composite Particle Size, and Activity Yield of Immobilized Glucose Isomerase

It is natural to suppose that the particle size of polymerized composite might affect the immobilized enzyme activity. The relation between monomer concentration in polymerization and the average diameter of polymerized particle is shown in Figure 30 for immobilized glucose isomerase.

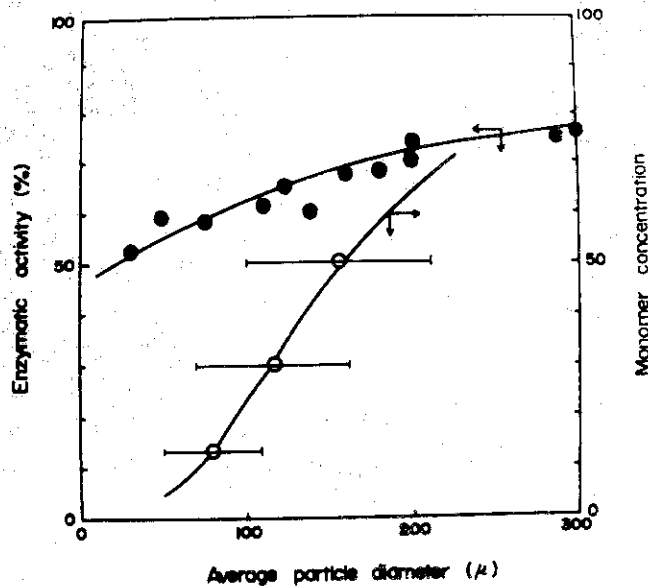


Figure 30 Relationship between polymerization monomer concentration, polymerized composite particle diameter, and activity yield of immobilized glucose isomerase. Monomer concentration: 30% ATMPT. Irradiation:  $-78^{\circ}\text{C}$ , 1 MR. Repeated enzyme reaction: 15 times

The average particle diameter increased with an increasing monomer concentration. Also activity yield was shown against average particle diameter in Figure 30. It increased with an increasing particle size in the range below 300  $\mu\text{m}$  in diameter. The reason might be that part of the total surface area of the monomer particle that catches and disperses the enzyme, increases with increasing particle size because particle number does not change as much by an increase in monomer concentration.

#### 3.1.4. Summary

Enzyme immobilization was studied by means of radiation-induced polymerization of hydrophobic glass-forming monomers at low temperatures. The polymerized composite was generally obtained in microspheric form. Enzymatic activity showed little decrease with repeated uses in these systems. The particle size of the microsphere increased with increasing monomer concentration, and activity yield had an optimum monomer concentration.

## 3-2. IMMOBILIZATION OF CELLULASE IN THE SWOLLEN POLYMER MICROSPHERE

### 3.2.1. Introduction

Entrapping of enzyme on polymer surface especially on a surface of hydrophobic particle is one of the characteristic feature of this method. Therefore, the obtained material can be used advantageously for the surface reaction with the substrate of high molecular weight or water insoluble property. The preparation of hydrophobic microsphere entrapping enzymes or microbial cells was studied already by radiation-induced suspension polymerization of glass-forming monomers<sup>2,59,67</sup>. However, effective surface area of polymer sphere for enzyme reaction is very important for activity of the material.

In this CHAPTER, an improved immobilization method for the increased surface area of hydrophobic microsphere containing cellulase was proposed using radiation-induced polymerization of glycidyl methacrylate as a glass-forming monomer in the presence of vinyl polymer such as poly(styrene) at low temperatures.

### 3.2.2. Experimental

#### 3.2.2.1. Materials

Cellulase from Trichoderma viride used as an enzyme was the same as described in CHAPTER 1. Glass-forming monomers such as glycidyl methacrylate (GMA), trimethylolpropane trimethacrylate (TMPT) and diethylene glycol dimethacrylate (DGDA) (see, in CHAPTER 3-1) were obtained from Shin-Nakamura Chemical Co. and purified by the same methods in CHAPTER 3-1. Poly(styrene) (PSt) obtained from Kishida Chemical Co. was used as a polymer. Its degree of polymerization is about 1700. Precipitation media such as methanol, ethanol, n-propanol, acetone, toluene and tetrahydrofuran (THF) obtained from Tokyo Kasei Kogyo Co. were used without further purification. Swelling solvents such as acetone, benzene and toluene from Tokyo Kasei Kogyo Co. were used without purification. Carboxymethyl cellulose (sodium salt) (CMC), n=500, used as a substrate was the same as described in CHAPTER 1.

#### 3.2.2.2. Preparation of Radiation Polymerized Particles

The preparation of polymerized particles was carried out as follows. PSt was completely dissolved in GMA monomer at 40-80°C. Five mg of cellulase and 1 ml of the PSt-GMA mixture were mixed and charged in a glass ampoule. After shaking, the enzyme-monomer suspension was dropped in cold precipitation medium as described previously<sup>68</sup>, with a pipette (1 mm fine tip). Then, the monomeric particles obtained were irradiated at -78°C for 2 hrs at a dose rate of  $5 \times 10^5$  R/hr, with  $\gamma$ -ray from a <sup>60</sup>Co source, in the presence of the precipitation media. After irradiation, the polymerized particles were dried and then treated with various swelling solvents at room temperature.

Mean diameter of dried particle ( $D_{av}$ ) was measured with optical microscope, Model SMZ-6, Nippon Kogaku Co. The cellulase content per particle ( $W_e$ ) was estimated from the initial enzyme concentration and number of particles ( $N_p$ ) which was read by microscopic observation. Degree of swelling ( $S_w$ ) was determined according to the following Equation;

$$S_w = \frac{W_s}{W_p} \quad (6)$$

where  $W_s$  and  $W_p$  are the weight of solvent absorbed in the polymer particle and that of dried polymer particle.

### 3.2.2.3. Assay of Cellulase Activity

The swollen particles were washed for 48 hrs at 25-35°C with 1000 ml of ethanol and then with 1000 ml of 0.1M acetate buffer solution (pH 4.5) to remove the solvent. The immobilized enzyme was shaken with 10 ml of 0.5% CMC solution (pH 4.5) at 40°C for 60 min. Activity assay was carried out under the same conditions as described in CHAPTER 1.

### 3.2.2.4. Measurement of Particle Structure

The particle structure was observed by optical microscope, Model Nikon F, Nippon Kogaku Co. and scanning electron microscope, Model JSM-03, Japan Electron Optics Laboratory Co.

### 3.2.3. Results and Discussion



### 3.2.3.1. Trapping of Cellulase by Polymerization of GMA in the Presence of PSt

The mixture of PSt, GMA and cellulase was added to various media below  $-24^{\circ}\text{C}$  to make particle through a nozzle and the results are summarized in Table II. The use of a glass-forming monomer such as GMA is advantageous, since the coagulation of monomeric micro-particles can be prevented owing to the high viscosity of supercooled solution. The addition of polymer such as PSt insoluble to the precipitation media is necessary to cover the monomer particle with polymer skin to keep it from being dissolved in the medium. Almost perfect spherical particles were obtained when alcohols such as methanol, ethanol and propanol were used as the shaping media, though no particle formed without the addition of PSt. However, acetone, toluene and tetrahydrofuran were not suitable as shaping media even at  $-78^{\circ}\text{C}$ ,

Table II Preparation of spherical-form particles in radiation polymerization at low temperatures

Sample	Monomer system	Preparation condition		Property of polymerized-particle		
		Medium	Temperature ( $^{\circ}\text{C}$ )	$D_{av}$ (nm)	$N_p$ (particles)	$W_e$ ( $\mu\text{g}/\text{particle}$ )
1		Methanol	-78	3.2	38	132
2		Ethanol	-78	3.0	42	119
3		n-Propanol	-78	3.4	35	143
4	10% PSt-90% GMA	Acetone	-78	Nonparticle (thin membrane-like composite)		
5		Toluene	-78	Nonparticle (curdy composite)		
6		THF	-78	Nonparticle (ring-like composite)		
7		Methanol	-24	Nonparticle (block composite)		
8	10% PSt-90% DGEA	Ethanol	-78	3.1	38	132
9	10% PSt-90% TMPT	Ethanol	-78	3.0	44	114

no particles could form owing to the considerable solubility of PSt skin in these media. The optical photograph of polymerized spherical particles (sample 2 in Table II) is shown in Figure 33 (a). However, it is important to further increase the surface area of these particles for more efficient contact of the substrate with enzyme. For this purpose, the polymerized particle was swollen by acetone, toluene and benzene. The swollen particles changed from a rigid matrix to an expanded elastic marshmallow-like matrix in shaping and softness.

The absorbed swelling agents were gradually washed away with water from polymer matrix while using the particles for an enzyme reaction with

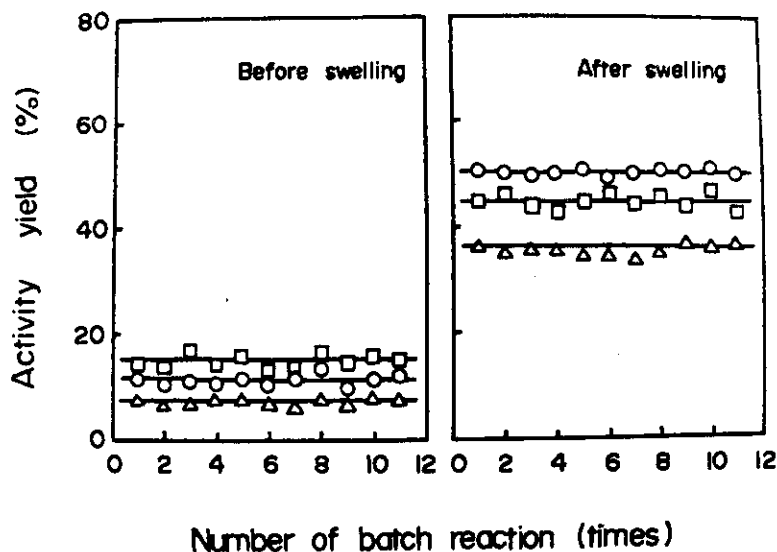


Figure 31 Relationship between the activity yield of cellulase in swollen particles and the repeated use. The polymerized particles (see, samples 1-3 in Table II) were treated at room temperature with various swelling solvents. The  $S_w$  values were prepared to be about 2.5 in all cases. Swelling solvent: (O) acetone, sample 1, ( $\Delta$ ) toluene, sample 2, ( $\square$ ) benzene, sample 3

an aqueous suspension of substrate. As the result, the particles having large surface areas due to wrinkles and micropores were formed. However, in the case of polyfunctional monomers such as DGDA and TMPT, the polymer particles were hardly swollen by any swelling agent owing to highly cross-linked structure of the polymers.

### 3.2.3.2. Activity Yield of Cellulase in the Hydrophobic Particles

The activity yield of cellulase in the hydrophobic particles are plotted against the number of batch enzyme reaction (repeated use) in Figure 31

It is remarkable that the activity yield did not change with repeated use as in a previous work<sup>56</sup>. However, the activity yield in swollen particles was about 4-6 times larger than that of rigid particles before the swelling treatment. The activity yield increases with increase in the degree of swelling for all cases in Figure 32. Acetone was the most effective solvent having the greatest capacity of all the solvents to induce swelling. The saturated  $S_w$  values in acetone, benzene and toluene were 5.0, 3.6, and 2.7, respectively. This increase in activity through swelling may be attributed to the increase in the surface area owing to the wrinkles and porous structures in the matrix. That is, certain active

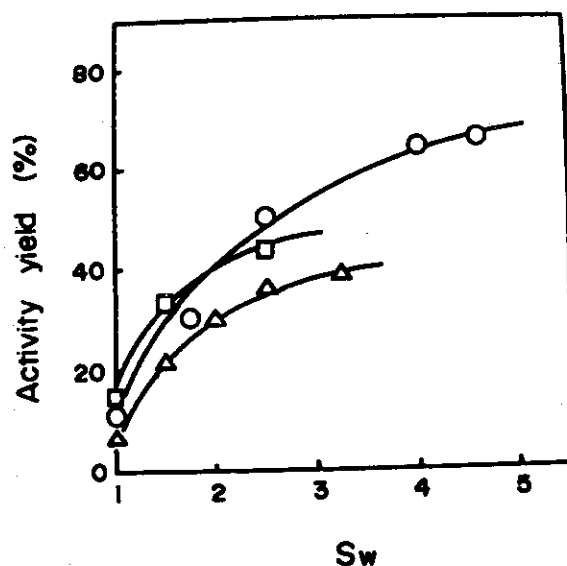


Figure 32 Relationship between the activity yield of cellulase in swollen particles and the degree of swelling. Swelling solvent: (O) acetone, (Δ) toluene, (□) benzene

sites of enzyme occluded in the matrix are perhaps exposed to enhance activity by surface area increase. At the same time, the substrate might diffuse into the inner surface of the matrix through the wrinkles and porous structures more easily and frequently to make contact with the enzyme in consequence of this increase. Since the substrate can hardly diffuse inside hydrophobic matrix, the enzymatic reaction has to be carried out on the matrix surface. Moreover, the swollen particles can be used repeatedly with no activity decrease due to enzyme leakage. Consequently, the swelling technique is the most advantageous method for increasing the activity of hydrophobic immobilized particles without lessening the other benefits of the hydrophobic carrier as well as the stable activity retention in repeated use. However, the activity yield for particles of 10% PSt-90% DGDA and 10% PSt-90% TMPT systems did not increase after treatment by solvent. The activity yield was only 5-10% of the swollen particles.

### 3.2.3.3. Observation of Particle Structure

The structure of a hydrophobic particle was observed by microscopic photograph. After swelling ( $S_w = 2.5$ ), the particle size became about 2 times that of the original particle (before swelling) as shown in Figure 33

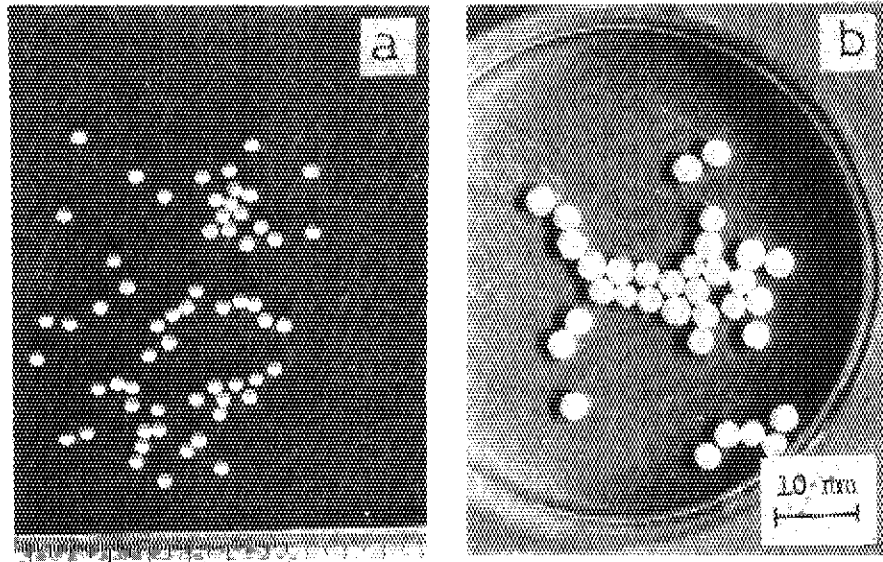


Figure 33 Optical microphotographs of swollen particles. The rigid particles were treated at room temperature for 16 hrs with acetone as a swelling solvent ( $S_w=2.5$ ). Treatment: (a) before (rigid matrix), (b) after (expanded elastic matrix)

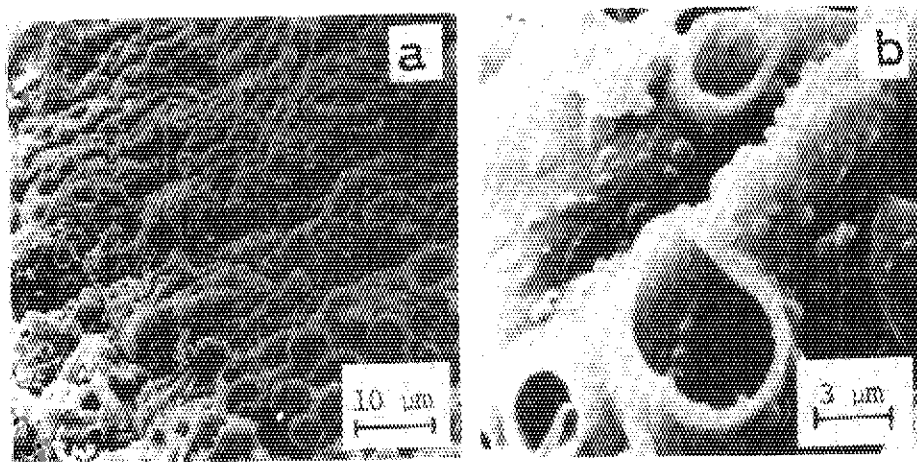


Figure 34 Scanning electron microphotographs of swollen particles. After swelling (see, b in Figure 33), the expanded elastic particles were washed with excess ethanol and then with excess water. After drying, the particle structure was observed by a scanning electron microscope. (a) x 1000, (b) x 10000

(optical microphotograph) and Figure 34 (electron microphotograph).

The surface of expanded elastic particles swollen with acetone is apparently contracted by contact with water to form many wrinkles and micropore structures of 1-3  $\mu\text{m}$  in diameter. It is obvious that the observed wrinkles and micropores as well as volume expansion greatly increases the surface area of the matrix. These results support the explanation described above owing to the activity increase in the present method.

#### 3.2.3.4. Summary

The immobilization of cellulase in hydrophobic particles was carried out by the radiation polymerization of GMA as a glass-forming monomer in the presence of PSt at low temperatures. When the monomer system containing cellulase was poured into cold alcohol, spheres were formed. Then, the rigid microspheres polymerized by radiation were swollen with acetone, benzene or toluene into soft elastic matrices. The activity yield of immobilized cellulase in swollen matrix increased to about 4-6 times than that of the rigid particles. The microscopic observation proved that the swelling treatment formed many wrinkles on the expanded particle surface, thus increasing the surface area greatly.

## CHAPTER 4

### CONTINUOUS ENZYME REACTION BY IMMOBILIZED ENZYMES

#### 4.1. Introduction

As described in CHAPTERS 1-3, a biologically active substance such as enzymes was immobilized on vinyl polymer of various forms using radiation-induced polymerization method, at low temperatures. Especially, enzymes were immobilized stably and firmly to endure the repeated reactions<sup>69-74</sup>.

The purpose of the present CHAPTER is to testify the function of immobilized enzymes by this method for the continuous enzyme reaction processes. The continuous enzyme reaction was investigated using porous immobilized composite containing Aspergillus niger glucoamylase, with substrates having different molecular weights such as maltose and starch.

#### 4.2. Experimental

##### 4.2.1. Materials

2-Hydroxyethyl methacrylate (HEMA) as a carrier, Aspergillus niger glucoamylase as an enzyme, 10% maltose solution (pH 4.5) or 10% soluble starch solution (pH 4.5) as substrates and drierite as an adsorbent were the same as described in CHAPTER 1.

##### 4.2.2. Preparation of Immobilized Glucoamylase

Glucoamylase was dissolved in 0.1M acetate buffer solution (pH 4.5). This solution was mixed with HEMA to total volume of 20 ml at a determined concentration. In the case of immobilized glucoamylase in the presence of drierite, drierite was added in the same method as described previously<sup>46</sup>.

The mixture was charged in an 20 mm diameter glass ampoule and sealed off under a vacuum of  $10^{-3}$  mmHg. The sample was irradiated for 1 hr at a dose rate of  $5 \times 10^5$  R/hr, at  $-78^\circ\text{C}$ . The polymerized composite was cut to  $2 \times 2 \times 2$  mm<sup>3</sup> pieces, filled to the small column and used continuous enzyme reaction.

##### 4.2.3. Continuous Enzyme Reaction

Continuous enzyme reaction was carried out at 45°C by the apparatus as shown in Figure 35. Other experiments were the same as described in CHAPTER 1.

#### 4.3. Results and Discussion

##### 4.3.1. Continuous Enzyme Reaction Using Immobilized Glucoamylase

Continuous enzyme reaction was carried out using an immobilized glucoamylase column prepared by low temperature polymerization. The results are shown in Figures 36 and 37. According to these results, glucose formation decreased to about 15% of its original value after 30 days continuous operation in glucoamylase immobilized by 60% HEMA, while it scarcely decreased after the same operation in glucoamylase immobilized by 90% HEMA. Glucose formation decreased to 10-20% of its original value in immobilized glucoamylase with an enzyme concentration greater than

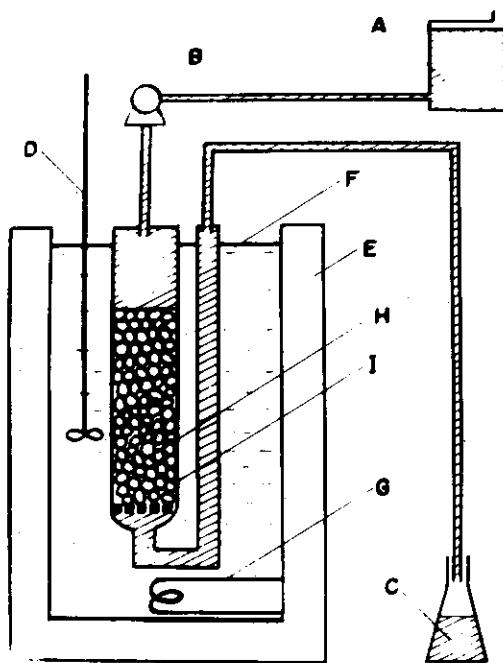


Figure 35 Column apparatus for continuous enzyme reaction. A: substrate, B: pump, C: product, D: stirrer, E: water bath, F: water, G: heater, H: immobilized glucoamylase ( $2 \times 2 \times 2 \text{ mm}^3/\text{pieces}$ ), I: column (16 mm diameter glass tube)

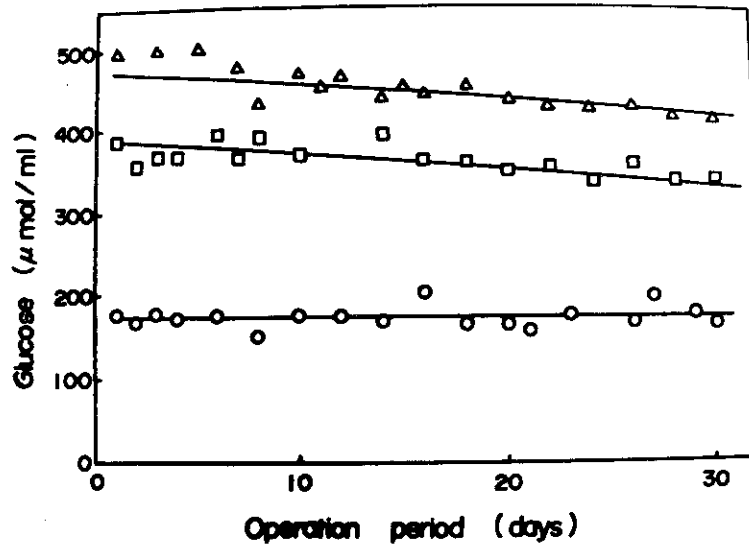


Figure 36 Effect of enzyme concentration on glucose formation as a function of operation period in continuous enzyme reaction. Monomer concentration: 60% HEMA. Irradiation:  $-78^{\circ}\text{C}$ ; 0.5 MR, in vacuo. Enzyme concentration (mg/20 ml): (○) 40, (□) 150, (Δ) 600. Flow rate: 10 ml/hr (SV 0.5). Reaction temperature:  $45^{\circ}\text{C}$

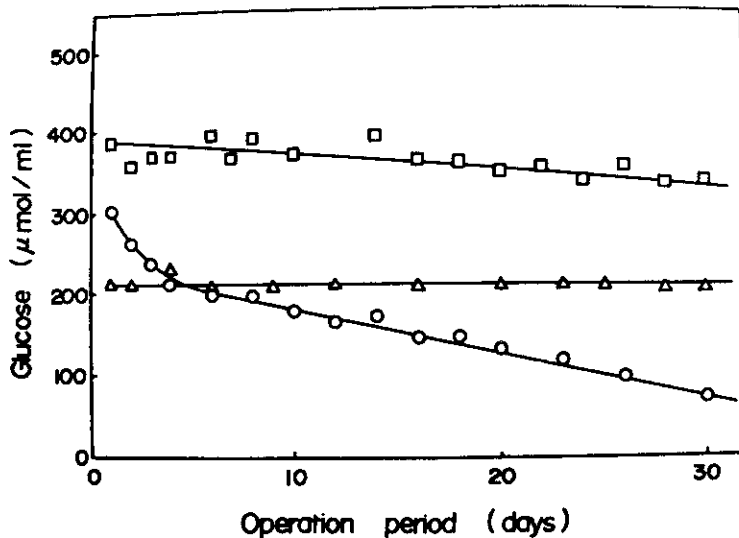


Figure 37 Effect of polymerization monomer concentration on glucose formation as a function of operation period in continuous enzyme reaction. Enzyme concentration: 150 mg/20 ml. Monomer concentration: (○) 30% HEMA, (□) 60% HEMA, (Δ) 90% HEMA. The other conditions were the same as those in Figure 36



40 mg/20 ml, while almost no decrease was observed in immobilized glucoamylase having an enzyme concentration less than 40 mg/20 ml after 30 days continuous operation. These results agreed with those of batch reaction studies and similar results were also obtained in continuous reactions using various immobilized enzymes by the same polymerization method.

In immobilization of enzyme by radiation-induced polymerization of HEMA at low temperature, it was proposed that enzyme was mainly entrapped in pore structure of the composite<sup>1</sup>. In this case, apparent activity yield of immobilized enzyme was affected by diffusion rate of substrate. Therefore, the effect of substrate on glucose formation was investigated. The result was shown in Figure 38. It was found that the glucose formation in maltose was greater than in starch. The similar effect of substrate molecular size has been reported by Melrose<sup>32</sup>. In the case of starch, contamination occurred during continuous enzyme reaction at 40°C<sup>75</sup>, but not occurred in this CHAPTER, at 45°C. It was found that various adsorbents have a remarkable effect for the increase of activity yield and prevent of the leakage of enzyme<sup>46</sup>. Drierite was one of the effective adsorbent. The continuous enzyme reaction was carried out using immobilized glucoamylase containing drierite. The result is shown in Figure 39. The

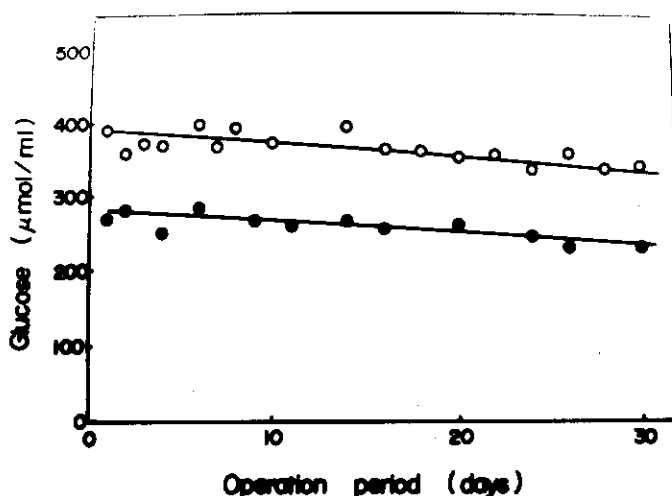


Figure 38 Effect of substrate on glucose formation as a function of operation period in continuous enzyme reaction. Enzyme concentration: 150 mg/20 ml. Monomer concentration: 60% HEMA. Substrate: (○) 10% maltose solution, pH 4.5, (●) 10% soluble starch solution, pH 4.5. The other conditions were the same as those in Figure 36

immobilized glucoamylase showed no leakage during 30 days at 45°C. The enzymatic activity was 75% after continuous enzyme reaction.

The continuous enzyme reaction was further carried out at 50°C. The amount of glucose formation after 1 and 30 days was 430 and 200  $\mu\text{mole/ml}$ , respectively.

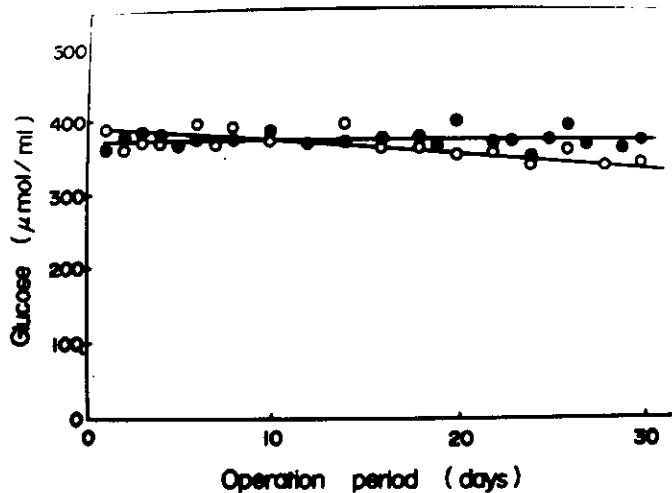


Figure 39 Effect of adsorbent on glucose formation as a function of operation period in continuous enzyme reaction. Enzyme concentration: 150 mg/20 ml. Monomer concentration: 60% HEMA. Drierite concentration: (O) none, (●) 6 g/20 ml. The other conditions were the same as those in Figure 36

#### 4.4. Summary

The continuous enzyme reaction was carried out at 45°C in small column, using glucoamylase from *Aspergillus niger* immobilized by the present immobilization method. In the case of glucoamylase immobilized at 60% HEMA concentration, no leakage of enzyme from the matrix was observed at enzyme concentration below 40 mg/20 ml, and at a flow rate of 10 ml/hr (SV 0.5) even after 30 days. The leakage of enzyme could be depressed in the presence of drierite as an adsorbent. The hydrolysis rate of maltose by immobilized glucoamylase was about 50% larger as compared with that of soluble starch.

In conclusion, the stability of the enzymes immobilized was excellent in view of the durable long use. However, many problems will still remain for further development in industrial scales.

## PART II

ENTRAPPING AND CONTROLLED RELEASE OF DRUGS BY RADIATION-INDUCED  
POLYMERIZATION OF GLASS-FORMING MONOMERS AT LOW TEMPERATURES

In the method described in the former PART, the enzymes were physically immobilized in porous sponge-like or rigid microsphere matrices in principle. Therefore, it was found that the enzyme leakage from the matrix often occurred under the conditions of large porous structure (small monomer concentration) and large hydrophilicity of the matrices. The leakage could be retarded easily by controlling these factors.

On the other hand, in this PART the drugs were physically entrapped in variously shaped matrices by radiation-induced polymerization of glass-forming monomers at low temperatures for the purpose of controlled release. The controlled release of drug is desired for protection of drug, prevention of severe secondary effect, and durability of efficacy. In CHAPTERS 5-6, the flat circular tablet containing drugs was prepared by radiation-induced polymerization of various glass-forming monomers. Their release profiles in the stationary state were examined according to Noyes-Whitney's and Higuchi's equations. The release profiles were affected by various factors. The hydrophilicity of polymer matrix gave an important effect on diffusion and release rate. In CHAPTERS 7-9, anticancers were entrapped in the matrices. The polymer-drug capsule was shaped into various forms to be implanted directly on the cancered part.

## CHAPTER 5

### ENTRAPPING AND CONTROLLED RELEASE OF POTASSIUM CHLORIDE FROM VARIOUS MATRICES

#### 5.1. Introduction

Controlled drug dissolution by polymer entrapment is an attractive research field for durable and moderate pharmaceutical effects<sup>77-85</sup>.

The author has studied radiation-induced polymerization of glass-forming monomers<sup>3</sup>, at low temperatures for the preparation of polymer matrices containing biologically active substances<sup>76,86-88</sup> such as enzymes and microbial cells. Glass-forming monomers were found to be suitable and advantageous as entrapping matrix. This characteristic method can be applied to the controlled release of biologically active substance such as drugs. The release of low molecular substances from the matrices depends on diffusivity through matrix membranes swollen by water, as well as on porous structure in matrix.

In this CHAPTER, the release behaviour of potassium chloride from radiation polymerized capsules was investigated, in relation to hydrophilicity (water content) and porosity of matrix according to Noyes-Whitney's and Higuchi's equations.

#### 5.2. Experimental

##### 5.2.1. Materials

Potassium chloride (KCl) (> 48 mesh) (Otsuka Pharmaceuticals Co.) was dried over silica gel in vacuum. Commercial methyl methacrylate (MMA), methyl acrylate (MA), and 2-hydroxyethyl methacrylate (HEMA) were obtained from Tokyo Kasei Kogyo Co. and purified by distillation before use. Commercial polyethylene glycol #600 diacrylate (PGD 600), polyethylene glycol #400 dimethacrylate (PGDM 400), diethylene glycol dimethacrylate (DGDA), trimethylolpropane trimethacrylate (TMPT), and trimethylolpropane triacrylate (ATMPT) were obtained from Shin-Nakamura Chemical Co. and purified by washing with 1% aqueous sodium hydroxide, passed over Amberlyst A-27 (Rohm & Haas), and dried over molecular sieves 4A. Polyethylene glycol #600 (PEG 600) obtained from Wako Pure Chemical Co. was used as a

pore-making agent and not purified.

### 5.2.2. Preparation of Radiation Polymerized Flat Circular Capsules

In the preparation of radiation polymerized flat circular capsules comprising KCl, 600 mg of KCl was charged into a flat bottom glass ampoule 14 mm in diameter, 0.5 ml of various vinyl monomers was added and then ampoule was sealed off under a vacuum of  $10^{-3}$  mmHg at a temperature of  $-196^{\circ}\text{C}$ . In this case, KCl in the ampoule was homogeneously coated by monomer. The sealed ampoule was irradiated at room temperature with a  $^{60}\text{Co}$  source at a dose rate of  $5 \times 10^5$  R/hr. The polymerized matrix obtained by an irradiation dose of 4 MR as a flat circular capsule of 14 mm in diameter, 4 mm long and  $4.84 \text{ cm}^2$  surface area was used for the dissolution test. After irradiation, no monomer or other impurity was detected in the capsule by gas chromatographic techniques.

### 5.2.3. Preparation of the Polymer-Drug Composition Having A Heterogeneous Disperse Phase

The polymer-drug composite was prepared as described above, but using DGDA-PEG 600 mixtures. The ampoule was irradiated for 8 hrs at a dose rate of  $5 \times 10^5$  R/hr at a temperature of  $-78^{\circ}\text{C}$  (dry ice-ethanol). No DGDA remaining in the matrix was detected by gas chromatographic techniques. The polymer-drug composites obtained from a composition of 30% DGDA-70% PEG 600, 50% DGDA-50% PEG 600, 70% DGDA-30% PEG 600 and 100% DGDA were flat circular composites of 14 mm in diameter and 4 mm long having  $4.84 \text{ cm}^2$  surface area.

### 5.2.4. Dissolution of KCl from the Capsules

The dissolution test was carried out at  $37^{\circ}\text{C}$  at a rate of 100 rpm with a Toyama Sangyo dissolution apparatus, Model TR-5S, based on United States Pharmacopeia XIX as shown in Figure 40. The basket was immersed in 1000 ml purified water, pH 6.0 and at selected time intervals over a total period of 480 min, 10 ml of the elution medium was sampled and KCl assayed spectrophotometrically using a Shimadzu double beam spectrophotometer, Model UV-200<sup>89</sup>.

### 5.2.5. Measurement of Porous Structure in the Matrix

The average diameter of this phase (pore),  $D_{av}$  and the apparent density of dispersed particle phase (porosity),  $W'_a$  in the matrix estimated from microscopic observation were the same as described in CHAPTER 1.

## 5.3. Results and Discussion

### 5.3.1. Time-Release Curves from Various Matrix Capsules Containing KCl

KCl, a known drug for oral treatment of hypo-potassemeia, was chosen as a model drug for the controlled release study. The amount of released KCl was measured at various times and the results are shown in Figure 41. It was evident that the release property depended on the kind of polymer

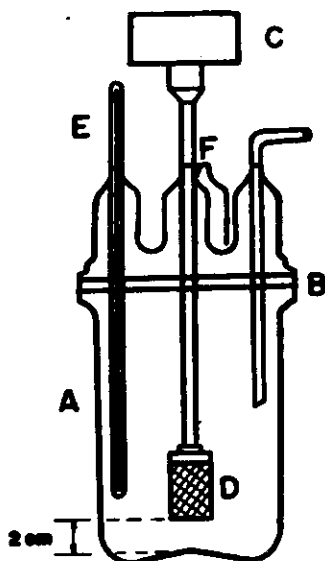


Figure 40 Apparatus for dissolution test.  
 A: cylindrical vessel, B: fitted cover, C: motor, D: basket (40 mesh stainless steel cloth) 3.66 cm high and 2.5 cm diameter,  
 E: thermometer (37°C), F: sampling

and this may be related to the hydrophilic property of the polymer as discussed later. It was also recognized that the release process could be divided into three parts; a relatively quick release process in the initial stage, followed by a stationary release process in the second

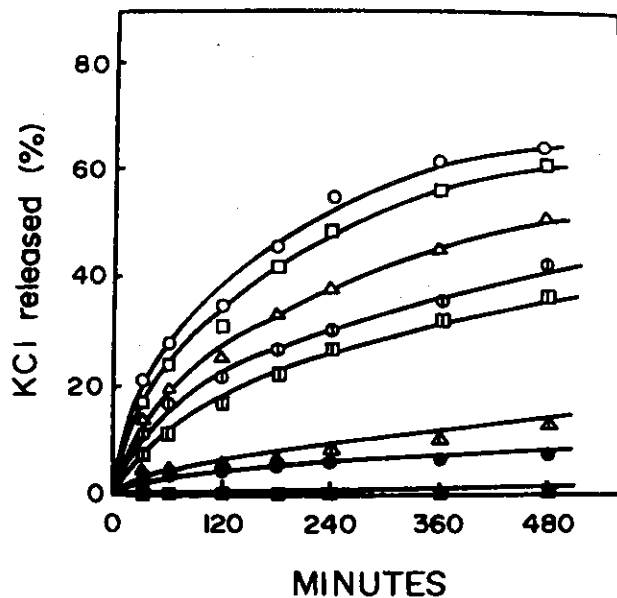


Figure 41 Relationship between the release of drug (%) from polymer capsules containing 600 mg of KCl and the time. Monomer: (○) HEMA, (□) PGD 600, (△) PGDM 400, (⊙) MA, (◻) MMA, (▴) DGDA, (●) ATMPT, (■) TMPT

stage, and a related slow release process in the later stage. The initial rapid process could be attributed to the quick dissolution of KCl present on the surface of polymer caused by the rapid swelling of the polymer by water. The second step; a stationary state release process through the polymer matrix is analyzed in the next section. The last process is probably a release rate decreasing step caused by a shortage of KCl in the matrix.

### 5.3.2. Analysis of Stationary State Release Process by Noyes-Whitney Equation

The Noyes-Whitney equation is applicable for the kinetic analysis of first order release from the matrix medium<sup>90-91</sup>. The release rate and the concentration (C) of the drug at a certain time t can be expressed as follows;

$$-\frac{dC}{dt} = K_r(C - C_1) \quad (7)$$

$$C = \frac{VC_0}{V_0 + V} \left\{ 1 + \frac{V_0}{V} \exp - \frac{-K_r(V_0 + V)t}{V_0} \right\} \quad (8)$$

where  $C_1 = (C_0 - C)V/V_0$ ,  $C_1$  is the drug concentration in fluid medium,  $C_0$  is the initial drug concentration in the matrix;  $V_0$  and  $V$  are the volumes of water used for release and of matrix per unit weight, and  $K_r$  is the rate constant for release. Since  $V_0 \gg V$  ( $V_0$  is 1000 ml and  $V$  is about 0.5 ml), equation (8) may be written;

$$K_r t = \ln \frac{\alpha C_0}{(\alpha C_0 - C_1)} \quad (9)$$

where  $\alpha$  is  $V/V_0$ . The relation between  $t$  and  $\log[\alpha C_0 / (\alpha C_0 - C_1)]$  is shown in Figure 42. The three stages in the release behaviour are clearly shown.

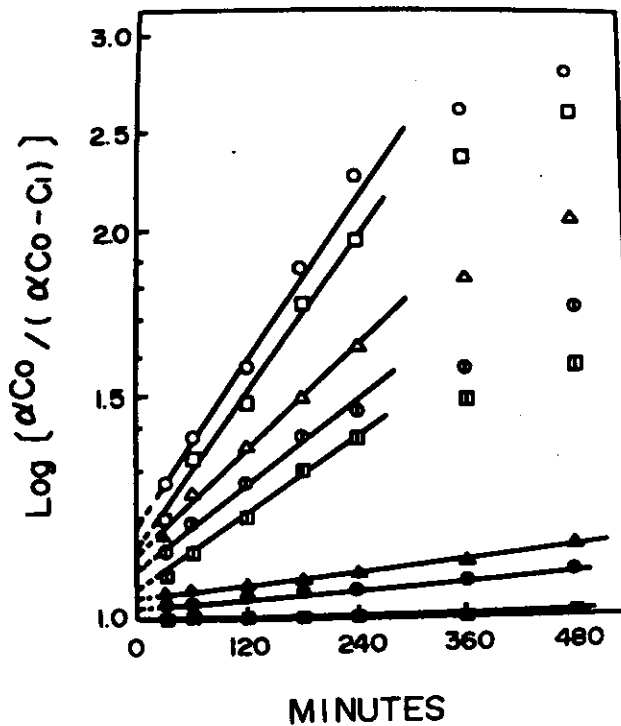


Figure 42 Semilogarithmic relationship between  $\alpha C_0 / (\alpha C_0 - C_1)$  and the time.



The linear relation in the stationary release stage shows that analysis by the Noyes-Whitney equation is approximately applicable to these matrices. Exact kinetic analysis for this release is complicated by the fact that the concentration of KCl in the matrix changes as the matrix polymer swells with water. In addition the polymer swelling in the presence of salt might be different to that in pure water and this difference may affect the drug concentration and diffusivity in the polymer matrix. However it was ascertained that the major step in the polymer swelling is completed within about 60 min; that is, within the initial, non-stationary, quick release stage, even in the most hydrophobic polymer used. The linear relationship in Figure 42 is therefore an approximate representation of experimental results using the value of drug concentration in polymer matrix saturated with pure water.

Though the theoretical value of  $\alpha C_0 / (\alpha C_0 - C_1)$  must be unity at  $t=0$ , the intersection of the straight line and the ordinate shows higher values. This deviation is probably due to the quick dissolution of KCl trapped on the surface of the matrix on swelling of the polymer. The values of intersection,  $Z$  vary with the polymer used and probably depend on the hydrophilic property or swelling tendency of the polymer. In order to estimate the hydrophilic property of the polymer, water content ( $W$ ) was determined as a rough measure of hydrophilicity, according to the following equation (though it might change in the presence of salt such as KCl);

$$W (\%) = \frac{W_w}{W_p + W_w} \times 100 \quad (10)$$

where  $W_w$  and  $W_p$  are the weight of the water absorbed to saturate the polymer and of dried polymer, respectively. These values are listed in Table III. Furthermore, the apparent dissolution coefficient of drug in the matrix capsules can be estimated according to;

$$D_p = \frac{K_r h}{S} \quad (11)$$

where  $h$  is the effective thickness of matrix membrane and  $S$  is the specific surface area. The values of  $D$  listed in Table III show that  $Z$  increased in correspondence with the increase of water content and diffusion coefficient. It is clear that the rapid increase in rate in the initial release stage could be related to hydrophilic property and to the quick dissolution and release on swelling of the aqueous polymer matrices.

### 5.3.3. Treatment of Release Property by the Higuchi Equation

Higuchi proposed the following equation for the amount of drug released in non-capillary matrices<sup>44</sup>,

$$Q = (2A - C_s) \left( \frac{Dt}{1 + \frac{2(A - C_s)}{C_s}} \right)^{1/2} \quad (12)$$

For the common case of  $C_s \ll A$ , equation (12) can be simplified to;

$$Q = (2ADC_s t)^{1/2} \quad (13)$$

where  $A$  is the concentration of drug expressed in units/cm<sup>3</sup>,  $C_s$  is the concentration of drug in the external polymer phase of the matrix,  $D$  is the diffusion constant of the drug in the external polymer phase of the matrix,

Table III Parameters for release of KCl from the polymer-drug matrix capsules

Monomer	$W$ (%)	$Z$ (%)	$K_r$ ( $\times 10^{-3} \text{ min}^{-1}$ )	$D_p$ ( $\times 10^{-5} \text{ g/cm min}$ )	$A$ ( $\text{mg/cm}^3$ )	$C_s$ ( $\text{mg/cm}^3$ )	$Q/t^{1/2}$ ( $\text{ng/cm}^2 \text{ min}^{1/2}$ )
HEMA	32.5	16	2.60	5.37	843	150	4.37
PGD 600	30.7	12	2.23	4.61	884	140	3.87
PGEM 400	21.6	11	1.54	3.18	940	90	3.01
MA	7.6	9	1.14	2.35	1129	20	2.41
MMA	4.8	6	1.10	2.27	1185	10	2.06
DGDA	3.8	3	0.22	0.45	1242	8	0.69
ADMP	3.3	1	0.21	0.43	1200	7	0.33
TMPT	2.4	0	0.04	0.08	1189	6	0.03

$t$  is the time and  $Q$  is the amount of drug released up to time  $t$  per unit area of exposure.

Experimental results (Table III) on the release between  $Q$  and the square root of  $t$  show that the linear relation is obeyed within certain time ranges and then gradually changes to the saturated curve. It is clear that the main release step agrees approximately with equation (13). Although  $C_s$  and  $D$  in equation (13) depends on the matrix swelling, values in saturated aqueous matrix can be used approximately for the stationary state release step in the linear parts of curves in Figure 43 as well as in Figure 42. In later stages of release, deviation from linearity was observed owing to non-stationary state (non-first order) release.

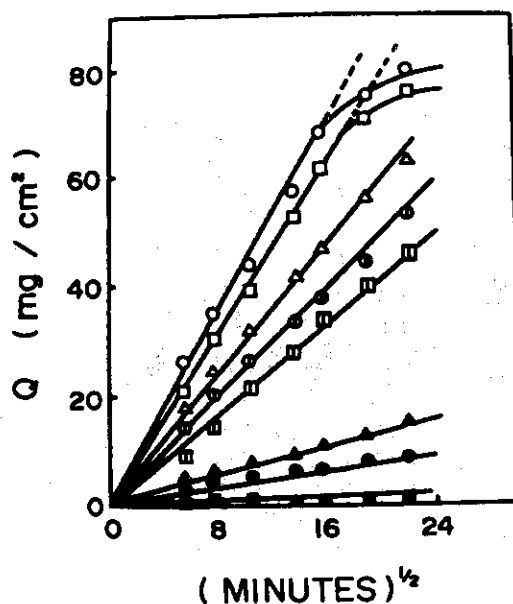


Figure 43 Linear relationship between the cumulative amount of drug release per unit area of polymer capsule and the square root of time.

It may be concluded that KCl is effectively trapped and released with control in various acrylate and methacrylate polymers formed by radiation-induced polymerization. The hydrophilic property of these polymer matrices had the most important effect on release property, the release rate being very small in less hydrophilic or hydrophobic matrices. Practically it would be useful if the hydrophobic polymer had the preferable release rate and further, investigation on this point is reported in a following section.

### 5.3.4. Release Property from Porous Capsules Containing KCl

The structure of the polymerized matrix observed by scanning electron microscopy, after complete leaking of KCl and PEG 600 is shown in Figure 44. As the dispersed water-particle phase could be hardly observed in Figure 44 (d), it is clear that the dispersed phase is formed by the addition of PEG 600 which crystallized at temperatures below 0°C. The PEG 600 crystal dispersed in supercooled DGDA monomer at low temperatures formed a heterogeneous dispersion structure in the matrix by melting and leaking out (replacing by water) after polymerization. These structures consisted of independently closed cells as seen clearly in Figure 44. The formation of such a heterogeneous dispersion structure is the most

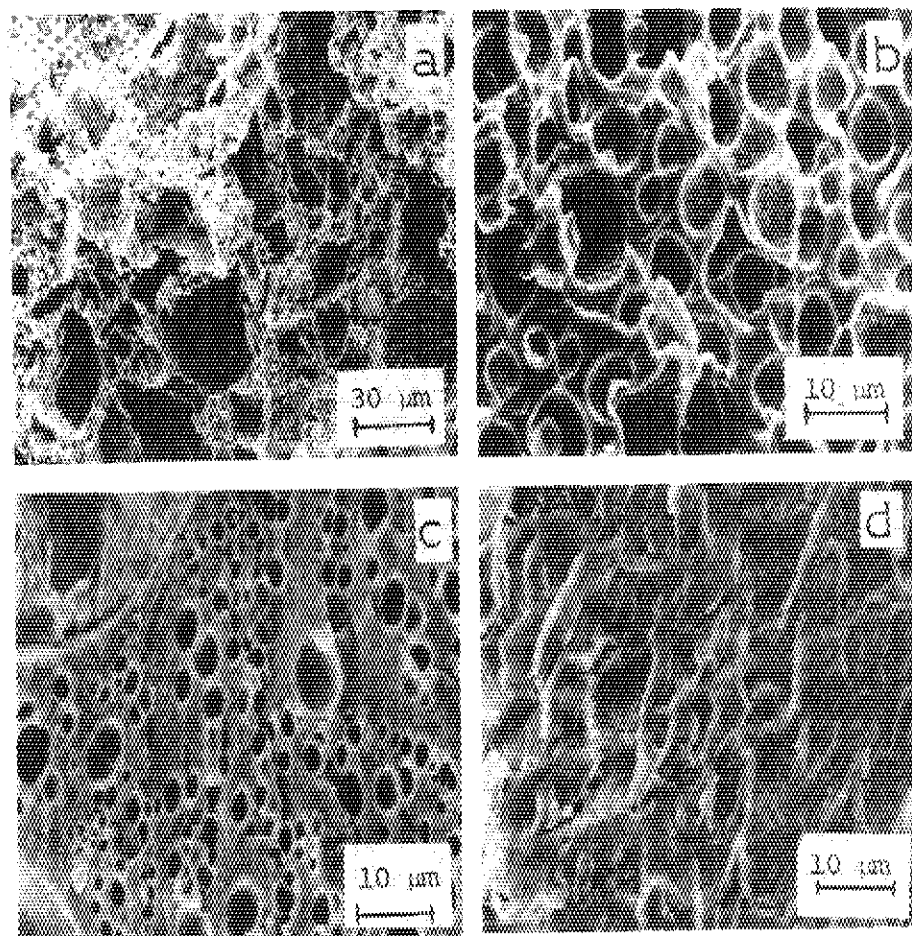


Figure 44 Scanning electron microphotographs of porous structure in the polymer-drug composite. Composition: (a) 30% DGDA-70% PEG 600, (b) 50% DGDA-50% PEG 600, (c) 70% DGDA-30% PEG 600, (d) 100% DGDA

characteristic property of polymers obtained by low temperature polymerization of supercooling monomer containing a crystallizable solvent. The distribution of average diameter of dispersed phase and their number determined by microscopic observation was shown in Table IV. These distributions can be controlled by changing the combination and composition of supercooling and crystalizing components. The average diameter of dispersed phase decreased but their average number increased with decreasing PEG 600 concentration. This fact might be due to the nature of the crystal growth at low PEG 600 concentration. The apparent content

Table IV Effect of porous structure on the  $Q/t^{1/2}$  of KCl from the polymer-drug composite

Sample	Composition (vol %)		W (%)	$Q/t^{1/2}$ ( $\text{mg}/\text{cm}^2/\text{min}^{1/2}$ ) ( $\times 10^{-4} \text{ cm}^2/\text{min}$ )	D	Porous structure		
	DGDA	PEG 600				$D_{av}$ ( $\mu\text{m}$ )	Number of $D_{av}$ (pieces/ $\text{cm}^2$ )	$W'_a$ (%)
1	30	70	56.7	3.00	4.43	15.5	$2.2 \times 10^5$	41.7
2	50	50	46.1	2.31	2.63	6.6	$1.2 \times 10^6$	30.7
3	70	30	24.8	1.54	1.17	2.2	$2.9 \times 10^6$	11.4
4	100	0	3.8	0.69	0.23	—	—	—

of dispersed water particle phase,  $W'_a$  was estimated also from the result of microscopic observation and compared to W obtained from water content in Table IV. The value from microscopic observation was smaller than that from water content, but its dependence on monomer concentration agreed with the trend observed in the water content study. This difference might be attributed to a low estimation of average diameter in the visual field of electron microscopy in Figure 44 (b) and Figure 44 (c), because relatively few water-particle phase will be sliced at their maximum length or diameter. Values  $Q/t^{1/2}$  (Table IV) plotted as a function of water content (W) (Figure 45) gave a linear plot, showing that the release rate ( $Q/t^{1/2}$ ) increases roughly in proportion to the water content (W). Furthermore, the apparent diffusivity (D) of drug in the porous matrix are shown in Table IV. The diffusivity in the matrix itself should not change applicably since the polymer matrix is always methacrylate and its water absorption is hardly changed by the PEG 600. However, apparent diffusivity in Table IV increased markedly with increasing PEG 600 and the results support the

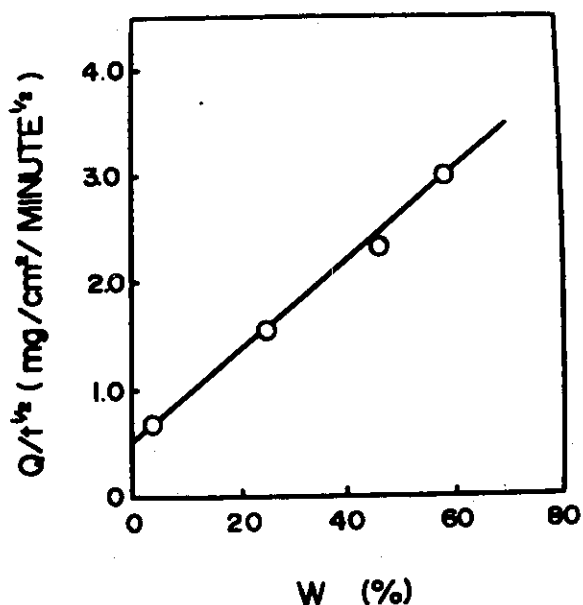


Figure 45 Relationship between the flux of KCl and the water content.

conclusion that dispersed water-particle phase made by PEG 600 markedly promote the release rate. It is certain that this promoting effect is due to the apparent increased effect of drug diffusion in the matrix due to the presence of the dispersed water phase as well as to the decrease in thickness of matrix membrane by decreased monomer concentration. Clearly, the release rate can be controlled by the composition of monomer and PEG 600.

#### 5.4. Summary

The release behaviour of KCl from flat circular capsules of various hydrophilicities obtained by radiation-induced polymerization was studied. The release process could be divided into three parts, an initial quick release stage, a stationary state release stage and a retarded stage. Release behaviour in the stationary state was examined using Noyes-Whitney and Higuchi equations. It was found that the hydrophilic property of polymer matrix expressed by water content was the most important factor affecting on diffusion and release rate. Rigidity of the polymer also affect diffusivity. The first quick release step was attributed to rapid dissolution of drug in the matrix surface by polymer swelling. The pore structure formed in PDGDA matrix by the addition of PEG 600. The release

of KCl from the matrix increased linearly with the square root of time in the stationary state release stage.

## CHAPTER 6

### CONTROLLED RELEASE OF DRUGS FROM MATRIX HAVING pH DEPENDENCY OF SOLUBILITY

#### 6.1. Introduction

In controlled drug dissolution, it is often required to release a drug within a specific pH range. In order to satisfy this require addition of some specific polymers having pH dependency of solubility was tried as a component of matrix.

This CHAPTER describes the drug dissolution from solid tablets prepared by radiation-induced polymerization in the presence of dimethylaminoethyl methacrylate-methyl methacrylate copolymer or methacrylic acid-methyl acrylate copolymer to carry out the controlled release at pH 3.0-8.0.

#### 6.2. Experimental

##### 6.2.1. Materials

2-Hydroxyethyl methacrylate (HEMA) (see, CHAPTER 1), hydroxyethyl acrylate (HEA) (see, CHAPTER 2) and glycidyl methacrylate (GMA) (see, CHAPTER 3) were used as carriers.

Aspirin (Nipponkayaku Co.), sulfanilamide (Kanto Chemical Co.), salicylic acid (Kanto Chemical Co.), colchicine (Kanto Chemical Co.) and pottasium chloride (KCl) (see, CHAPTER 5) were used as drugs.

Copolymer (Eudragit E: Rohm Pharm GMBH) of dimethylaminoethyl methacrylate (DAMA)-methyl methacrylate (MMA) (cation-type copolymer) and copolymer (Eudragit L: Rohm Pharm GMBH) of methacrylic acid (MAc)-methyl acrylate (MA) (anion-type copolymer) were used as copolymers. The cation-type copolymer was dissolved only in a medium corresponding to the gastric juice at  $\text{pH} < 5.0$ ; the anion-type copolymer was dissolved in a medium corresponding to the intestinal juice at  $\text{pH} > 6.0$ .

##### 6.2.2. Porous Polymer-Drug Tablet Preparation

Polymer tablets containing drugs were made as follows. Drug, 600 mg, was put in a flat-bottom glass ampoule, 14 mm in diameter, and then 0.5 ml of the copolymer-glass-forming monomer mixture was added. Powdered



copolymers, such as anion- and cation-type copolymers; completely dissolved at 30-80°C in glass-forming monomers such as HEMA, HEA and GMA. The ampoule was sealed under a vacuum of  $10^{-3}$  mmHg at -196°C (liquid nitrogen) and was irradiated for 2 hrs at  $5 \times 10^5$  R/hr at -78°C with  $\gamma$ -ray from a  $^{60}\text{Co}$  source. After irradiation, the polymer-drug matrix was obtained as a homogeneous tablet, 14 mm in diameter and 4 mm long.

### 6.2.3. Drug Dissolution from Tablets

The dissolution test was carried out under the same conditions as described in CHAPTER 5. The dissolved drug was assayed spectrophotometrically (Shimazu double beam spectrophotometer, Model UV-200) at 460 nm by a mercury thiocyanate method for  $\text{KCl}^{89}$ , at 258 nm for sulfanilamide, at 296 nm for salicylic acid, at 273 nm for aspirin and at 353 nm for colchicine.

### 6.2.4. Other Experiments

The other experiments were the same as described in CHAPTER 5.

## 6.3. Results and Discussion

### 6.3.1. Effect of Irradiation on Drugs

It is necessary to know the irradiation effect on drug activity before polymer tablet preparation. The relation between untreated drug relative activity and the irradiation conditions used in experimental tablet preparation is shown in Figure 46. Under the present experimental temperature, energy and irradiation duration, there was no detectable drug decomposition. Since drug radiation damage is enhanced in the presence of oxygen, the irradiation in a vacuum is desirable.

### 6.3.2. Drug Dissolution-Time Curves of Tablets in the Presence of Anion-Type Copolymer

KCl, salicylic acid, sulfanilamide, aspirin or colchicine was entrapped in the polymer matrix by radiation-induced polymerization of a glass-forming monomer at low temperature in the presence of an anion-type copolymer.

The dissolved drugs in the dissolution medium at pH 8.0 was measured at certain time intervals.

First-order drug dissolution kinetics were investigated using the Noyes-Whitney equation<sup>90-91</sup>, as described in CHAPTER 5.

The relation between  $t$  and  $\alpha C_0 / (\alpha C_0 - C_1)$  in tablets of various anion-type copolymer concentrations and various polymer matrices and drug components is shown in Figure 47. The dissolution rate constant ( $K$ ) was calculated from the initial slope of linear graphs (Table V). For samples

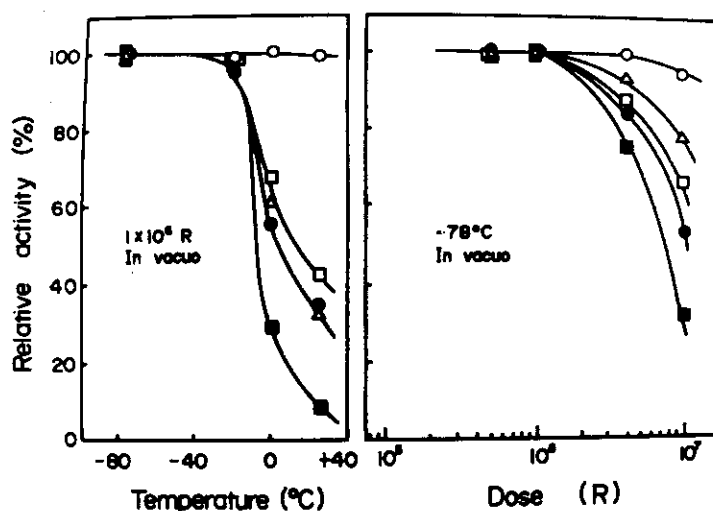


Figure 46 Effect of irradiation conditions on drug activity. Drug was dissolved in distilled water (pH 6.0) and put into a glass ampoule. The ampoule was sealed in vacuo. The irradiation was carried out under 1 MR/hr, in vacuo. The untreated drug activity was taken as 100%. Drug concentration: (O) 60  $\mu$ g of KCl/ml (as Cl), (□) 25  $\mu$ g of salicylic acid/ml, ( $\Delta$ ) 8  $\mu$ g of sulfanilamide/ml, (●) 60  $\mu$ g of aspirin/ml, (■) 20  $\mu$ g of colchicine/ml

1-4 (Figure 47), aspirin dissolution from the tablet increased with anion-type copolymer concentration. This increase was attributed to anion-type copolymer dissolution in the tablet at pH 8.0, although the copolymer barely dissolved in HEMA monomer at concentrations above 30%. The results for samples 3, 5 and 6 in Figure 47, showing aspirin dissolution from various polymer tablets, depended on the kind of glass-forming monomer or matrix. This dissolution was related to the hydrophilic property of the matrix, which is indicated in Table V in relation to the polymer matrix water content (W).

Drug dissolution from tablets in the presence of a 10% anion-type copolymer is shown for samples 3 and 7-10 in Figure 47. Dissolution

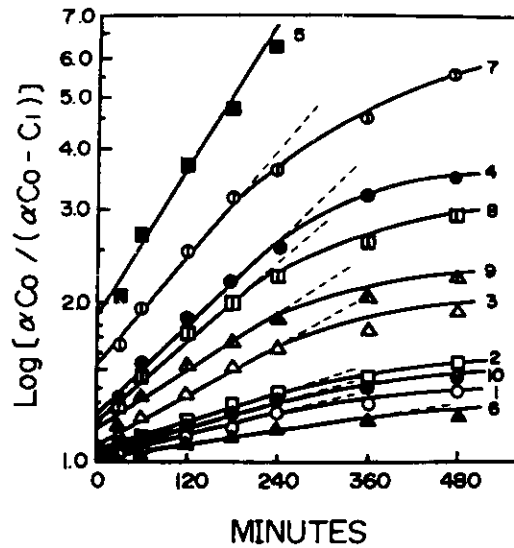


Figure 47 Semilogarithmic relationship between  $\alpha C_0 / (\alpha C_0 - C_1)$  and dissolution time for polymer tablets in the presence of an anion-type copolymer. Sample number refers to compositions in Table V. The dissolution medium was at pH 8.0. Tablet system and drug: (○) 100% HEMA (aspirin), (□) 95% HEMA (aspirin), (△) 90% HEMA (aspirin), (●) 80% HEMA (aspirin), (■) 90% HEA (aspirin), (▲) 90% GMA (aspirin), (⊙) 90% HEMA (KCl), (⊞) 90% HEMA (salicylic acid), (⊚) 90% HEMA (sulfanilamide), (⊗) 90% HEMA (colchicine)

Table V Parameters for drug dissolution from polymer tablets, 14 mm in diameter and 4 mm thick, in the presence of anion-type copolymer

Sample	Composition (wt %)		Drug (mol. wt.)	K ( $\times 10^{-3} \text{ min}^{-1}$ )	W (%)
	Anion-type copolymer	Monomer			
1	—	100% HEMA	Aspirin (180.16)	0.89	31.2
2	5	95% HEMA	Aspirin (180.16)	1.24	34.9
3	10	90% HEMA	Aspirin (180.16)	1.99	39.3
4	20	80% HEMA	Aspirin (180.16)	3.41	47.4
5	10%	90% HEA	Aspirin (180.16)	7.26	57.9
6	10%	90% GMA	Aspirin (180.16)	0.50	7.2
7	10%	90% HEMA	KCl (74.55)	4.31	37.6
8	10%	90% HEMA	Salicylic acid (138.12)	2.88	40.1
9	10%	90% HEMA	Sulfanilamide (172.21)	2.36	37.2
10	10%	90% HEMA	Colchicine (399.45)	1.00	38.6

decreased in the order of KCl, salicylic acid, sulfanilamide, aspirin and colchicine, perhaps due to differences in drug molecular weights (Table V). The larger the molecular weight of the trapped substances, the smaller was the dissolution rate from the matrix. The intersections of the straight lines and the axis of the ordinates show values higher than unity (Figure 47). This deviation was probably due to the rapid dissolution of drugs and anion- or cation-type copolymers trapped on the surface by polymer swelling.

### 6.3.3. Effect of Medium pH on Aspirin Dissolution from PHEMA Tablet

The anion-type copolymer dissolved in the medium only at  $\text{pH} > 6.0$ , while the cation-type copolymer dissolved only at  $\text{pH} < 5.0$ . Aspirin dissolution from tablets containing various copolymers was investigated for dissolution media at various pHs<sup>92-93</sup> (Figure 48). The dissolution rate at  $\text{pH} 8.0$  was larger than that at  $\text{pH} 3.0$  for anion-type copolymer tablets, while the pH dependency of dissolution in the presence of the cation-type copolymer was the opposite to that in the presence of the anion-type copolymer. Therefore, dissolution of the formulation was markedly influenced by pH in the presence of a copolymer. Aspirin dissolution

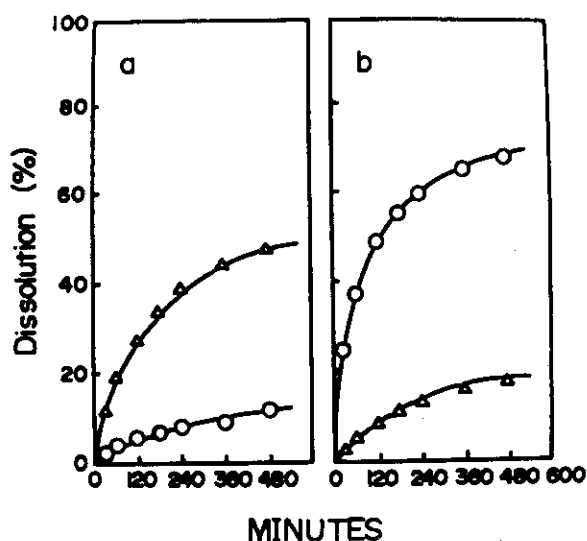


Figure 48 Effect of kind of copolymer [(a) anion-type and (b) cation-type] and dissolution medium pH [(O) pH 3.0 and (Δ) pH 8.0] on aspirin dissolution from PHEMA tablet. Tablet composition was 90% HEMA-10% copolymer

from a porous PHEMA tablet prepared with PEG 600 instead of with a copolymer also was investigated. Dissolution of the formulation was hardly influenced by dissolution medium pH (Figure 49).

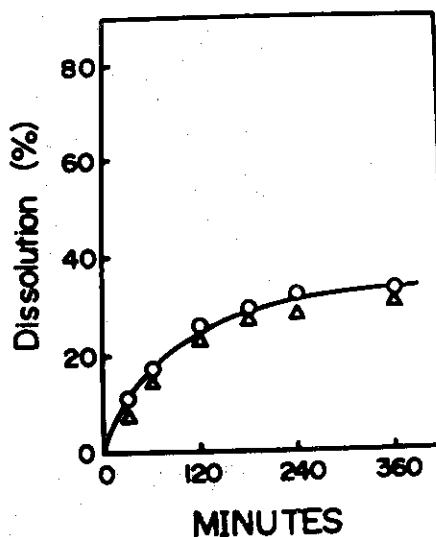


Figure 49 Effect of dissolution medium pH [(O) pH 3.0 and (Δ) pH 8.0] on aspirin dissolution from PHEMA tablet in the presence of PEG 600.

#### 6.3.4. Porous Structure

Polymer tablet structure was observed by scanning electron microscopy after complete removal of additives such as aspirin, PEG 600 and copolymers (Figure 50). Since the porous structure is hardly observable in Figure 50 (a), it must have been a consequence of the dissolution of copolymer or PEG 600. The porous polymer matrix obtained in the presence of copolymer is shown in Figures 50 (b) and (c), and the porous matrix obtained in the presence of PEG 600 is shown in Figure 50 (d). The porous structures in Figures 50 (b) and (c) are quite similar but are different from the structure in Figure 50 (d). The reason may be the difference in dispersion form of those additives (copolymer and PEG 600) in HEMA monomer before polymerization. That is, the anion- or cation-type copolymer may be dispersed in the fibrous molecular form, and the pore structure forms in the polymer after polymerization as shown in Figures 50 (b) and (c). On the other hand, PEG 600 may be dispersed in the monomer in the spherical form owing to its crystallization at low temperatures, and then the pore structure in the tablets can be controlled by varying the kinds of

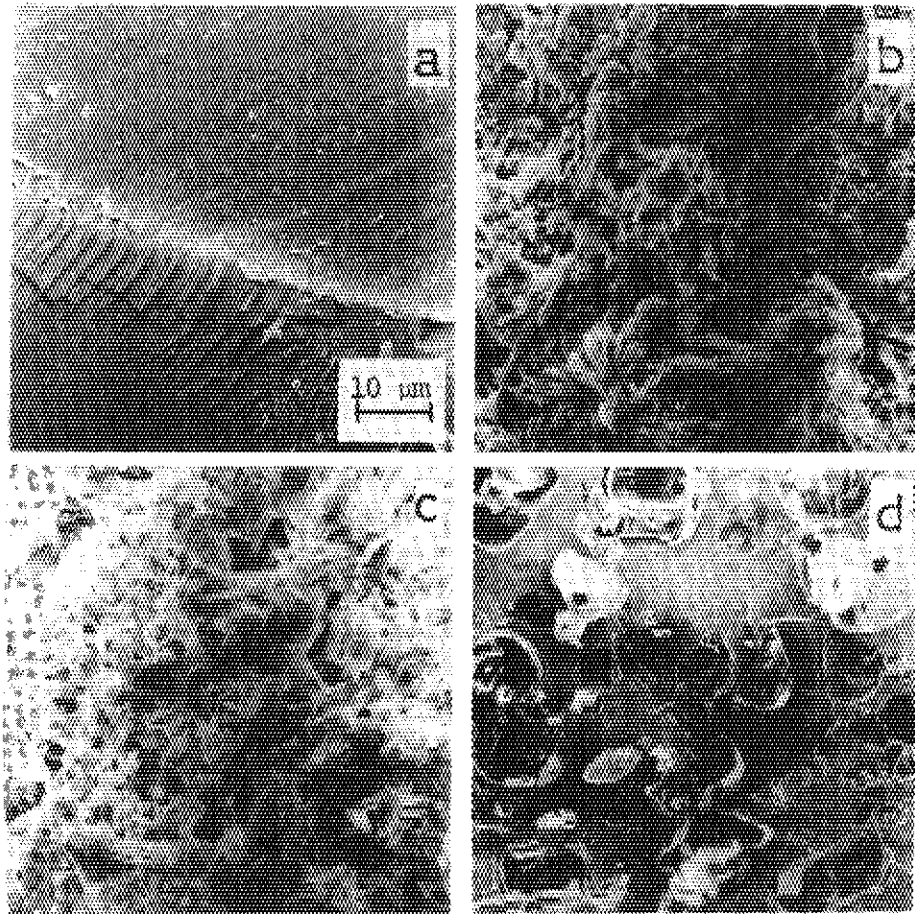


Figure 50 Scanning electron microphotographs of porous structure of PHEMA tablets containing aspirin in the presence of various additives. (a) tablet in the presence of 10% anion-type copolymer before treatment with dissolution medium, (b) tablet in the presence of 10% anion-type copolymer after treatment with dissolution medium at pH 8.0, (c) tablet in the presence of 10% cation-type copolymer after treatment with dissolution medium at pH 3.0, (d) tablet in the presence of 10% PEG 600 after treatment with dissolution medium at pH 3.0

additives and their concentrations.

#### 6.4. Summary

A copolymer obtained in the tablets dissolved in the dissolution medium at a specific pH. Drug dissolution from tablets took place rapidly at pH >6.0 in the presence of MAC-MA copolymer and at pH < 5.0 in the presence of DAMA-MMA copolymer. The polymers had fibrous or capillary pore structures in contrast to the spherical pore structures in PEG 600.

## CHAPTER 7

## CONTROLLED RELEASE OF DRUGS FROM VARIOUSLY SHAPED MATRICES

## 7-1. RELEASE OF DRUGS FROM POLYMERIZED BEADS

## 7.1.1. Introduction

Entrapped drugs in fine particle form such as microsphere could give various merits in practical usage. Trapped enzymes or microbial cells on a carrier surface is desirable for the contact of substrate<sup>26,94</sup>. Immobilized enzyme or microbial cell microspheres were obtained by suspension polymerization of a hydrophobic glass-forming monomer at low temperatures or by polymerization of the salt-out hydrophilic glass-forming monomer.

Drugs also can be entrapped inside microsphere polymer matrix, because low molecular weight substances leach rapidly from the surface-sorbed state<sup>67</sup>. In this CHAPTER, a new method for small solid particle preparation incorporating drugs by radiation-induced polymerization at low temperatures was investigated.

## 7.1.2. Experimental

## 7.1.2.1. Materials

Potassium chloride (KCl) used as a drug, 2-hydroxyethyl methacrylate (HEMA), hydroxyethyl acrylate (HEA), diethylene glycol dimethacrylate (DGDA) and trimethylolpropane trimethacrylate (TMPT) used as carriers (glass-forming monomers), methanol, ethanol, n-butanol, n-hexane and 1,4-butanediol used as precipitation media, and poly(methyl methacrylate) (PMMA) used as a polymer were the same as described in CHAPTER 3 except for a drug (see, CHAPTER 5).

Methyl methacrylate (MMA) was used as a non-glass-forming monomer (as described in CHAPTER 2).

## 7.1.2.2. Preparation of Radiation Polymerized Beads

Drops of polymer, monomer and drug (KCl) mixtures were allowed to fall into a cold (-78°C) precipitation medium with the equipment shown in

Figure 51(a). The solid globules were irradiated at  $-78^{\circ}\text{C}$  (dry ice-methanol) or  $-24^{\circ}\text{C}$  for 2 hrs at  $1 \times 10^6$  R/hr with a  $^{60}\text{Co}$  source. After irradiation, the polymerized spheres were removed and dried. When polyethylene glycol #600 (PEG 600) replaced the polymers PMMA or poly(styrene) (PSt), the solidified globules were irradiated for 1 hr at  $1 \times 10^6$  R/hr. Then the original n-hexane precipitation medium was replaced by cooled 1,4-butanediol, and polymerization was continued for 2 hrs at room temperature at the same rate.

### 7.1.2.3. Other Experiments

The mean particle diameter ( $D_{av}$ ), mean KCl amount ( $C_{KCl}$ ), water content (to estimate the polymer hydrophilicity) were carried out by the same method as described in CHAPTER 4. On the other hand, the dissolution test was the same as described in CHAPTER 5.

## 7.1.3. Results and Discussion

### 7.1.3.1. Non-Glass-Forming Monomers

MMA required at least 6% PMMA to form stabilized globules when dropped into cold methanol. Otherwise, the monomer-polymer-drug mixture formed threads or simply coalesced into an immiscible layer. Other precipitation media produced similar results. MMA polymerization did not yield solid spheres at cold temperatures and merely coalesced above  $0^{\circ}\text{C}$ .

### 7.1.3.2. Glass-Forming Monomers

These monomers gave well-formed solid globules when mixed with polymer and KCl and supercooled. They were easily polymerized by irradiation at the low temperatures used.

### 7.1.3.3. Globule Formation

Ethanol as the supercooled precipitation medium yields spherical globules (Figure 52). Methanol, n-butanol and n-hexane formed ellipsoidal globules. Globule formation seemed dependent on the polymer present in the mixture and a precipitation medium temperature not above  $-24^{\circ}\text{C}$ . When



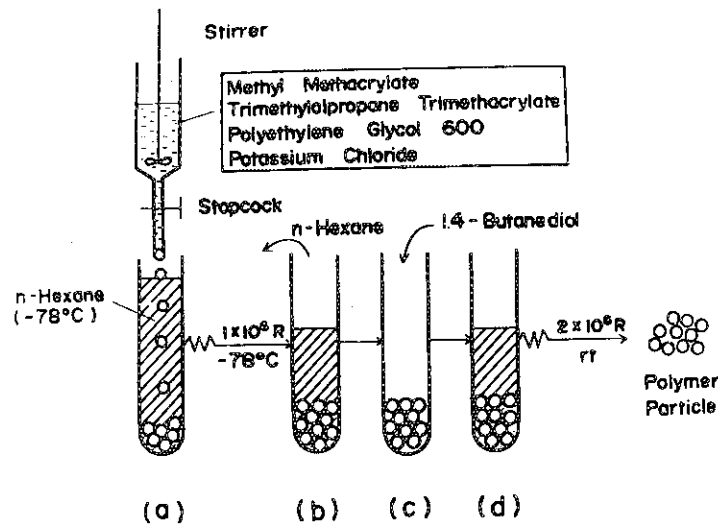


Figure 51 Preparation methods for porous polymerized spheres containing KCl.

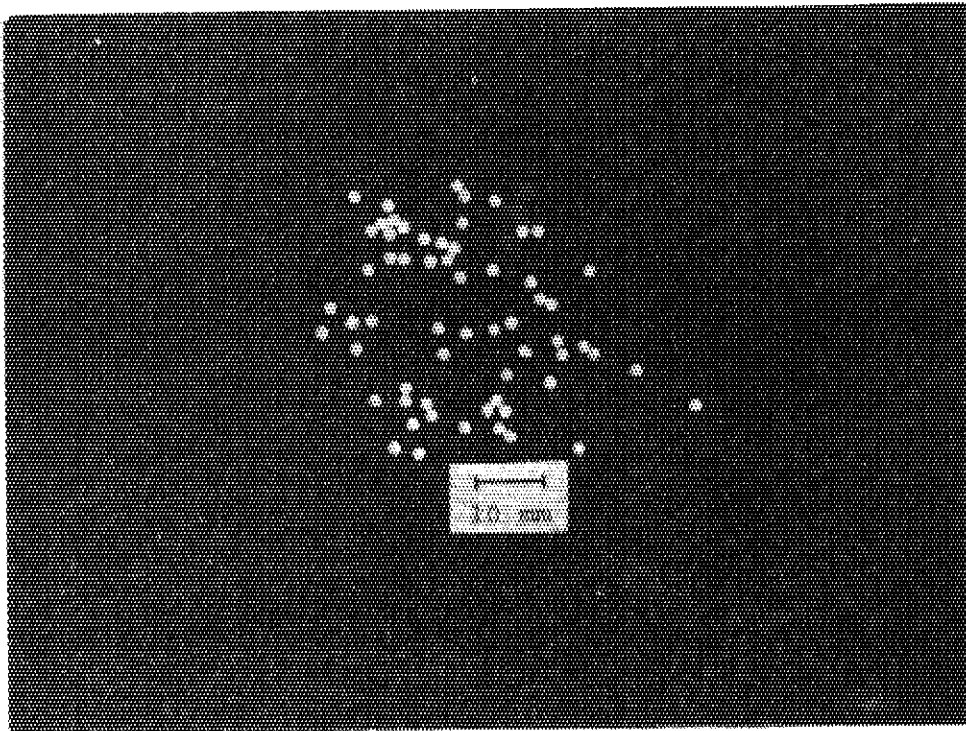


Figure 52 Photograph of spherical particles

Table VI Properties and preparation of polymer, glass-forming monomer, and KCl beads in low temperature polymerization

Sample	Polymer-monomer composition (%)	Precipitation condition		W (%)	Property of beads		
		Medium	Temperature (°C)		Shape	D <sub>av</sub> (nm)	C <sub>KCl</sub> (mg/particle)
1	100% DGDA	Methanol	-78	3.8	Nonparticle (block composite)	—	—
2	5% PMMA-95% DGDA	Methanol	-78	3.3	Ellipsoid	—	19
3	10% PMMA-90% DGDA	Methanol	-78	3.6	Ellipsoid	—	21
4	20% PMMA-80% DGDA	Methanol	-78	3.1	Ellipsoid	—	23
5	10% PMMA-90% DGDA	Ethanol	-78	2.7	Sphere	2.2 ± 0.1	18
6	10% PMMA-90% DGDA	n-Butanol	-78	3.6	Ellipsoid	—	20
7	10% PMMA-90% DGDA	n-Hexane	-78	3.4	Ellipsoid	—	19
8	10% PMMA-90% DGDA	Ethanol	-24	—	Nonparticle (block composite)	—	—
9	10% PMMA-90% HEA	Ethanol	-78	64.5	Sphere	2.1 ± 0.1	16
10	10% PMMA-90% GMA	Ethanol	-78	4.2	Sphere	1.9 ± 0.1	17
11	10% PMMA-90% HEMA	Ethanol	-78	32.0	Sphere	2.0 ± 0.1	17
12	10% PMMA-90% TMPT	Ethanol	-78	2.6	Sphere	2.1 ± 0.1	20
13	100% GMA	Ethanol	-78	4.0	Nonparticle	—	—
14	10% PST-90% GMA	Ethanol	-78	3.8	Sphere	2.0 ± 0.1	23
15	20% PST-90% GMA	Ethanol	-78	3.5	Sphere	2.2 ± 0.1	21

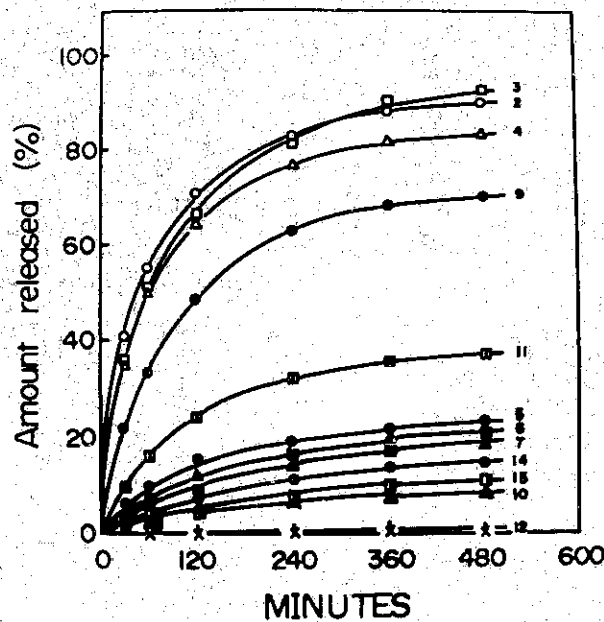


Figure 53 KCl release profile from polymerized particles. Numbers refer to compositions (table VI)

those conditions were not met, coalescence but not stabilization occurred (Table IV).

#### 7.1.3.4. Release of KCl

In the spheres containing PMMA as the polymer and DGDA as the monomer (samples 2-7), the methanol precipitation medium increased KCl release (Figure 53).

In non-methanol precipitation media, release from relatively strongly hydrophilic beads (samples 9 and 11) was faster than that from less hydrophilic matrices.

#### 7.1.4. Summary

The preparation of beads including polymer, vinyl monomer and drug was carried out by low temperature, radiation-induced polymerization. Complete spherical particles were obtained when ethanol was the precipitation medium. Polymers such as PMMA and PSt were dissolved in various glass-forming monomers, and the drug was dispersed in the mixture. The mixture was dropped into cold precipitation media. The formed monomeric particle was irradiated at low temperatures to produce polymerization. The drug release profiles from polymerized particles were changed by varying the glass-forming monomer and the precipitation medium.

## 7-2. RELEASE OF CHEMOTHERAPEUTIC DRUGS FROM VARIOUSLY SHAPED MATRICES

### 7.2.1. Introduction

A convenient entrapping method of chemotherapeutic agents for cancer was studied by radiation polymerized vinyl polymer matrices and release profiles of variously shaped matrices in vitro were obtained. Among drugs, the chemotherapeutic agent for cancer may be the most urgent and important one to be applied for this technique<sup>55,95</sup>. Because, it is seriously desired to give the chemotherapeutic drugs a durable and moderate effect, preventing the harmful second reactions and increased bioavailability. In hitherto used oral dosage and injection it has been difficult to satisfy the above conditions, because the drugs should have been absorbed in blood vessel to reach the cancered part.

On the other hand, it is expected that the drugs can attack a cancer directly and efficiently with less secondary reaction, by insertion or implantation of them into the cancered part. Therefore, it is necessary to give the drugs of the suitable sizes, forms and composite structures to be implanted and also the durable release effect for long times in vitro usage by polymer entrapping.

### 7.2.2. Experimental

#### 7.2.2.1. Materials

##### 7.2.2.1.1. Glass-Forming Monomer

Diethylene glycol dimethacrylate (DGDA) was obtained from Shin-Nakamura Chemical Co. and purified by passing through an ion exchange resin to remove polymerization inhibitor.

##### 7.2.2.1.2. Polymers

Poly(styrene) (PSt), poly(methyl methacrylate) (PMMA), poly(vinyl formal) (PVF), poly(methyl acrylate) (PMA) and poly(vinyl acetate) (PVAc) were obtained from Kishida Chemical Co. and used without further purification. Polyethylene glycol #600 (PEG 600) was also used without purification, Kishida Chemical Co.

#### 7.2.2.1.3. Chemotherapeutic Drugs

Mitomycin C (MMC) was obtained from Kyowa Hakko Kogyo Co.  
5-Fluorouracil (5-FU) and bleomycin hydrochloride (BLM) were obtained from Nipponkayaku Co.

#### 7.2.2.1.4. Precipitation Medium

Ethanol was used without further purification, Tokyo Kasei Kogyo Co.

#### 7.2.2.2. Preparation of Polymer-Drug Composites of Various Shapes by Radiation-Induced Polymerization

The polymer-drug composite was prepared by irradiating a mixture of drug, DGDA monomer and a polymer such as PSt, PMA, PMMA, PVF and PVAc. The concentrations (compositions) of each component are described in Figure and Table captions of each experimental result. In some cases, PEG 600 was used instead of polymer as a pore-making agent. In all cases, the irradiation was carried out at  $-78^{\circ}\text{C}$  in dry ice-methanol system with a dose rate of  $5 \times 10^5$  R/hr from a  $^{60}\text{Co}$  source. After irradiation, the polymer yield (conversion) was measured by isolating with methanol, drying and weighing the polymer. The conversion was almost 100% in all cases for the original monomer as shown in Figure 54. Therefore, it is sure that the unreacted monomer might be trace amount even if it presents, and it would not affect the release profile.

##### 7.2.2.2.1. Preparation of a Rod Shape Composite

A mixture of drug and DGDA monomer comprising a polymer was charged into a 4-8 mm in diameter glass ampoule. The ampoule was sealed off under a vacuum of  $10^{-3}$  mmHg and stirred to mix the components homogeneously. Then the sample was cooled and irradiated at  $-78^{\circ}\text{C}$ . A rod-like shaped composite of 4-8 mm in diameter was obtained.

##### 7.2.2.2.2. Preparation of a Tablet Shape composite

A mixture of drug and DGDA monomer comprising a polymer was charged into a 14 mm in diameter glass ampoule of flat bottom type. The other

operation were the same as for the rod shape composite.

#### 7.2.2.2.3. Preparation of Powder Composite

The tablet composite prepared according to the above method (7.2.2.2.2) was crushed to a form and the finely divided particles of 32-115 mesh size was obtained.

#### 7.2.2.2.4. Preparation of a Membrane Form Composite

A mixture of drug and DGDA monomer comprising a polymer was charged into a frame which was constructed by the two glass plates and a 1.5 mm thick silicone rubber gasket. The irradiation was carried out under nitrogen atmosphere at  $-78^{\circ}\text{C}$ . The other operations were the same as that of rod shape composite preparation.

#### 7.2.2.2.5. Preparation of a Spherical Shape Composite

A mixture of drug and DGDA monomer comprising a polymer was dropped to a cold precipitation medium such as ethanol kept at  $-78^{\circ}\text{C}$  with a pipette according to the previous method<sup>87</sup>. Then the formed monomeric particle was irradiated at  $-78^{\circ}\text{C}$  with the precipitation medium.

#### 7.2.2.3. Other Experiments

The dissolution test (usually distilled water, pH 6.0, 1000 ml) was carried out by the same methods as described in CHAPTER 5. At a selected time intervals, 5 ml of the dissolution medium was sampled and assayed spectrophotometrically with Shimazu double beam spectrophotometer, Model UV-200, measuring the absorption at 265 nm for 5-FU, 290 nm for BLM and 365 nm for MMC, respectively.

All measurements were carried out three times using three samples prepared under the same conditions. The results agreed each other within the error of 5%. The structure of polymer matrices was observed by the same methods as described in CHAPTER 3.

#### 7.2.3. Results and Discussion

### 7.2.3.1. Radiation Polymerization of DGDA Monomer in the Presence of Polymers

The glass-forming monomers have the large polymerization rate at low temperatures during an irradiation<sup>3</sup>. Moreover, they cause a remarkable post-polymerization during the treatment at the elevated temperature after the irradiation at low temperatures owing to the activity of trapped and living radicals. In this work, an irradiation of DGDA-polymer mixture was tested at  $-78^{\circ}\text{C}$  in order to the polymerizability of monomeric system. The result is shown in Figure 54. According to this result, the polymerization rate increased by a presence of polymer. That is, pure DGDA monomer polymerized to nearly 100% by the irradiation of  $5 \times 10^5 \text{ R}$ , but a mixture with a polymer reached nearly 100% conversion at a dose of  $3 \times 10^5 \text{ R}$ . The very hard polymers were obtained by those polymerization.

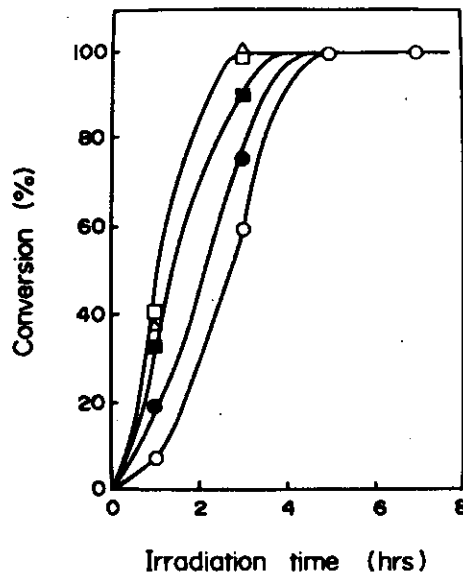


Figure 54 Time-conversion curves for the radiation-induced polymerization of DGDA monomer in the presence of various polymers. Irradiation:  $0.1 \text{ MR/hr}$  at  $-78^{\circ}\text{C}$ , in vacuo. Polymer: (O) none, (□) PSt, (Δ) PMMA, (■) PVF, (●) PEG 600. Composition:  $0.9 \text{ g DGDA}-0.1 \text{ g polymer}$

### 7.2.3.2. Effect of Irradiation on Drugs

It is necessary to study the radiation effect on the activity of

chemotherapeutic drugs themselves before an entrapping. Then after an irradiation of chemotherapeutic drugs, the sample activities were assayed by a colourimetric method and compared with that obtained by a biological method. The biological assays were carried out by measuring the inactivation ability of irradiated and unirradiated drugs for Micococcus flavus P.C.I. 1203 in the case of 5-FU, for Mycobacterium smegmatis ATCC 607 in the case of BLM and for Bacillus subtilis ATCC 6633 in the case of MMC, respectively. The results are shown in Table VII. These results show that there is no significant difference between the assay results obtained by the two methods. Therefore, it is reasonable to adopt the colourimetric assay in this CHAPTER. The effects of irradiation conditions on the activity of chemotherapeutic drugs are shown in Figure 55.

Table VII Comparison of the relative activities of chemotherapeutic drugs obtained by a biological assay and a colourimetric assay

Drug	Relative activity (%)	
	Biological assay	Colourimetric assay
BLM	90.2, 95.5 <sup>a)</sup>	92.5, 95.8
MMC	95.1, 98.0 <sup>b)</sup>	96.2, 97.2
5-FU	97.3 <sup>c)</sup>	100.0, 98.9

Irradiation:  $5 \times 10^5$  R/hr, 1 hr, at  $-78^\circ\text{C}$ , in vacuo.

Composition: 5 ml of distilled water (pH 6.0) was mixed with drugs to form the mixture of 60  $\mu\text{g/ml}$  for BLM, 10  $\mu\text{g/ml}$  for MMC, and 10  $\mu\text{g/ml}$  for 5-FU, respectively.

Assay: a) assayed with Mycobacterium smegmatis ATCC 607,

b) assayed with Bacillus subtilis ATCC 6633,

c) assayed with Micrococcus flavus P.C.I. 1203.

All assays were carried out at  $37^\circ\text{C}$  for 18 hrs.

Relative activity: the activity of non-irradiated drugs was taken as 100%.

According to this result, an inactivation of chemotherapeutic drug by irradiation can be remarkably retarded by choosing relatively low temperature (usually below  $-40^\circ\text{C}$ ) and smaller irradiation dose usually than  $5 \times 10^5$  R, at which DGDA monomer can be easily polymerized. Such radiation effect may well be a general tendency also for other irradiated drugs such as aspirin, sulfanilamide, salicylic acid and colchicine, as previous



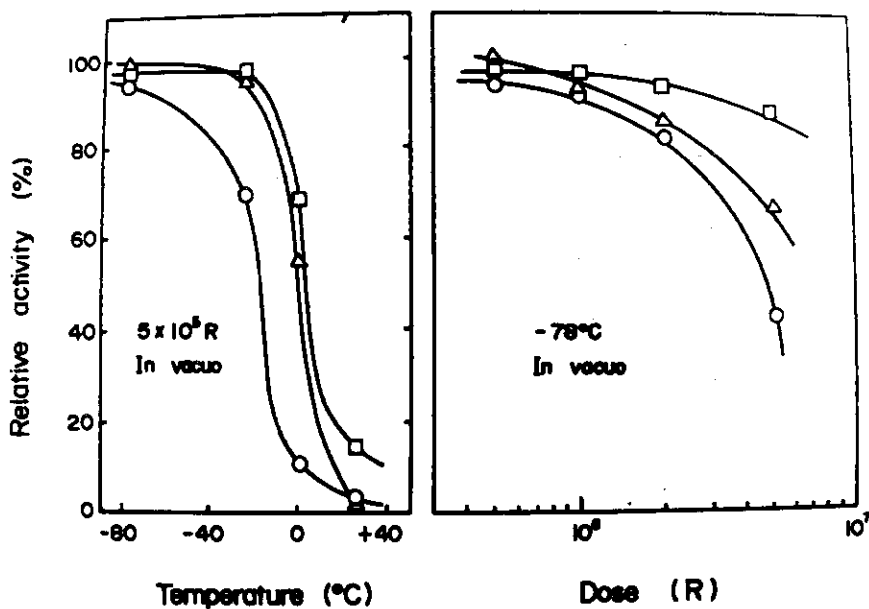


Figure 55 Effect of irradiation conditions on the activity of chemotherapeutic drugs. The activity of untreated chemotherapeutic drug was taken as 100%. Drug: (O) BLM, (□) MMC, (Δ) 5-FU

studied<sup>68</sup>. It was also found that an inactivation of biologically active substances by an irradiation was promoted by the oxygen and therefore the irradiation should be done under the vacuum.

#### 7.2.3.3. Time-Release Curve in the Polymerized Composite Comprising Drugs

Polymer-chemotherapeutic drug composites of various shapes were prepared by radiation-induced polymerization of DGDA monomer dissolving a polymer, at -78°C. The results are shown in Figures 56, 57, 58 and 59.

According to the result of Figure 56, the release rate of 5-FU from a rod shape polymer changed by the kind of added polymer. This may be attributed to the difference of hydrophilic property of polymer. In the case of addition of PEG 600, the spherical pores formed in the matrix owing to dissolving of PEG 600 from the matrix to the dissolving medium.

The effect of added PSt content in the matrix on the release property of 5-FU is shown in Figure 57. The release of 5-FU from the rod shape matrix decreased with the increase of PST concentration as shown in Figure 57 (a). However, in the case of spherical composite, no

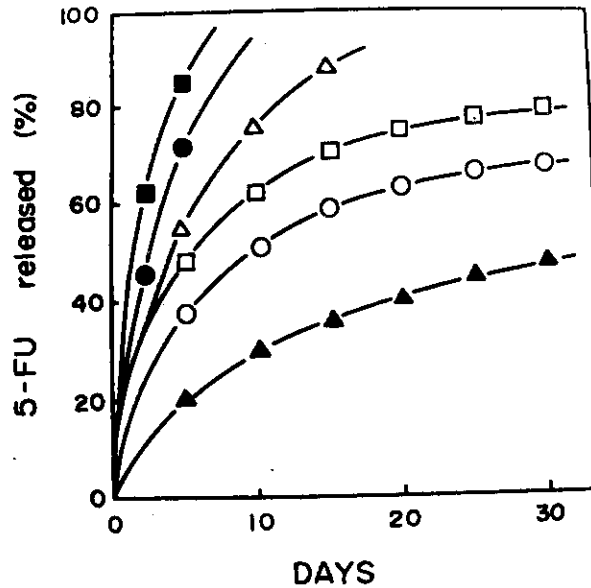


Figure 56 Release profile of 5-FU from the rod shaped PDGDA matrices comprising various kinds of polymers. Irradiation: 0.5 MR at  $-78^{\circ}\text{C}$ , in vacuo. Composition: 0.9 g DGDA-0.1 g polymer, and 100 mg 5-FU. Matrix size: 8 mm diameter and 20 mm length. Polymer: (○) PSt, (□) PMA, (●) PVAc, (△) PEG 600, (▲) PMMA, (■) PVF

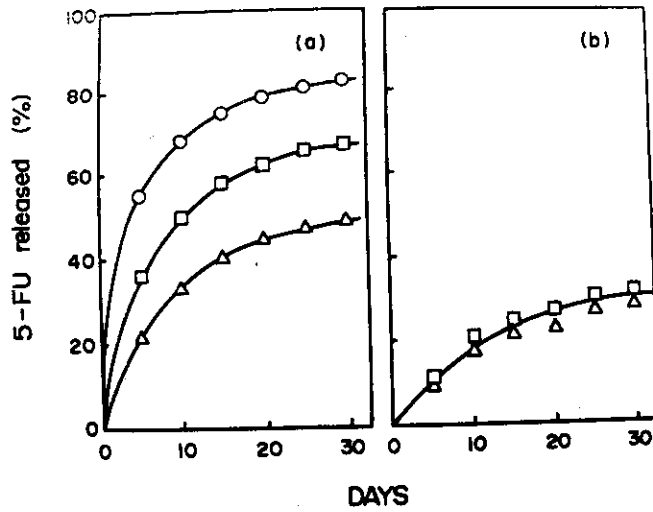


Figure 57 Effect of PSt content on the release of 5-FU from rod and spherical shaped PDGDA matrices. Irradiation: 0.5 MR at  $-78^{\circ}\text{C}$ , in vacuo. Shape of matrix: (a) rod shape (8 mm diameter and 20 mm length), (b) spherical shape (3 mm average diameter of particle and 40 particles in number). Composition: 100 mg 5-FU, (○) 1.0 g DGDA, (□) 0.9 g DGDA-0.1 g PSt, (△) 0.8 g DGDA-0.2 g PSt

difference was observed by the concentration as shown in Figure 57 (b). In a polymerization of pure DGDA monomer, no spherical polymer formed<sup>87</sup>. On the other hand, in the presence of PSt, the spherical matrix formed easily and the benzene soluble precipitate formed also in a cold precipitation medium phase during irradiation. This precipitate increased with increasing the PSt concentration and mainly consisted of excess PSt.

From these results, it is sure that the surface of spherical matrix is completely coated with a PSt to form a skin and an excess PSt is removed from the matrix to the precipitation medium as the benzene solution fraction. This might be reason for the formation of spherical matrix in the presence of PSt. On the other hand, all PSt is included inside the matrix and no skin formed in the rod shape polymer. As a

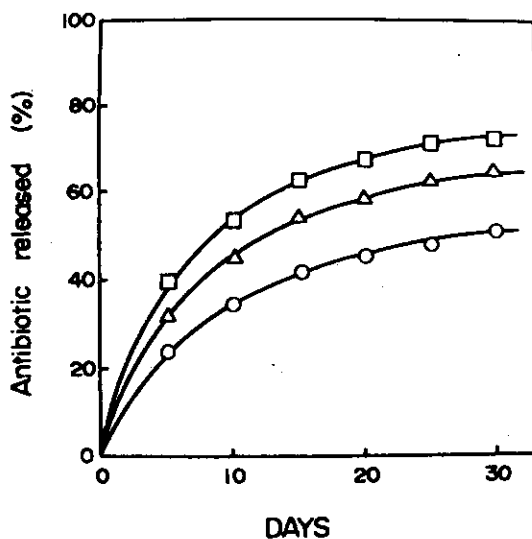


Figure 58 Release profiles of various chemotherapeutic drugs from the rod shaped PDGDA matrices. Irradiation: 0.5 MR at  $-78^{\circ}\text{C}$ , in vacuo. Composition: 20 mg drug, 0.45 g DGDA-0.05 g PSt. Matrix size: 8 mm diameter and 10 mm length. Drug: (O) BLM, (□) MMC, ( $\Delta$ ) 5-FU

result, the amount of 5-FU released per unit area and per unit time in a rod shape polymer was markedly larger than that in a spherical polymer as shown in Figure 57. This problem will be discussed in the later section in relation to the matrix structure observed by a scanning electron microscope.

The result of Figure 58 showed that the release of drug from a rod shape composite changed by the kind of drugs. This might be due to the

difference in the molecular size of drugs or in the affinity of drugs to the matrix polymer. The release profile of 5-FU from the matrices of various shapes was shown in Figure 59. From this result, it can be said that the release of 5-FU changed markedly by the shape of polymer matrix.

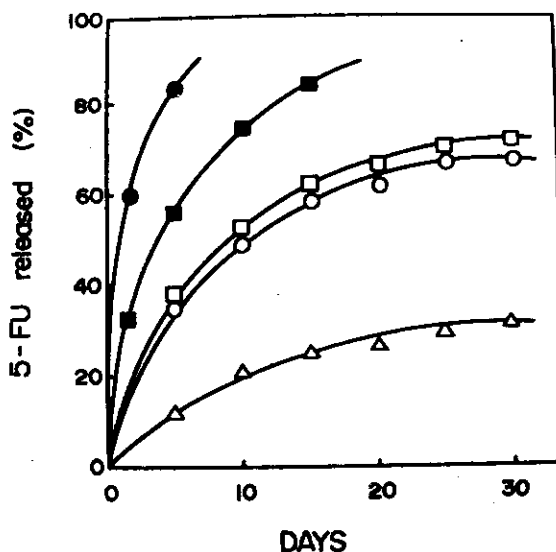


Figure 59 Release profile of 5-FU from the variously shaped PDGDA matrices. Irradiation: 0.5 MR at  $-78^{\circ}\text{C}$ , in vacuo. Composition: 0.9 g DGDA-0.1 g PSt, and 100 mg 5-FU. Shape of matrix: (○) rod (4 mm diameter and 40 mm length), (□) flat tablet (14 mm diameter and 7 mm thick), (Δ) spherical (3.2 mm average particle diameter and 38 particles in number), (●) powder (32-115 mesh), (■) membrane ( $20 \times 35 \times 1.5 \text{ mm}^3$ )

That is, the release rate decreased in the order of powder, membrane, tablet, rod and sphere. It is noticed that the matrices of various forms and shapes including chemotherapeutic drugs can be easily prepared by a molding or a casting polymerization of glass-forming monomers in a supercooled state.

#### 7.2.3.4. Phase Structure of Polymer Matrices

The optical photographs of polymer matrices of various shapes prepared by radiation polymerization were shown in Figure 60.

In the result of Figure 57, the amount of 5-FU released per unit area (about  $6 \text{ cm}^2$ ) of rod matrix was markedly larger than that (about  $11.3 \text{ cm}^2$ )

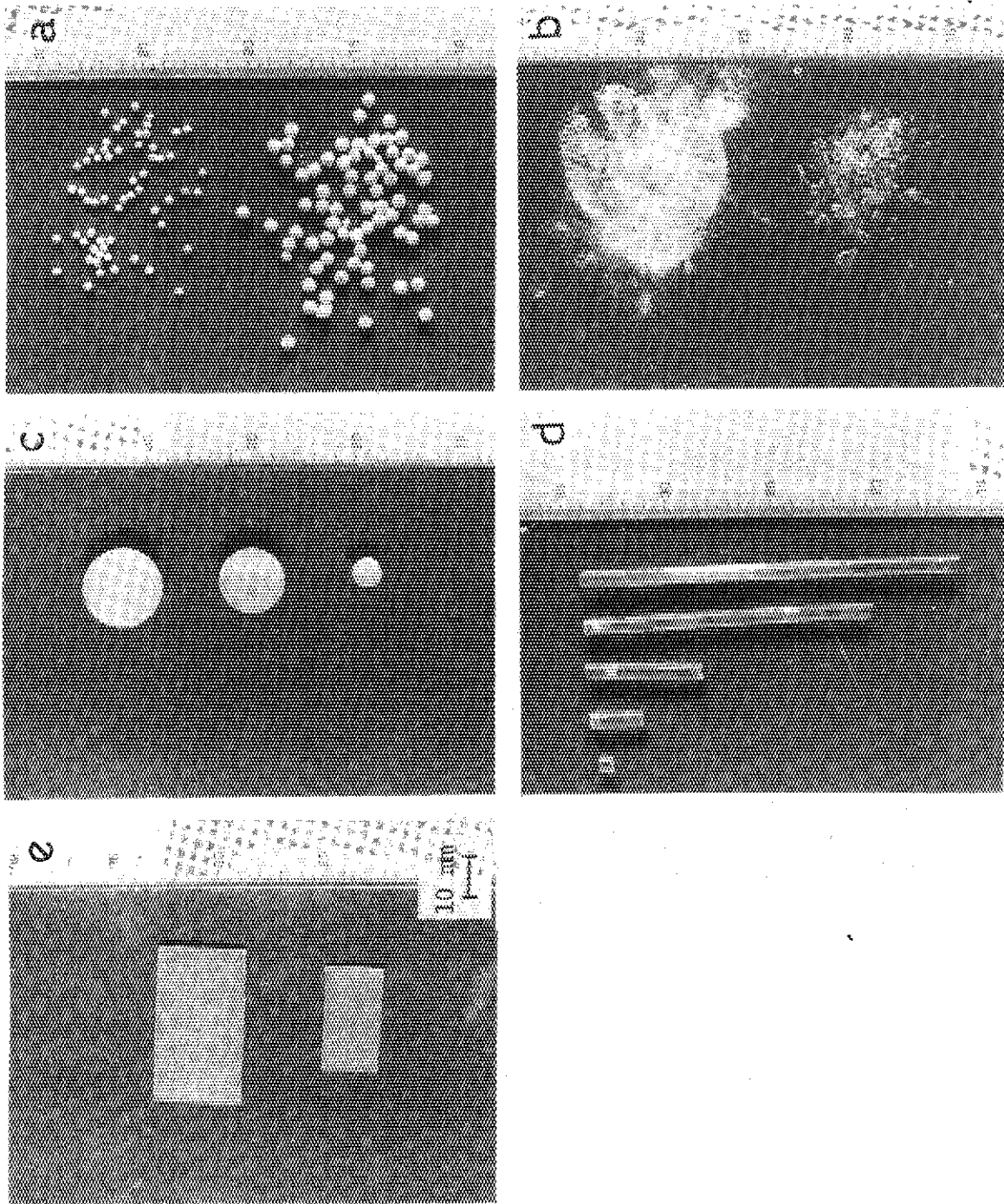


Figure 60 Photographs of variously shaped DGDA-chemotherapeutic drug composites obtained by radiation-induced polymerization. The composition and preparation conditions were the same as in Figure 59. Shape of matrix: (a) spherical matrix, (b) powder matrix, (c) flat circular tablet matrix, (d) rod matrix, (e) membrane matrix

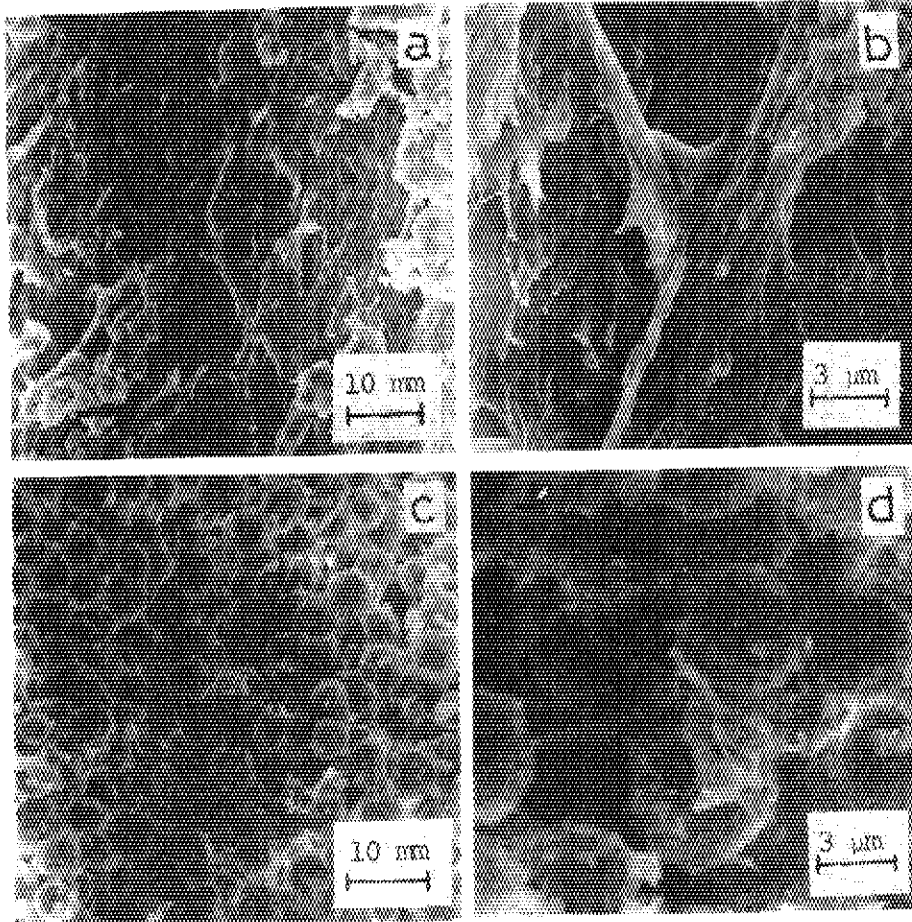


Figure 62 Scanning electron microphotographs of DGD A matrices after the removal treatment of PST. The preparation conditions of matrices are the same as those in Figure 57. Multiplication: (a) spherical matrix (300 times), (b) spherical matrix (1000 times), (c) rod matrix (300 times), (d) rod matrix (1000 times)

of spherical matrix. This difference can be attributed to the difference of phase structure in the two kinds of matrices. Both matrices were treated with boiling benzene in order to remove the PST. The photographs of matrices after this treatment were shown in Figure 61. According to this result of Figure 61, the shape of spherical matrix hardly changed by the benzene boiling treatment, but the shape of rod matrix was markedly deformed by the treatment and destroyed to the crumps. Since no poly(diethylene glycol dimethacrylate) (PDGD A) dissolves to benzene, so no

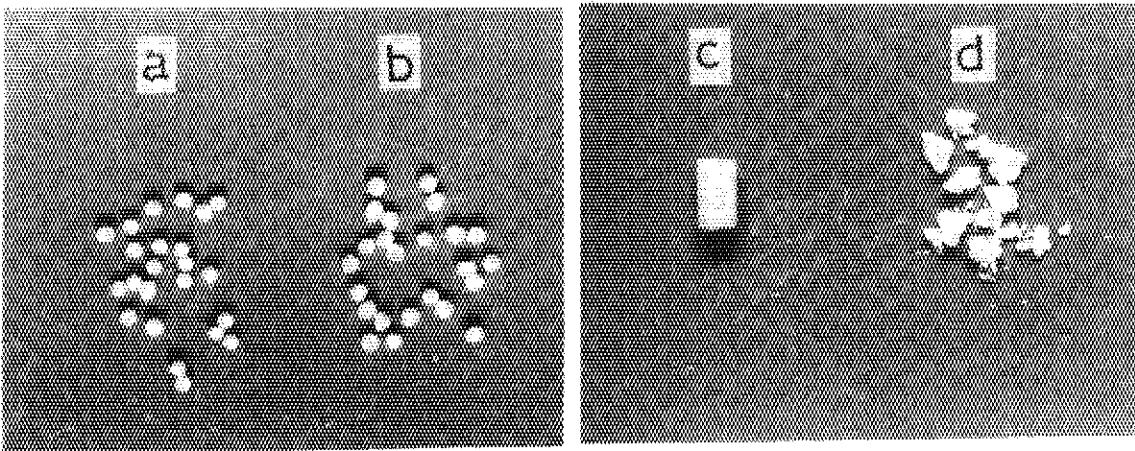


Figure 61 Photographs of DGD matrices before and after the removal of comprised PSt. The preparation conditions of matrices are the same as in Figure 57. PSt in the matrix was extracted with a boiling benzene for 24 hrs, (a) spherical matrix before removal treatment, (b) spherical matrix after removal treatment, (c) rod matrix before removal treatment, (d) rod matrix after removal treatment

PSt exists inside the matrix, but PSt covers the matrix surface in the case of spherical sample. On the other hand, PSt is homogeneously dispersed inside the matrix and then the drug can be dissolved out from the matrix without being prevented by the surface skin of PSt in the case of rod sample. This might be the reason for the greater release rate in a rod sample. The result of observation of those structure by a scanning electron microscope is shown in Figure 62. This result shows that a spherical composite consists of homogeneous PDGD phase and PSt skin, but a rod composite consists of blend mixture of spherical polymer blocks.

#### 7.2.4. Summary

The vinyl polymer-chemotherapeutic agent composites of various shapes such as rod, tablet, membrane, microsphere, and powder were prepared by radiation polymerization at low temperatures for the purpose of controlled slow and durable release of drugs from implanted matrices. BLM, MMC, and 5-FU were entrapped for testing in PDGD including small quantity of a polymer such as PSt, PVF, PMMA, PVAc, and PEG 600. The release rates from the matrices much depended on the kind of polymer, drug, and monomer concentration in polymerization and also the shape of composite.

## CHAPTER 8

## CONTROLLED RELEASE OF 5-FLUOROURACIL FROM POLYMER MATRICES CONTAINING ADSORBENTS

## 8.1. Introduction

It has been shown that the release rate of drugs could be controlled by various factors, for examples, the increase of the hydrophilicity of the matrix, the addition of soluble polymer, and the addition of pore-making components<sup>23,56,87,96</sup>. These methods were effective mainly in promoting the release of drugs. However, it is often desired to retard the release rate of drug without changing the properties of polymer.

In this CHAPTER, the matrix including 5-FU was prepared in the presence of various adsorbents to study the retardation effect of drug release by adsorbent addition.

## 8.2. Experimental

## 8.2.1. Materials

A glass-forming monomer such as 2-hydroxyethyl methacrylate (HEMA) was the same as described in CHAPTER 5. Silica gel (230-400 mesh), activated charcoal (fine powder), molecular sieves 4A (40-60 mesh) and activated clay (fine powder) were the product of E. Merck AG., Nishio Industries Co., Ltd and Kishida Chemical Co., Ltd, respectively. 5-Fluorouracil (5-FU) as an anticancer was obtained from Nipponkayaku Co., Ltd and pulverized to a powder (100-200 mesh).

## 8.2.2. Preparation of Radiation Polymerized-Matrices Containing 5-FU

A mixture of 1.5 ml of glass-forming monomers, 100 mg of 5-FU and 0-300 mg of adsorbents was charged into a glass ampoule of 8 mm inside diameter. The ampoule was degassed twice under cooling with liquid nitrogen and then was sealed under a vacuum of  $10^{-3}$  mmHg. After shaking the ampoule, it was frozen at a fixed low temperature. The irradiation from a  $^{60}\text{Co}$  source was carried out for 2 hrs at a dose rate of  $5 \times 10^5$  R/hr and at  $-78^\circ\text{C}$  in a Dewar vessel (dry ice-methanol). After irradiation, the



hard composites (8 mm diameter and 30 mm long) which formed were used for the dissolution test as in the polymerized state.

### 8.2.3. Other Experiments

The dissolution test (usually distilled water, pH 6.0, 1000 ml) and fine structure of the matrix were carried out by the same methods as described in CHAPTER 7.

## 8.3. Results and Discussion

### 8.3.1. Effect of Polymerization Conditions on Release of 5-FU

The time course for the release of 5-FU from a hydrophilic matrix such as PHEMA in the presence of adsorbents at 37°C are illustrated in Figures 63, 64 and 65.

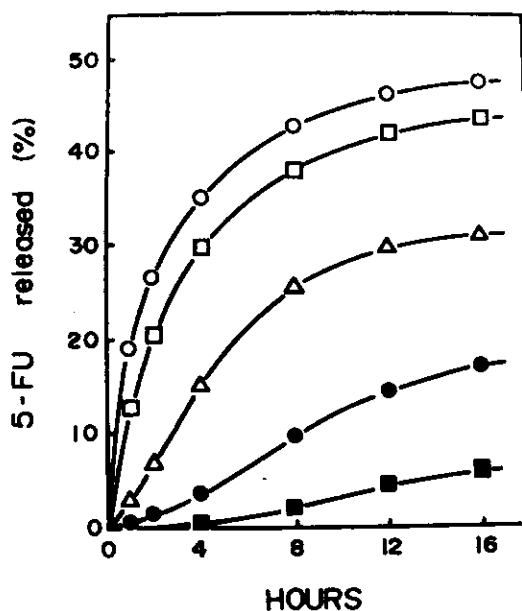


Figure 63 Drug release from PHEMA matrix containing 5-FU as a function of activated charcoal concentration in HEMA/drug/adsorbent system. Activated charcoal concentration (mg): (○) 0, (□) 10, (△) 50, (●) 100, (■) 300

Figure 63 shows the time-release curve as a function of activated charcoal concentration added in the matrix. Figure 63 shows that the release of 5-FU was remarkably affected by the addition of activated charcoal and the release rate of 5-FU was retarded in the early stage of dissolution in the high concentration. The dissolution was later accelerated and then suppressed again. The retarding effect caused by the adsorbent may be advantageous for the prolonged, durable release of drug from a large surface area matrix such as the finely divided one, from

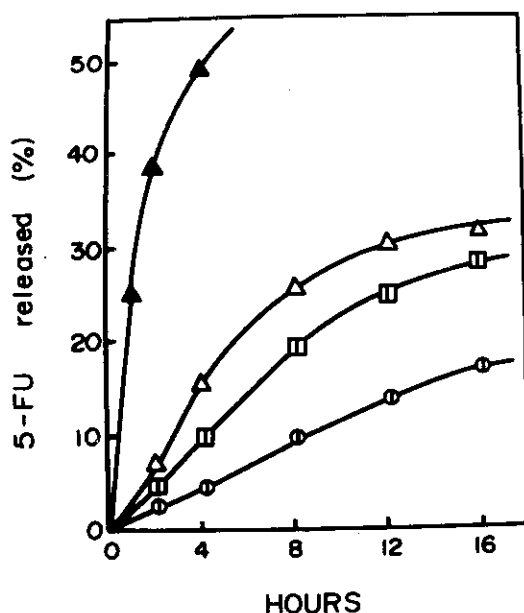


Figure 64 Drug release from PHEMA matrix containing 5-FU in the presence of various adsorbents in HEMA/drug/adsorbent systems. Adsorbent concentration: 50 mg, (▲) activated clay, (△) activated charcoal, (◻) molecular sieves 4A, (○) silica gel

which the release is usually too quick. A similar tendency was observed in other adsorbents such as silica gel and molecular sieves 4A, as shown in Figure 64. However, the effect of adsorbent on 5-FU release differs greatly according to the kind of adsorbent. The retardation effect on the release was in the order of silica gel, molecular sieves 4A, activated charcoal and activated clay. This can perhaps be attributed to differences in the adsorption properties of the drugs and in the physical structures of adsorbents inside the matrix. Figure 64 shows that the

release rate of 5-FU was very large in the presence of activated clay, which in a non-adsorbent. Adsorption with a adsorbent expected a big influence on the retardation of drug release.

Figure 65 shows the rate of release in two samples obtained by different mixing methods in the HEMA drug activated charcoal system. According to this result, the release rate was larger in the case of a matrix prepared simultaneously than in that prepared stepwise. The following mechanism for the adsorbent effect on the release property might be supposed. Solid drug and adsorbent are first dispersed separately in the matrix. However, with the swelling of the polymer, the drug dissolves in water and then can be easily adsorbed by the adsorbent. After that, the desorption of the drug occurs in a certain equilibrium with the adsorption. The desorbed drug may be released out of the matrix by

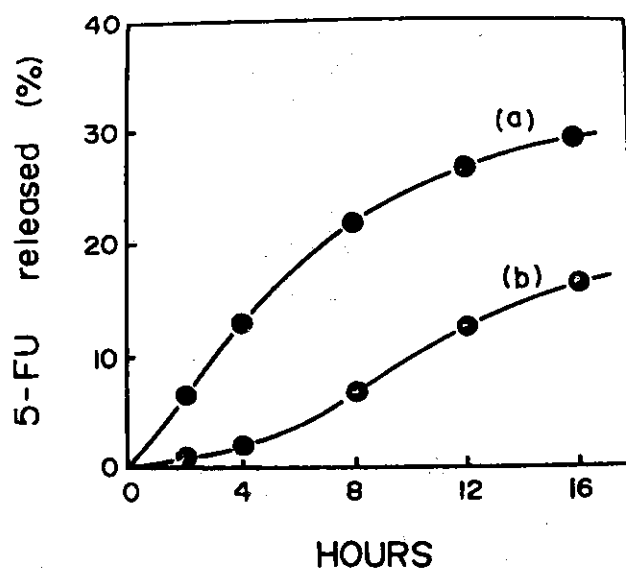


Figure 65 Effect of mixing method on release of 5-FU in HEMA/drug/activated charcoal system. Mixing method: (a) 1.5 ml HEMA, 50 mg activated charcoal and 30 mg 5-FU were mixed at the same time, (b) 2.0 ml aqueous solution containing 30 mg 5-FU and 50 mg activated charcoal were mixed and water containing in the system allowed to evaporate slowly under reduced pressure and finally 5-FU adsorbed with activated charcoal was mixed with 1.5 ml HEMA

diffusion. Consequently, the release of drug in the presence of adsorbent decreases owing to such a adsorption-desorption process by the adsorbent, in comparison with that in the absence of adsorbent. Most of the drug

would be released directly out of the matrix without being caught by adsorbent in the case of low adsorbent concentration, but the release of almost all the drug is retarded by the adsorption and the release becomes desorption-controlled in the system of high adsorbent concentration. This might be the reason for the different release behaviours in Figure 63 under various adsorbent concentrations. The swelling of polymer by water is almost completed within one hr and reaches a saturated state, so the swelling step is not a rate-determining process in the overall release in Figure 63.

### 8.3.2. Microscopic Observation of the Matrix

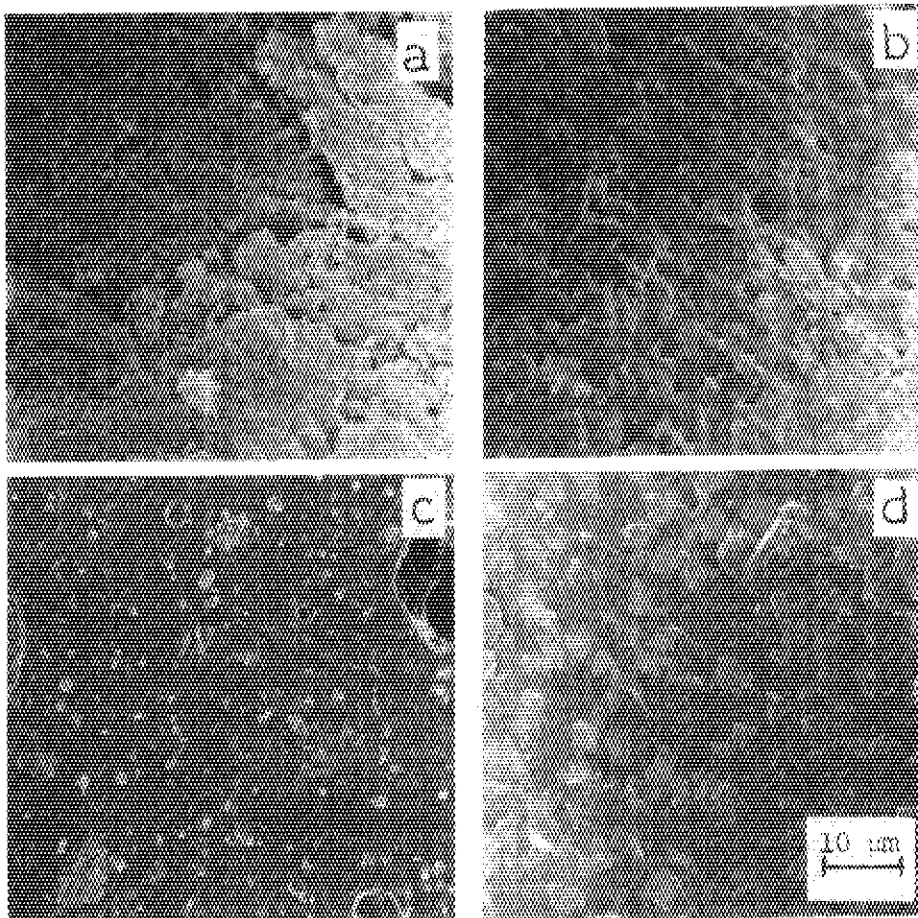


Figure 66 Scanning electron microphotographs of PHEMA matrices containing 5-FU in the presence of various adsorbents. The experimental conditions were the same as those in Figure 64. Adsorbent: (a) activated clay, (b) activated charcoal, (c) silica gel, (d) molecular sieves 4A

The microphotographs of the matrices obtained by radiation-induced polymerization in the presence of adsorbents are shown in Figure 66. It was found that adsorbents are homogeneously distributed in the matrix in all systems, but fine structures in the matrices differed according to the kind of adsorbent. However, it seems that there are some differences in the density or vacancy of matrices in the presence of various adsorbents. That is, there are relatively many vacancies in the matrices such as activated clay and activated charcoal. While, there are few vacancies in the matrices such as silica gel and molecular sieves 4A. The larger release rates in the former two systems compared with the later two cases (see, Figure 64) might be roughly explained by such differences of apparent matrix density.

### 8.3.3. Kinetics of Release

The author reported previously that the release of drugs from radiation polymerized-matrices, porous or non-porous, was carried out according to the Higuchi equation<sup>44</sup> for the diffusion-controlled release.

Figure 67 shows the relationship between the drug release and the square root of the time as a function of activated charcoal concentration,

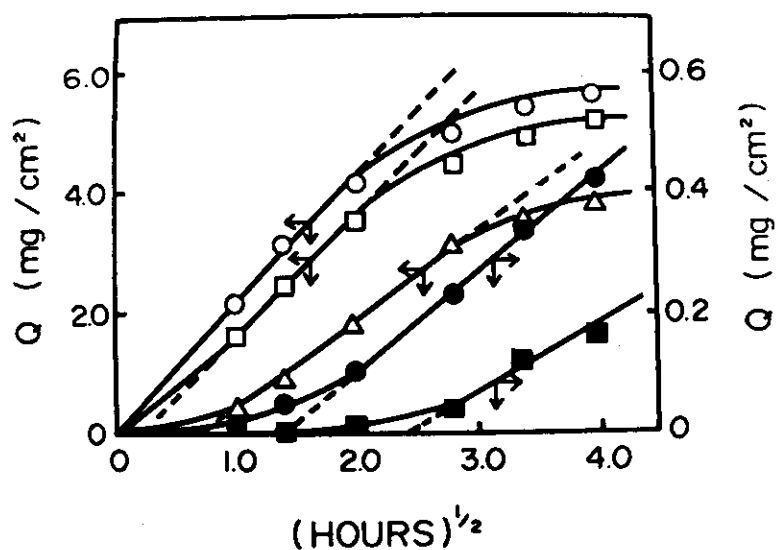


Figure 67 Linear  $Q-t^{1/2}$  relationship in HEMA/drug/activated charcoal system. The experimental conditions and symbols were the same as those in Figure 63

using the data given in Figure 63. Linear plots between  $Q$  and  $t^{1/2}$  were obtained over a certain time range for 5-FU from PHEMA matrix including activated charcoal, as seen in Figure 67. Furthermore, in the systems including activated charcoal, extrapolation to the x axis indicates a lag time before steady state release. In matrix systems including no adsorbent, no time lag due to initial retardation was observed. The result in Figure 67 suggests that no drug is trapped on the matrix surface but rather the drug is trapped inside, outside the matrix. That is, in those systems, the drug exists partly in a solid and partly in adsorbed state in adsorbent depending on the adsorbent concentration. These drugs are released from the matrix phase directly by diffusion or stepwise by diffusion via desorption into the dissolution phase. Therefore, Higuchi equation might be applicable over a certain equilibrium, assuming that the apparent overall drug concentration consists of both markedly dispersed drug and an adsorbed-desorbed drug.

#### 8.4. Summary

Entrapping of 5-FU was carried out by radiation-induced polymerization of glass-forming monomer, HEMA, at  $-78^{\circ}\text{C}$  in the presence of adsorbents. It was found that the release of 5-FU for the matrix was retarded by the addition of various adsorbents. The release rate decreased with increasing concentration of adsorbent. The manners of release of 5-FU from the matrices containing adsorbents were studied according to Higuchi equation. The observation by a scanning electron microscope proved that an adsorbent was homogeneously distributed in the matrix.

## CHAPTER 9

CONTROLLED RELEASE OF MULTI-COMPONENT CYTOTOXIC AGENTS FROM RADIATION  
POLYMERIZED COMPOSITES

## 9.1. Introduction

In this CHAPTER, the simultaneous entrapping of multi-components cytotoxic agents such as 1-(2-tetrahydrofuryl)-5-fluorouracil (FT-207), mitomycin C (MMC) and adryamicin (ADM) was studied for the purpose of controlled release of them in desired rates and ratios.

The author studied the entrapping of several anticancers for controlled release without secondary reaction in directly implanted state on the cancered part<sup>97</sup>. This technique has been proved to be very effective. However, each cancer has a specific adaptability for a specific kind of cancer. If multi-kinds of anticancers are entrapped and released from the single matrix to attack directly the cancered part, one of them would show an effect, without preliminary investigation on adaptabilities of each anticancer. Therefore, this technique may be useful for the cure of cancers, which are difficult to clarify its position, property or scope of spread.

## 9.2. Experimental

## 9.2.1. Materials

Diethylene glycol dimethacrylate (DGDA) as a glass-forming monomer and poly(methyl methacrylate) (PMMA) as a polymer were the same as described in CHAPTER 8.

Mitomycin C (MMC) and adryamicin (ADM) obtained from Kyowa Hakko Kogyo Co., Ltd and 1-(2-tetrahydrofuryl)-5-fluorouracil (FT-207) obtained from Taiho Pharmaceutical Co., Ltd were used as anticancers.

## 9.2.2. Preparation of Polymer-Cytotoxic Agent Composites

The polymer-cytotoxic agent composite was made by irradiation of the mixture of cytotoxic agent, monomers and polymers. In all cases, the irradiation was carried out for 2 hrs at  $-78^{\circ}\text{C}$ , achieved by use of solid

carbon dioxide and methanol, at a dose rate of  $5 \times 10^5$  R/hr from a  $^{60}\text{Co}$  source. No cytotoxic agents used in this study were dissolved in a monomer such as DGDA. However, in the 10% PMMA-90% DGDA system, PMMA was initially dissolved in DGDA monomer.

The composite formed in this study was a very hard, flat circular tablet, 0.7 cm diameter and  $5.4 \text{ cm}^2$  surface area. The glass-forming monomers easily reach 100% conversion under the above irradiation conditions<sup>96</sup>.

### 9.2.3. Release Test of Cytotoxic Agents from the Polymer-Cytotoxic Agent Composites

The release test was carried out by the same methods as described in CHAPTER 8. At selected time intervals, 5 ml samples of the elution medium were assayed spectrophotometrically with a Shimadzu double beam spectrophotometer, Model UV-200, measuring the absorption at 365 nm for MMC, 270 nm for FT-207, 254 nm (or 235 and 290 nm) for ADM and 278 nm for UK.

### 9.2.4. Thrombogenicity Test of the Composites

The thrombogenicity test was carried out by Imai's method<sup>98</sup>, using blood taken from human arm (100 parts) mixed with a 3.8% aqueous solution of citric acid (10 parts) and stored in a refrigerator. The blood (0.25 ml) was dropped on a sample film on a watch glass filled with distilled water. Then, 3.8% aqueous calcium chloride (25  $\mu\text{l}$ ) was added to the blood as a coagulation promoter to initiate the test. After a determined time, distilled water (20-30 ml) was added to the blood to stop the coagulation. The thrombus formed was dried and weighed. The thrombus percent expresses as a ratio the quantity of thrombus at a certain test time, to the quantity of thrombus obtained at the time when no blood dissolves in the distilled water added as a coagulation stopper.

## 9.3. Results and Discussion

### 9.3.1. Release Profiles of Each Cytotoxic Agent from the Individual and Common Matrices



The release profiles of each cytotoxic agent used in this CHAPTER were investigated and the result is shown in Figure 68. The release rates of each cytotoxic agent are found to differ depending on their kind. That

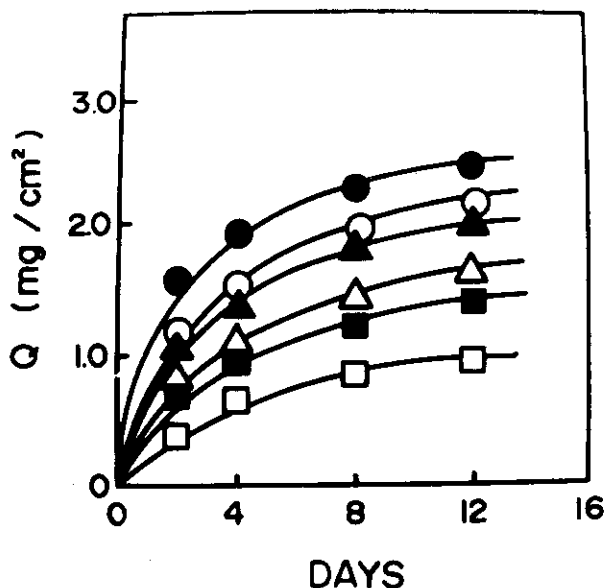


Figure 68 Release profiles of each anticancer from the common or the individual composites. In the individual composite [symbols in Figure: (○) for FT-207, (△) for MMC and (□) for ADM], 20 mg of an anticancer was entrapped, while 60 mg (consist of 20 mg of FT-207, 20 mg of MMC and 20 mg of ADM) of mixed anticancers was entrapped in the common composite [symbols in Figure: (●) for FT-207, (▲) for MMC and (■) for ADM]. Monomer system: 10% PMMA-90% DGDA (0.8 ml). Composite size: 0.7 cm diameter flat circular composite

is, the release decreased in the order of FT-207, MMC and ADM. This may be attributed to the difference in the molecular weight (Mw) of the cytotoxic agent. The Mw of FT-207, MMC and ADM are 200, 327 and 580, respectively. It was also found that the release of each cytotoxic agent from the common matrix, containing multi-component cytotoxic agents, was faster than that from the individual composite containing only a single cytotoxic agent. This may be due to the difference in the total content of cytotoxic agent contained in the composite.

Figure 69 shows the release profile of multi-component cytotoxic agents from the common composite, when the total contents and the composition ratios of each cytotoxic agent are changed. That is, the

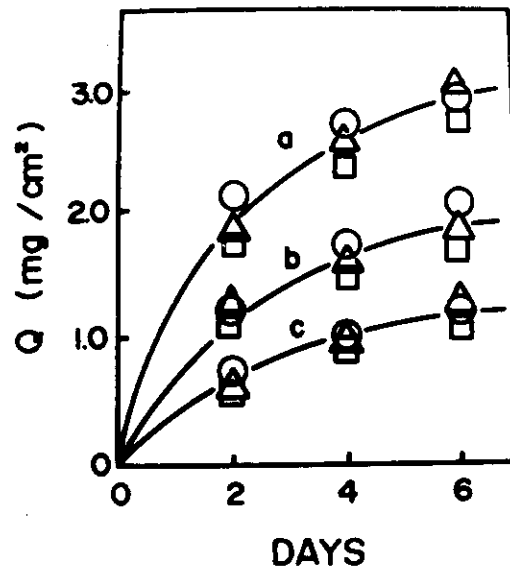


Figure 69 Release profiles of each anticancer from the common composite as a function of anticancer content added in the composite. Monomer system and composite size were the same as in Figure 68. Component of anticancer: (a) 35 mg of ADM, 25 mg of MMC and 20 mg of FT-207, (b) 30 mg of ADM, 20 mg of MMC and 15 mg of FT-207, (c) 20 mg of ADM, 15 mg of MMC and 10 mg of FT-207. Symbols in Figure: (○) FT-207, (□) MMC, (△) ADM

composition ratios of each cytotoxic agent were controlled according to the result of Figure 68 to give the same release rate. The result shown in Figure 69 is that the release behaviour of each cytotoxic agent in the common matrix is expressed by the single release curve. It is evident that multi-component cytotoxic agents entrapped in the common matrix can be released at a desired rate, that is, at quick or slow rates at united or different rates, by controlling the content and composition of cytotoxic agents. This property is convenient and useful for practical applications.

### 9.3.2. Thrombus Formation of the Composites

Thrombogenicities of radiation polymerized composites used in this CHAPTER were tested, because in some cases these materials might be used in contact with blood. The composite materials show (Figure 70) comparable thrombogenicity to that of commercially available polytetra-

fluoroethylene (PTFE). It has been reported<sup>99</sup> that a composite such as PDGDA caused no inflammation or foreign body reaction for the adjacent tissue of animals.

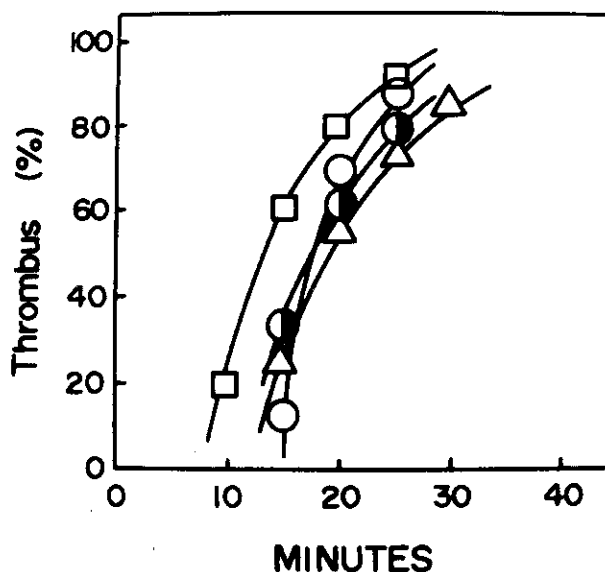


Figure 70 Thrombogenicities of various composites made by radiation polymerization at low temperatures. Composite film: (○) PTFE, (□) poly(10% PMMA-90% DGDA), (△) PDGDA, (●) PIMPT

### 9.3.3. In Vivo Animal Experiments

The monomeric capsules (0.8 g/capsule) of two kinds containing 20 mg MMC such as 10% PMMA-90% DGDA (Lot 747) and 10% PMMA-90% HEA (Lot 748) systems were irradiated for 2 hrs at a dose rate of  $5 \times 10^5$  R/hr at  $-78^\circ\text{C}$ , in vacuo. The two polymeric capsules obtained were directly implanted on the cancered part of animal. The result is shown in Figure 71<sup>99</sup>.

Ehrlich ascites carcinoma ( $5 \times 10^6$ /0.2 ml) was inoculated into the abdominal cavity of females ICR mice of 5 weeks old. The author was used two kinds of capsules with different water absorption ratio, one with faster effusion and other with slower effusion. Each has two kinds of drug concentrations, low concentration of MMC (0.25 mg/kg/day) and high concentration (0.5 mg/kg/day). Average survival of control group without bearing capsule was 11.1 days. The group of low concentration of capsule

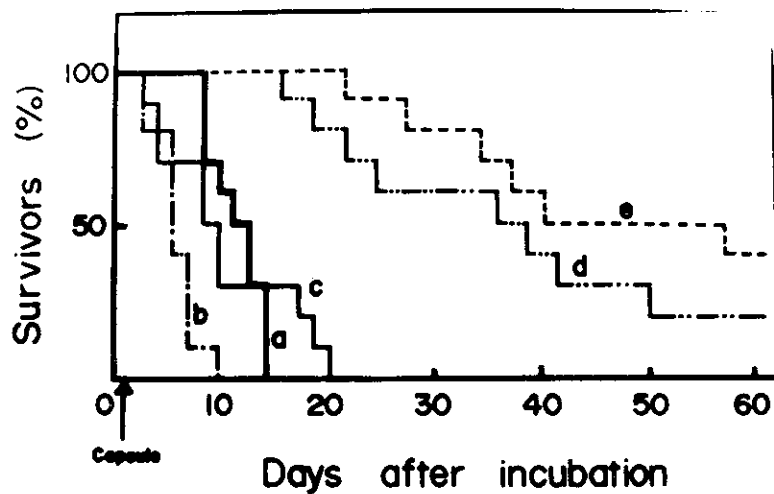


Figure 71 Survival ratio on mice bearing ehrlich ascited carcinoma after treatment with MMC capsule. LC: 0.25 mg/kg/day, HC: 0.5 mg/kg/day. (a) control, (b) Lot 748 HC, (c) Lot 748 LC, (d) Lot 747 HC, (e) Lot 747 LC

Table VIII Hematological data on mice after 1 week of treatment with MMC capsule

Group	No. of mice used	RBC ( $\times 10^4/\text{mm}^3$ )	WBC ( $\times 10^2/\text{mm}^3$ )
Control	10	847.70 $\pm$ 18.30	45.80 $\pm$ 8.05
Experimental	10	765.00 $\pm$ 14.67*	48.78 $\pm$ 5.32

Values are the mean  $\pm$  S.E.

\* Significantly different from the control at  $p < 0.001$

with slower effusion indicated average survival above 46.5 days and percentage of the prolongation life was more than percentage of 418 with increase of body weight. No leucocytoenia appeared. This capsule acted on local malignant cells effectively. This anticancer (cytotoxic agent) drug capsule is recommendid in order to minimize the influence on blood cells and to achieve prolongation of life for inoperable patients (Table VIII)<sup>99</sup>.

#### 9.4. Summary

The multi-component cytotoxic agents such as MMC, ADM and FT-207 were entrapped in a single common composite by radiation-induced polymerization of glass-forming monomers in the presence of polymers. It was found that the release profiles of each cytotoxic agent from the single matrix were controlled freely by the contents and compositions of three cytotoxic agents in the matrix.

The controlled release delivery devices containing cytotoxic agents had excellent healing effects in animal experiments, as described in CHAPTER 9. This method is characterized that the polymer-drug capsule was directly implanted on the cancered part. At present, the bedside and clinical using the controlled release delivery devices is practiced.

## REFERENCES

1. M. Yoshida, M. Kumakura and I. Kaetsu; Polymer, 20 3-8 (1979).  
[Immobilization of enzymes by radiation-induced polymerization of glass-forming monomers: I. Immobilization of some enzymes by poly(2-hydroxyethyl methacrylate)].
2. M. Yoshida, M. Kumakura and I. Kaetsu; J. Macromol. Sci.-Chem.,  
in press.  
[Immobilization of enzymes by radiation-induced copolymerization of 2-hydroxyethyl methacrylate and other hydrophilic or hydrophobic comonomers].
3. I. Kaetsu, H. Okubo, A. Ito and K. Hayashi; J. Polymer Sci., A1  
2203 (1972).
4. I. Langmuir and V.J. Schaefer; J. Amer. Chem. Soc., 60 1351 (1938).
5. A Schejter and A. Bar-Eli; Arch. Biochem. Biophys., 136 325 (1970).
6. A.N. Glazer, A. Bar-Eli and E. Katchalski; J. Biol. Chem., 237  
1832 (1962).
7. A. Mitz; Science, 123 1076 (1956).
8. T. Wagner, C.J. Hsu and G. Kelleher; Biochem. J., 108 892 (1968).
9. H. Brandenberger; Helv. Chim. Acta, 40 61 (1957).
10. G. Manecke and G. Guezel; Makromol. Chem., 91 136 (1966).
11. S. Borodokin and F.E. Fucker; J. Pharm. Sci., 64 1289 (1975).
12. T.J. Roseman and W.I. Higuchi; J. Pharm. Sci., 59 353 (1970).
13. R.W. Crosswell and C.H. Becker; J. Pharm. Sci., 63 440 (1974).
14. T. Higuchi; J. Pharm. Sci., 52 1145 (1963).
15. J.B. Schwarz, A.P. Simonelli and W.I. Higuchi; J. Pharm. Sci., 57  
274 (1968).
16. J.T. Carstensen and M. Patel; J. Pharm. Sci., 64 1770 (1975).
17. W.H. Thomas; J. Pharm. Pharmacol., 25 27 (1973).
18. R.I. Leininger, C.W. Cooper, R.D. Falb and G.A. Grode; Science,  
152 1625 (1966).
19. K. Catt, H.D. Nail and G.W. Tregear; J. Lab. Clin. Med., 70  
820 (1967).
20. H. Maeda, H. Suzuki and A. Yamaguchi; Biotechnol. Bioeng., 15  
607 (1973).
21. H. Maeda, K. Yamada, H. Kumagai, T. Hino and S. Okamura;  
Enzyme Engineering, 3 57 (1978).

22. K. Kawashima and K. Umeda; Biotechnol. Bioeng., 16 609 (1974).
23. M. Yoshida, M. Kumakura and I. Kaetsu; Polymer, 19 1375-1378 (1978).  
[Controlled release of biofunctional substances by radiation-induced polymerization : I. Release of potassium chloride by polymerization of various vinyl monomers].
24. P. Bernfeld and J. Wang; Science, 142 678 (1963).
25. T.M.S. Chang and M.J. Poznasky; Nature, 218 243 (1968).
26. M. Yoshida, M. Kumakura and I. Kaetsu; Polymer J., 11 915-919 (1979).  
[Immobilization of cellulase in the swollen microsphere by radiation polymerization].
27. M. Yoshida, M. Kumakura and I. Kaetsu; Polymer J., 11 775-779 (1979).
28. I. Kaetsu, H. Okubo, A. Ito and K. Hayashi; J. Polymer Sci., A1 2215 (1972).
29. M. Yoshida, M. Kumakura and I. Kaetsu; Polymer, 19 1379-1381 (1978).  
[Controlled release of biofunctional substances by radiation-induced polymerization II. Release of potassium chloride from porous poly(diethylene glycol dimethacrylate)].
30. S. Suzuki; Kagaku no Ryoiki, 28 281 (1974).
31. S. Gondo and K. Kusunoki; Kagaku Kogaku, 38 357 (1974).
32. G.S.J. Melrose; Rev. Pure Appl. Chem., 21 83 (1971).
33. I. Chibata; Koteika Koso, Kodansha, Tokyo, 1977.
34. L. Goldstein; Methods Enzymol., 19 935 (1971).
35. E. Katchalski, I. Silman and R. Goldman; Advanc. Enzymol., 34 445 (1971).
36. G. Maneck; Naturwissenschaften, 51 25 (1964).
37. K. Mosbach; Sci. Am., 224 26 (1971).
38. H. Maeda, H. Suzuki and A. Yamaguchi; Biotechnol. Bioeng., 15 827 (1973).
39. F.G. Sandret, A. Guilbot and J. Bure; Acta Chim. Acad. Sci. Hung., 23 513 (1960).
40. J. Bure; Getreide u. Mehl, 9 133 (1959).
41. T. Kitamikado and N. Toyama; Hakko Kyokaiishi, 40 85 (1962).
42. G. Noeling and P. Berenfeld; Helv. Chim. Acta, 31 286 (1948).
43. L. Sialoman and J.E. Johnson; Anal. Chem., 31 453 (1959).
44. T. Higuchi; J. Pharm. Sci., 50 874 (1961).
45. M. Yoshida, M. Kumakura and I. Kaetsu; Polymer, 20 9-13 (1979).  
[Immobilization of enzymes by radiation-induced polymerization of glass-forming monomers II. Effects of cooling rate and solvent

- on porosity and activity of immobilized enzymes].
46. M. Kumakura, M. Yoshida, M. Asano and I. Kaetsu; J. Solid-Phase Biochem., 2 279-288 (1978).  
[Immobilization of enzymes by radiation-induced polymerization of glass-forming monomers. Double entrapping of enzymes in the presence of various additives].
  47. H.P. Gregor and P.W. Rauf; Biotechnol. Bioeng., 17 445 (1976).
  48. K. Hirano, I. Karube, T. Matsunaga and S. Suzuki; J. Ferment. Technol., 55 401 (1977).
  49. K. Kawashima and K. Umeda; Agri. Biol. Chem., 50 1143 (1976).
  50. K. Toda and M. Shoda; Biotechnol. Bioeng., 17 481 (1975).
  51. J.F. Kennedy, S.A. Barker and J.D. Humphreys; Nature (London), 261 242 (1976).
  52. A.M. Klivanov, G.P. Samoklin, K. Martinek and I.V. Berezin; Biotechnol. Bioeng., 19 211 (1977).
  53. S. Sai, Y. Tani and K. Ogata; J. Ferment. Technol., 53 380 (1975).
  54. Y.K. Cho and J.E. Baily; Biotechnol. Bioeng., 19 769 (1977).
  55. I. Kaetsu, M. Kumakura, M. Yoshida and M. Asano; Proc. 26th IUPAC Congress, Tokyo, 1977, p262.  
[Immobilization of enzymes by radiation-induced polymerization at low temperatures].
  56. M. Kumakura, M. Yoshida and I. Kaetsu; European J. Appl. Microbiol. Biotechnol., 6 13-22 (1978).  
[Immobilization of *Streptomyces phaeochromogenes* cells at a high concentration by radiation-induced polymerization of glass-forming monomers].
  57. M. Yoshida, M. Kumakura and I. Kaetsu; Yakuzaigaku, 39 69-74 (1979).  
[Controlled release of potassium chloride from radiation-polymerized copolymer matrices].
  58. M. Yoshida, M. Kumakura and I. Kaetsu; Kobunshi Ronbunshu; 36 35-40 (1979).  
[Preparation and its drug release property of radiation-polymerized poly(methyl methacrylate) capsule including potassium chloride].
  59. I. Kaetsu, M. Kumakura and M. Yoshida; Biotechnol. Bioeng., 21 863-873 (1979).  
[Enzyme immobilization by radiation-induced polymerization of hydrophobic glass-forming monomers at low temperatures].



60. I. Kaetsu, M. Kumakura and M. Yoshida; Biotechnol. Bioeng., 21 847-861 (1979).  
[Enzyme immobilization by radiation-induced polymerization of 2-hydroxyethyl methacrylate at low temperatures].
61. M. Yoshida, M. Kumakura and I. Kaetsu; unpublished data.
62. M. Yoshida, M. Kumakura and I. Kaetsu; J. Macromol. Sci.-Chem., in press.  
[Immobilization mechanism of enzymes by radiation-induced polymerization of glass-forming monomers].
63. S. Nishizaki; Iyakuin Kenkyu, 5 895 (1969).
64. S. Dische and E. Borenfreund; J. Biol. Chem., 193 583 (1951).
65. A.J. Johnson, D.L. Kline and N.A. Alkjaersig; Thrombosis Diathesis Haemorrhagica, 21 259 (1959).
66. Y. Takasaki; Agr. Biol. Chem., 30 1248 (1966).
67. M. Kumakura, M. Yoshida and I. Kaetsu; Appl. Environmental Microbiol., 37 310-315 (1979).  
[Immobilization of glucose isomerase containing *Streptomyces phaeochromogenes* cells in fine-particle form]
68. M. Yoshida, M. Kumakura and I. Kaetsu; J. Pharm. Sci., 68 628-631 (1979).  
[Drug entrapment for controlled release in radiation-polymerized beads].
69. K. Kawashima and K. Umeda; Nippon Shokuhin Kogyo Gakkaishi, 23 206 (1976).
70. H. Maeda; Biotechnol. Bioeng., 17 1571 (1975).
71. G.P. Hicks and S.J. Updike; Anal. Chem., 38 726 (1966).
72. H. Maeda, H. Suzuki, A. Yamauchi and S. Sakimae; Biotechnol. Bioeng., 17 119 (1975).
73. H. Maeda, A. Yamauchi and S. Suzuki; Biotechnol. Bioeng., 315 18 (1973).
74. K. Kawashima and K. Umeda; Biotechnol. Bioeng., 17 599 (1975).
75. H. Maeda, S. Miyago and H. Suzuki; Hakko Kyokaishi; 28 391 (1970).
76. G. Manecke and H.G. Vogt; Makromol. Chem., 177 725 (1976).
77. J.C. Fu, C. Hagemer and D.L. Moyer; J. Biomed. Mater. Res., 10 743 (1976).
78. S. Borodkin and F.E. Tucker; J. Pharm. Sci., 64 1269 (1975).
79. K. Juni, M. Nakano and Y. Arita; Yakuzaigaku, 36 129 (1976).
80. Y.W. Chin and E.P.K. Lau; J. Pharm. Sci., 65 488 (1976).

81. J.J. Sciarra and S.P. Patel; J. Pharm. Sci., 65 1519 (1976).
82. H.D. Orth and W. Brummer; Angew. Chem. (Int. Edn.), 11 249 (1972).
83. K. Smiley and G.W. Strandberg; Advances in Applied Microbiology, Academic Press, New York, vol. 15, p13 (1972).
84. Y.W. Chin, H.J. Lambert and D.E. Grant; J. Pharm. Sci., 63 365 (1974).
85. V.W. Winkler, S. Borodkin, S.K. Webel and J.T. Mannebach; J. Pharm. Sci., 66 816 (1977).
86. R.W. Crosswell and C.H. Becker; J. Pharm. Sci., 63 440 (1974).
87. M. Yoshida, M. Kumakura and I. Kaetsu; J. Pharm. Sci., 68 860-862 (1979).  
[Controlled drug dissolution by radiation-induced polymerization in the presence of dimethylaminoethyl methacrylate-methyl methacrylate or methacrylic acid-methyl acrylate copolymer].
88. M. Yoshida, M. Kumakura and I. Kaetsu; Polymer Preprints, 26 698-701 (1977).  
[Immobilization of enzymes by radiation-induced polymerization at low temperatures in various forms].
89. W. Uchiumi; Nippon Kagaku Zasshi, 73 835 (1952).
90. A.A. Noyes and W.R. Whitney; J. Amer. Chem. Soc., 19 930 (1897).
91. Y. Nozawa, T. Ushikawa, T. Yonezawa and F. Higashide; Yakuzaigaku, 36 7 (1976).
92. T. Saito, S. Suzuki, N. Nanbu, S. Sakurai and T. Nagai; Yakuzaigaku, 36 111 (1976).
93. K. Kishi, S. Nishii, A. Yamaji and E. Hiraoka; Biyojin Yakugaku, 3 150 (1977).
94. M. Kumakura, M. Yoshida and I. Kaetsu; Biotechnol. Bioeng., 21 679-688 (1979).  
[Immobilization of *Streptomyces phaeochromogenes* by radiation-induced polymerization of glass-forming monomers].
95. S.K. Chandrasekaran, R. Cappozza and P.S.L. Wong; J. Membrane Sci., 3 271 (1978).
96. I. Kaetsu, M. Yoshida and A. Yamada; J. Biomed. Mater. Res., in press.  
[Controlled slow release of chemotherapeutic drugs from matrices prepared by radiation polymerization at low temperatures].
97. A. Yamada, E. Machiyama, N. Kabei, M. Kikuchi, Y. Sakurai, M. Yoshida, M. Kumakura and I. Kaetsu; Jinko Zoki, 8 97-100 (1979).

[Controlled release of anticancer drug based on radiation-induced polymerization at low temperature].

98. Y. Imai and H. Nose; J. Biomed. Mater. Res., 6 165 (1972).
99. A. Yamada, E. Machiyama, N. Kabei, M. Kikuchi, Y. Sakurai, F. Hanyu, M. Yoshida, M. Kumakura and I. Kaetsu; J. Tokyo Wom. Med. Coll., 49 481-490 (1979).

[Study on controlled release from anticancer drug capsule made by radiation-induced polymerization at low temperature].

ACKNOWLEDGEMENT

The author wishes to express the sincere thanks to Dr Isao Kaetsu (Chief, Process Laboratory III) and Dr Minoru Kumakura of our Establishment for their helps and discussions during this work.

The author is deeply indebted to Dr Tadao Seguchi for his help with scanning electron microscope and to Associate Professor Akio Yamada of Tokyo Women's Medical College for useful discussions.